Thesis

On

EXPERIMENTATION FOR IMPROVEMENT IN SURFACE PROPERTIES AND PROCESS OPTIMIZATION OF DIE STEELS BY USING POWDER MIXED DIELECTRIC IN EDM PROCESS

Submitted in partial fulfillment of the requirement for the award of the degree of

Master of Engineering

IN

PRODUCTION & INDUSTRIAL ENGINEERING

Submitted By

GURPREET SINGH

Roll No. 800882003

Under the Guidance of

Dr. Ajay Batish
Associate Professor
Thapar University, Patiala

Mr. Anirban Bhattacharya
Assistant Professor
Thapar University, Patiala

DEPARTMENT OF MECHANICAL ENGINEERING
THAPAR UNIVERSITY
PATIALA-147004, INDIA

DECLARATION

I hereby declare that the thesis entitled "**EXPERIMENTATION FOR IMPROVEMENT IN SURFACE PROPERTIES AND PROCESS OPTIMIZATION OF DIE STEELS BY USING POWDER MIXED DIELECTRIC IN EDM PROCESS**" is an authentic record of my study carried out as requirements for the award of degree of **Master of Engineering** in **Production and Industrial Engineering** at **Thapar University, Patiala,** under the guidance of Dr. Ajay batish, Associate Professor and Mr. Anirban Bhattacharya, Assistant Professor, of Department of Mechanical Engineering, Thapar University, Patiala during July 2009 to June 2010. The matter embodied in this thesis has not been submitted in part or full to any other university or institute for the award of any degree.

Gurpreet Singh

This is to certify that above declaration made by the student concerned is correct to the best of my knowledge & belief.

15/7/2010

(Dr. AJAY BATISH)
Associate Professor,
Thapar University,
Patiala, 147004.

Anirban Bhattacharya

(ANIRBAN BHATTACHARYA)
Assistant Professor,
Thapar University,
Patiala, 147004.

Countersigned by:

(Dr. S.K. MOHAPATRA)
Professor & Head,
Department of Mechanical Engineering,
Thapar University, Patiala, 147004.

29.7.10

(Dr.R.K. SHARMA)
Dean of Academic Affairs,
Thapar University,
Patiala, 147004.

ACKNOWLEDGEMENTS

With deep sense of gratitude I express my sincere thanks to my guides, ***Dr. Ajay Batish*** and ***Mr. Anirban Bhattacharya,*** for their valuable guidance, proper advice and constant encouragement during the my thesis work from the initial level to final level.I also feel very much obliged to ***Dr. S.K. Mohapatra***, Professor & Head, of Mechanical Engineering Department.

I would like also thanks to *Department of Science and Technology (DST)* for providing the equipment and other sources for my thesis work.

I am grateful to the Mr. Baljeet Singh for helping to run smoothly and for assisting me in many different ways.

I am also very thankful to my friends for their cooperation.

I offer my regards to all of those who supported me in any respect during the completion of the work.

Lastly, and most importantly, I wish to thank my parents. They supported me and loved me. To them I dedicate this thesis.

GURPREET SINGH

Registration No. 800882003

ABSTRACT

Electric discharge machining (EDM) is one of most popular machining methods to manufacture dies and press tools because of its capability to produce complicated shapes and machine very hard materials. The present study has been done to study the effect of different input parameters, namely, current, workpiece material, electrode material, dielectric medium, pulse on time, pulse off time and powder and some their interactions on the MRR, TWR, micro hardness and surface roughness. The effect of various input parameters on output responses have been analyzed using Analysis of Variance (ANOVA). Deposition of the powder material either in pure form or in compound form was also studied. XRD and microstructure analysis was completed to understand the form and amount of deposition on the surface of the workpiece material. Main effect plot and interaction plot has been used to determine the optimal design for each output response.

CONTENTS

TITLE	**PAGE NO.**
Declarations	i
Acknowledgements	ii
Abstract	iii
List of Figures	vii
List of Tables	x
Abbrevations	xii
Notations	xiii
Chapter 1 INTODUCTION	**1-14**
1.1 Introduction to Non-Conventional Machining	1
1.2 Electrical Discharge Machining	2
1.3 History of EDM	2
1.4 Working Principle of EDM	3
1.5 EDM Discharge Phenomenon	5
1.6 Sinker EDM	7
1.7 EDM Process Parameters	8
1.8 Organization of Seminar	13

Chapter 2 LITERATURE REVIEW 15-26

2.1 Review of Literature 15

2.2 Categorization of Literature 15

2.2.1 Surface Modification with Powder Mixing 15

2.2.2 Surface Modification with Electrode Material 21

2.3 Summary of the Literature Review 25

2.4 Gap in literature 25

Chapter 3 PILOT EXPERIMENT & DESIGN OF STUDY 27-47

3.1 Pilot Experimentation 27

3.2 Methodology 30

3.3 Procedure of Experimental Design 31

3.4 Establishment of Objective Function 31

3.5 Degree of Freedom 31

3.6 Dummy Treatment 32

3.7 Selection of Factors and Interactions 32

3.8 Orthogonal Array 33

3.9 Experimental Setup 36

3.10 Measuring and Test Equipment used 39

3.10.1 Surface Roughness Tester 39

3.10.2 Micro Hardness Tester 40

3.10.3 X-Ray Diffraction Machine 40

3.10.4 Scanning Electron Microscope 40

3.11 Analysis of Results 41

3.12 Test Results for Workpiece & Electrode Materials 45

CHAPTER 4 RESULTS AND ANALYSIS OF MRR 48-57

4.1 Introduction 48

4.2 Results for MRR 48

4.3 Analysis of Variance- MRR 50

4.4 Results for S/N Ratio- MRR 53

4.5 Optimal Design 55

CHAPTER 5 RESULTS AND ANALYSIS OF TWR 58-66

5.1 Introduction 58

5.2 Results for TWR 58

5.3 Analysis of Variance- TWR 59

5.4 Results for S/N Ratio- TWR 62

5.5 Optimal Design 65

CHAPTER 6 RESULTS AND ANALYSIS OF MICRO HARDNESS 67-83

6.1 Introduction 67

6.2 Results for Micro Hardness 67

6.3 ANOVA-Micro Hardness at Non-Deposited Region 69

6.4 Results for S/N Ratio- Micro Hardness at Non-Deposited Region 71

6.5 Optimal Design 74

6.6 ANOVA-Micro Hardness at Deposited Region 76

6.7 Results for S/N Ratio- Micro Hardness at Deposited Region 79

6.8 Optimal Design 81

CHAPTER 7 RESULTS AND ANALYSIS OF SURFACE ROUGHNESS 84-106

7.1 Introduction 84

7.2 Results for Surface Roughness 84

7.3 ANOVA- Surface Roughness at Center Position 85

7.4 Results for S/N Ratio- Surface Roughness at Center Position 88

7.5 Optimal Design 91

7.6 ANOVA- Surface Roughness at Left Position 93

7.7 Results for S/N Ratio- Surface Roughness at Left Position 95

7.8 Optimal Design 98

7.9 ANOVA- Surface Roughness at Right Position 99

7.10 Results for S/N Ratio- Surface Roughness at Right Position 102

7.11 Optimal Design 104

CHAPTER 8 FURTHER ANALYSIS **107-129**

8.1 Introduction 107

8.2 XRD Analysis 108

8.2.1 XRD Analysis of HCHCr 109

8.2.2 XRD Analysis of EN31 112

8.2.3 XRD Analysis of HDS 115

8.3 Summary of XRD Analysis 119

8.4 Microstructure Analysis 120

8.4.1. Method of Sample Preparation 121

CHAPTER 9 RESULTS, CONCLUSIONS AND RECOMMENDATIONS **130- 134**

9.1 Results 130

9.1.1 Pilot Experiment 130

9.1.2 MRR 130

9.1.2 TWR 131

9.1.3 Micro Hardness 131

9.1.4 Surface Roughness 132

9.1.5 XRD Analysis 132

9.1.6 Microstructure Analysis 133

9.2 Conclusions 133

9.3 Recommendations For Future Work 134

APPENDIX -A 135

APPENDIX -B 136

APPENDIX -C 137

REFERENCES 138-142

LIST OF FIGURES

Figure No.	Title	Page No.
Figure 1.1	Relaxation circuit	3
Figure 1.2	Variation of capacitor voltage with time	4
Figure 1.3	Pulse waveform of controlled pulse generator	5
Figure 1.4	Preparation phase	5
Figure 1.5	Discharge phase	6
Figure 1.6	Interval phase	7
Figure 1.7	Sinker EDM system	8
Figure 1.8	Concept of normal polarity and reverse polarity	8
Figure 3.1	Main effect plot for MRR during pilot experimentation	29
Figure 3.2	Main effect plot for TWR during pilot experimentation	30
Figure 3.3	L27 Linear Graph	35
Figure 3.4	Electrical Discharge Machine	38
Figure 3.5	Schematic diagram of set up	38
Figure 3.6	Dielectric Tank with stirrer attachments	39
Figure 3.7	Workpiece materials before machining	46
Figure 3.8	Workpiece materials after machining	46
Figure 3.9	Electrodes	47
Figure 4.1	Main effect plot for Mean MRR	52

Figure 4.2 Interaction plot for MRR 52

Figure 4.3 Main effect plot for of S/N ratio of MRR 54

Figure 4.4 Interaction plot for S/N ratio of MRR 55

Figure 5.1 Main effect plot for Mean TWR 61

Figure 5.2 Interaction plot for TWR 62

Figure 5.3 Main effect plot for of S/N ratio of TWR 64

Figure 5.4 Interaction plot for S/N ratio of TWR 64

Figure 6.1 Main effect plots for mean micro hardness at non-deposited region 70

Figure 6.2 Interaction plot for micro hardness at non deposited region 71

Figure 6.3 Main effect plot for S/N ratio of micro hardness at non-deposited region 73

Figure 6.4 Interaction plot for S/N ratio of micro hardness at non-deposited region 74

Figure 6.5 Main effect plots for mean micro hardness at deposited region 78

Figure 6.6 Interaction plot for micro hardness at deposited region 78

Figure 6.7 Main effect plot for S/N ratio of micro hardness at deposited region 80

Figure 6.8 Interaction plot for S/N ratio of micro hardness at deposited region 81

Figure 7.1 Main effect plot for mean surface roughness at center position 87

Figure 7.2 Interaction plot surface roughness at center position 88

Figure 7.3 Main effect plot for S/N ratio of surface roughness at center position 90

Figure 7.4 Interaction plot for of S/N ratio of surface roughness center position 90

Figure 7.5 Main effect plot for mean surface roughness at left position 94

Figure 7.6 Interaction plot surface roughness at left position 95

Figure 7.7 Main effect plot for S/N ratio of surface roughness at left position 97

Figure 7.8 Interaction plot for of S/N ratio of surface roughness left position 97

Figure 7.9 Main effect plot for mean surface roughness at right position 101

Figure 7.10 Interaction plot surface roughness at right position 101

Figure 7.11 Main effect plot for S/N ratio of surface roughness at right position 103

Figure 7.12 Interaction plot for of S/N ratio of surface roughness right position 104

Figure 8.1 XRD pattern of HCHCr, W-Cu electrode, powder No 108

Figure 8.2 XRD pattern of HCHCr, W-Cu electrode, tungsten powder 110

Figure 8.3 XRD pattern of HCHCr, graphite electrode, Cu powder 111

Figure 8.4 XRD pattern of EN31, graphite electrode, tungsten powder 113

Figure 8.5 XRD pattern of EN31, graphite electrode, Cu powder 114

Figure 8.6 XRD pattern of EN31, W-Cu electrode, Cu powder 115

Figure 8.7 XRD pattern of HDS, graphite electrode, Cu powder 116

Figure 8.8 XRD pattern of HDS, graphite electrode, tungsten powder 117

Figure 8.9 XRD pattern of HDS, W-Cu electrode, Cu powder 118

Figure 8.10 SEM at 200× of HCHCr, W-Cu electrode, powder no 121

Figure 8.11 SEM at 500× of HCHCr, W-Cu electrode, powder no 122

Figure 8.12 SEM at 1000× of HCHCr, W-Cu electrode, powder no 122

Figure 8.13 SEM at 200× of HCHCr, graphite electrode, Cu powder 123

Figure 8.14 SEM at 500× of HCHCr, graphite electrode, Cu powder 123

Figure 8.15 SEM at 1000× of HCHCr, graphite electrode, Cu powder 124

Figure 8.16 SEM at 200× of EN31, graphite electrode, Cu powder 124

Figure 8.17 SEM at 500× of EN31, graphite electrode, Cu powder 125

Figure 8.18 SEM at 1000× of EN31, graphite electrode, Cu powder 125

Figure 8.19 SEM at 200× of EN31, graphite electrode, tungsten powder 126

Figure 8.20 SEM at 500× of EN31, graphite electrode, tungsten powder 126

Figure 8.21 SEM at 1000× of EN31, graphite electrode, tungsten powder 127

Figure 8.22 Different layer formed on EDM machined surface 128

LIST OF TABLES

Table No.	Description	Page No
Table 3.1	L18 OA along with results for pilot experimentation	27
Table 3.2	ANOVA for MRR	28
Table 3.3	ANOVA for TWR	29
Table 3.4	Factors interested and their levels	32
Table 3.5	Degree of freedom	33
Table 3.6	L27 Experimental design	35
Table 3.7	Constant input parameters	37
Table 3.8	Response Characteristics	42
Table 3.9	Chemical composition of workpiece materials	45
Table 3.10	Chemical composition of electrode materials	45
Table 3.11	Micro hardness of worpiece materials before machining	47
Table 4.1	Results for MRR	48
Table 4.2	ANOVA for MRR	50
Table 4.3	Response table for means of MRR	51
Table 4.4	ANOVA for S/N ratio of MRR	53
Table 4.5	Response table for S/N ratio of MRR	54
Table 4.6	Significant factors and interactions for MRR	56
Table 5.1	Results for TWR	58

Table 5.2 ANOVA for TWR 60

Table 5.3 Response table for means of TWR 61

Table 5.4 ANOVA for S/N of TWR 63

Table 5.5 Response table for S/N ratio of TWR 63

Table 5.6 Significant factors and interactions for TWR 65

Table 6.1 Results for micro hardness at non-deposited and deposited region 67

Table 6.2 ANOVA for micro hardness at non-deposited region 69

Table 6.3 Response table for means of micro hardness at non-deposited region 70

Table 6.4 ANOVA for S/N ratio of micro hardness at non-deposited region 72

Table 6.5 Response table for S/N ratio of micro hardness at non-deposited region 73

Table 6.6 Significant factors and interactions for micro hardness 74

Table 6.7 ANOVA for micro hardness at deposited region 77

Table 6.8 Response table for means of micro hardness at deposited region 77

Table 6.9 ANOVA for S/N ratio of micro hardness at deposited region 79

Table 6.10 Response table for S/N ratio of micro hardness at deposited region 80

Table 6.11 Significant factors & interactions for micro hardness at deposited region 81

Table 7.1 Results for surface roughness at center, left and right position 84

Table 7.2 ANOVA for surface roughness at center position 86

Table 7.3 Response table for means of surface roughness at center position 87

Table 7.4 ANOVA for S/N ratio of surface roughness at center position 89

Table 7.5 Response table for S/N ratio of roughness at center position 89

Table 7.6 Significant factors & interactions for surface roughness center position 91

Table 7.7 ANOVA for surface roughness at left position 93

Table 7.8 Response table for means of surface roughness at left position 94

Table 7.9 ANOVA for S/N ratio of surface roughness at left position 96

Table 7.10 Response table for S/N ratio of surface roughness at left position 96

Table 7.11 Significant factors & interactions for surface roughness at left position 98

Table 7.12 ANOVA for surface roughness at right position 100

Table 7.13 Response table for means of surface roughness at right position 100

Table 7.14 ANOVA for S/N ratio of surface roughness at right position 102

Table 7.15 Response table for S/N ratio of surface roughness at right position 103

Table 7.16 Significant factors interactions for surface roughness right position 105

Table 8.1 XRD pattern list of HCHCr, Electrode W-Cu, Powder No 108

Table 8.2 Changes in chemical composition of HCHCr after machining 109

Table 8.3 XRD pattern list of HCHCr, Electrode W-Cu, Powder W 110

Table 8.4 XRD pattern list of HCHCr, Electrode graphite, Powder Cu 111

Table 8.5 Changes in chemical composition of EN31 after machining 112

Table 8.6 XRD pattern list of EN31, Electrode graphite, Powder W 113

Table 8.7 XRD pattern list of EN31, Electrode graphite, Powder Cu 114

Table 8.8 XRD pattern list of HCHCr, Electrode W-cu, Powder Cu 115

Table 8.9 XRD pattern list of HDS, Electrode graphite, Powder Cu 116

Table 8.10 XRD pattern list of HDS, Electrode graphite, Powder W 117

Table 8.11 XRD pattern list of HDS, Electrode W-Cu, Powder Cu 118

Table 8.12 Summary of XRD Analysis 119

ANOVA	Analysis of Variance
DC	Direct Current
Dof	Degree of Freedom
EDM	Electric Discharge Machining
HCHCr	High-Carbon High-Chromium
HDS	Hot Die Steel
RC	Relaxation Circuit
MRR	Material Removal Rate
TWR	Tool Wear Rate
SR	Surface Roughness
SEM	Scanning Electron Microscope
X-RD	X-Ray diffraction
S/N	Signal to Noise Ratio

OA	Orthogonal Array
A	Worpiece Material
B	Dielectric
C	Electrode Material
D	Pulse off Time
E	Pulse on Time
F	Current
G	Powder
Gr	Graphite Electrode
W-Cu	Tungsten-Copper Electrode
CI	Confidence Interval
SS	Sum of Squares

CHAPTER 1

INTRODUCTION

1.1 INTRODUCTION TO NON-CONVENTIONAL MACHINING

The industries always face problems in manufacturing of components because of several reasons such as the complexity of the job profile or may be due to surface requirements with higher accuracy and surface finish or due to the strength of the materials. It is no longer possible to find tool material which are sufficiently hard and strong to cut materials like stainless steel, titanium and high strength temperature resistant alloys, fiber reinforced composites, satellites, ceramics, and difficult to machine alloys. Production of complex shapes with better surface finish, precise tolerances and higher production rates in such materials by traditional methods is even more difficult. In industries like aerospace, nuclear reactors, turbines etc. to meet such demands, a different class of machining processes have been developed which are termed as non-traditional machining processes or advanced machining processes. Such processes can which can accurately and easily machine the most difficult-to-machine materials to intricate and accurate shapes. Advanced machining processes can be classified into three basic categories, i.e. mechanical, electro-thermal, and electro-chemical machining processes. Some of them can be used only for electrically conductive materials, while others can be used for both electrically conductive and electrically non-conductive materials. In mechanical advanced machining methods, (abrasive jet machining, ultrasonic machining, and water jet machining) kinetic energy of either abrasive particles or water jet is utilized to remove material from the work piece. In electro-thermal methods, (laser beam machining, electron beam machining, and plasma arc machining), the energy is supplied in the form of heat and energy is concentrated onto a small area of work piece resulting in melting, or vaporization and melting both. In electrochemical (electrochemical machining), is a process which is reverse of electroplating. In some of above mentioned above cases, productivity can be increased as compared to conventional methods either by performing the operations faster or by reducing the total number of manufacturing operations. In non-conventional machining methods, there is no direct contact between the tool and the work piece;

hence the tool need not be harder than the workpiece. Further, in spite of the recent technical advancements, the conventional machining processes are inadequate to produce complex geometrical shapes in the hard and temperature resistant alloys and die steels. Keeping these requirements in mind, a number of non-conventional methods have been developed.

1.2 ELECTRIC DISCHARGE MACHINING

Electric discharge machining (EDM) is one of most popular machining methods to manufacture dies and press tools because of its capability to produce complicated shapes and machine very hard materials. This process enables machining of any conducting material, which is electrically conductive. The process removes the metal with sparks generated between electrode tool and the workpiece. The electrode tool made of copper or graphite, gradually makes the cavity that is a mirror image of the shape of the tool. There is no direct contact between the electrode tool and workpiece. The sparks flow through the dielectric fluid at a controlled distance. [1-3]

1.3 HISTORY OF ELECTRIC DISCHARGE MACHINING

In1768, the English scientist, Sir Joseph Priestly first observed the metal erosion by spark discharges. More than hundred years elapsed before some practical use was effected. In 1943, two Russians, B.R. and N.I. Lazarenko, whilst investigating the wear of switch contacts, deduced that spark discharge could be utilized for machining recently developed new metals which were proving to be difficult to shape by established methods. [4] The first British patent was granted to Rudorff in 1950. USA, Japan and Switzerland further developed electric discharge machining around 1950. A machine for spark machining by ‘method x’ was patented in USA in 1952. After the investigations of Lazarenko, the EDM process has attracted worldwide attention as a technique for metal machining and since then considerable research and development has been carried out and an improved form is being used in many current applications. [5]

1.4 WORKING PRINCIPLE OF EDM

The basic principle of the EDM process is the conversion of electrical energy into thermal energy through a series of discrete electrical discharges occurring between the electrode tool and the workpiece immersed in dielectric fluid. The insulating effect of dielectric fluid is important in avoiding electrolysis of electrodes during EDM process. The spark is initiated at the point of

smallest inter-electrode gap by high voltage, overcoming the strength of the dielectric thus breaking down dielectric. Erosion of metal takes place from both electrodes (work piece and tool). After each discharge, the capacitor is recharged from DC source through a resistor, and the spark that follows is transferred to the next narrowest gap (Figure 1.1). The cumulative effect of a succession of sparks spread over the entire workpiece surface leads to erosion, or machining to a shape, which is approximately complementary to that of the tool.

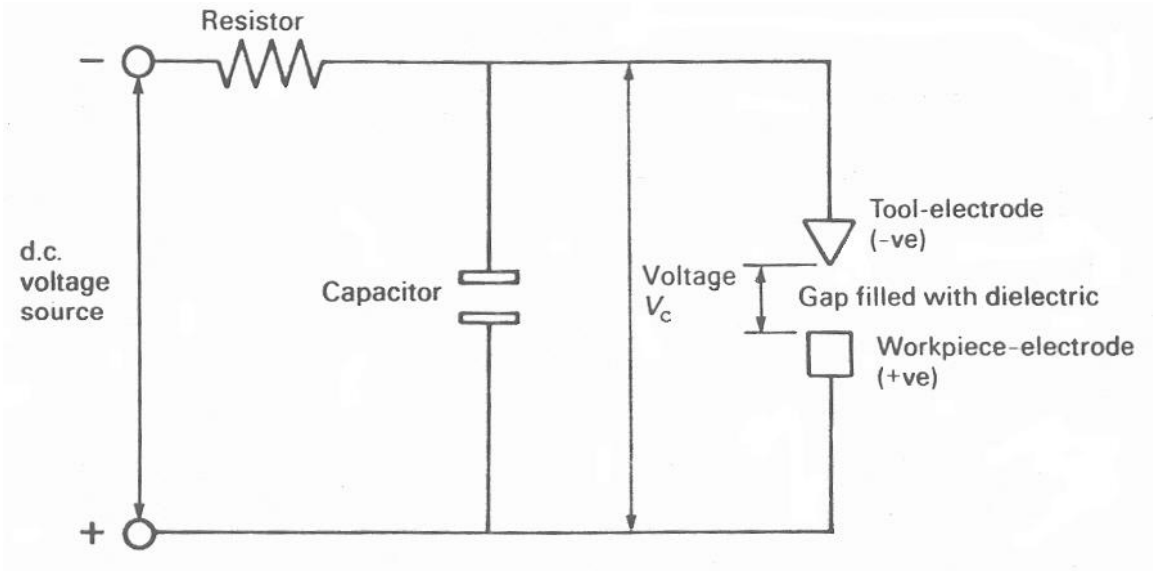

Figure 1.1: Relaxation circuit [4]

The Lazarenko relaxation circuit (RC) does not give good material removal rate (MRR), and higher MRR is possible only by sacrificing surface finish [6]. As indicated in Figure 1.2, the increase in voltage of capacitor should be larger than the breakdown voltage and hence great enough to create a spark between electrode tool and workpiece, at region of least electrical resistance, which usually occurs at the smallest inter electrode gap [4]. A major portion of machining time is spent on charging the capacitor. There is a very high peak value of current at the instant of spark initiation, followed by a rapid rate of decline. The spark temperature resulting from this high current peak is much higher than needed to remove material and results in thermal damage of tool electrode. Reduction in the peak

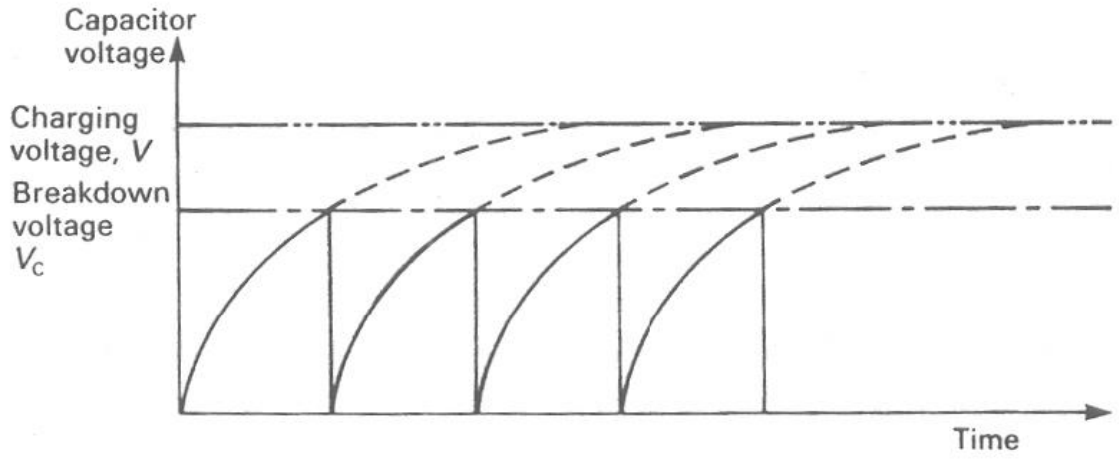

Figure 1.2: Variation of capacitor voltage with time [4]

current and increase in spark duration would result in lower electrode wear and improved machining efficiency [6].

Comparatively less metal is eroded from the tool as compared to the workpiece due to following reasons:

a) The momentum with which positive ions strike the cathode surface is much less than the momentum with which the electron stream impinges on the anode surface.
b) A compressive force is generated on the cathode surface by spark which helps reduce tool wear [2].

This has been achieved with advent controlled pulse generator. Its typical wave forms are shown in Figure 1.3. In this, as comparison to RC circuit there is increase in pulse duration and less peak current value and shortened idle period [6].

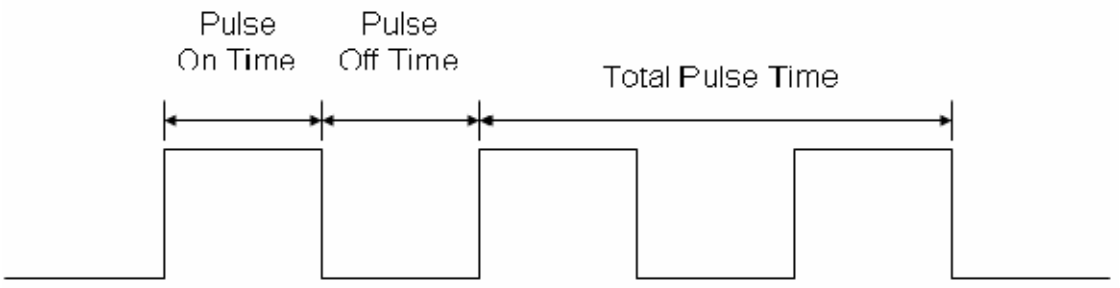

Figure 1.3: Pulse waveform of controlled pulse generator [3]

1.5 EDM DISCHARGE PHENOMENON

The discharge process during EDM is separated into three main phases which are: preparation phase, discharge phase and interval phase.

1.5.1 Preparation phase

When the generator switches voltage on, the electrical field reaches highest strength in the between the electrode. Ignition will not take place in former discharge channel. Spark location is determined by the gap distance and the gap conditions. In the presence of electrically conductive particles in the gap, thin particle bridges are formed. When the strength of the electric field exceeds the dielectric strength of the medium, electric breakdown of the medium takes place. Ionization of the particle bridges takes place and a plasma channel is formed in the gap between the electrodes. A minimum 3A current is needed to start the discharge. The steps in this phase are shown in the Figure 1.4.

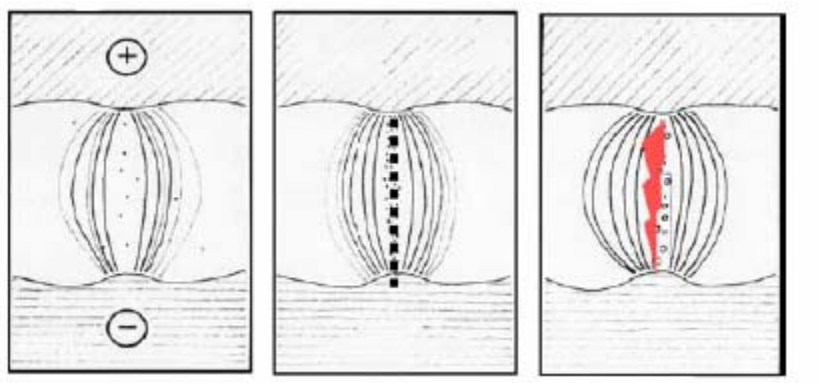

Figure 1.4: Preparation phase [8]

1.5.2 Discharge phase

In the discharge phase, the first plasma channel has to be developed in the shortest time against dielectric and a very high pressure inside the channel creating shock wave distribution within the liquid. The current passing the gap creates the high temperatures causing material evaporation from both electrodes. As the electron-processes show quicker reaction, anode material is worn and this effect causing minimum wear of tool electrode which is more important in surface finishing operations. Current density and temperature decrease quickly with continuous growth

of plasma channel. More energy is distributed to cathode where material at plasma spots become molten. Steps, during the discharge phase, are shown in Figure 1.5.

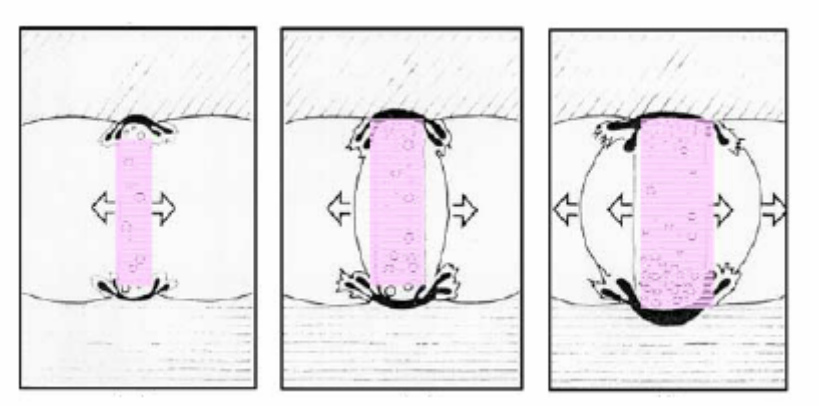

Figure 1.5: Discharge phase [8]

1.5.3 Interval phase

When the discharge is ended by switch off the generator, the plasma channel is de-ionize. The gas bubble collapsed and material is ejected out from the surface of electrodes in the form of vapors. The evaporated material solidifies quickly when it comes in contact with cold dielectric and debris are flushed away from the discharge gap. The debris concentration around earlier discharges creates a conductivity level in the gap, which defines the minimum off-time before a new ignition can be started. This moment is reached after 5-15 micro seconds when the de-ionization level of former plasma channel lowers beyond the average of gap conductivity. Power is switched on again for the next cycle after sufficient de-ionization of dielectric has occurred. The steps in this phase are shown in Figure 1.6 [8].

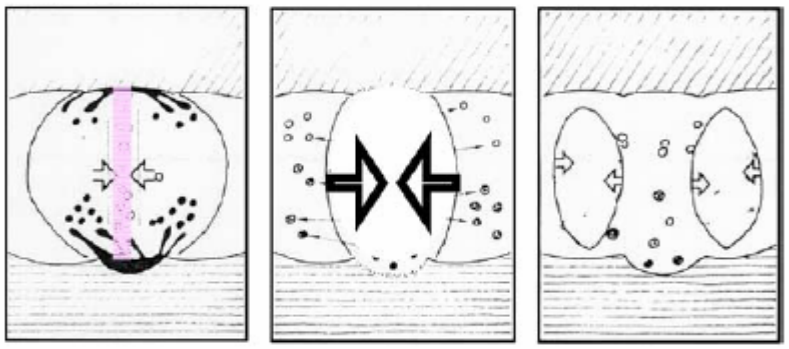

Figure 1.6: Interval phase [8]

1.6 SINKER EDM

Sinker EDM is also known as the cavity EDM or volume EDM. Sinker EDM consists of an electrode tool and workpiece, both are electrically conductive and submerged in the dielectric fluid like kerosene oil or EDM oil. The electrode tool and workpiece are connected with power supply and power supply generates an electrical potential between two parts. As the electrode tool approaches the workpiece, dielectric breakdown occurs in the fluid forming ionization channel, and a small sparks jumps. The resulting heat and cavitation vaporize the base material and electrode. These sparks strike one at a time in huge numbers at seemingly random locations between the electrode tool and the workpiece. As the base metal is eroded, and the spark gap increased, thus electrode has to be lowered automatically by the machine so that the process can continue uninterrupted. When, gap between tool and workpiece increases, flushing takes place to remove the eroded metal. Several hundred thousand sparks occur per second in this process, with the actual duty cycle being carefully controlled by the setup parameters. These controlling cycles are sometimes known as "on time" and "off time". The on time setting determines the length or duration of the spark. Hence, a longer on time produces a deeper cavity for that spark and all subsequent sparks for that cycle creating a rougher finish on the workpiece. The reverse is true for a shorter on time. Off time is the period of time that one spark is replaced by another. A longer off time for example, allows the flushing of dielectric fluid through a nozzle to clean out the eroded debris, thereby avoiding a short circuit. Sinker EDM system is shown in the Figure 1.7.

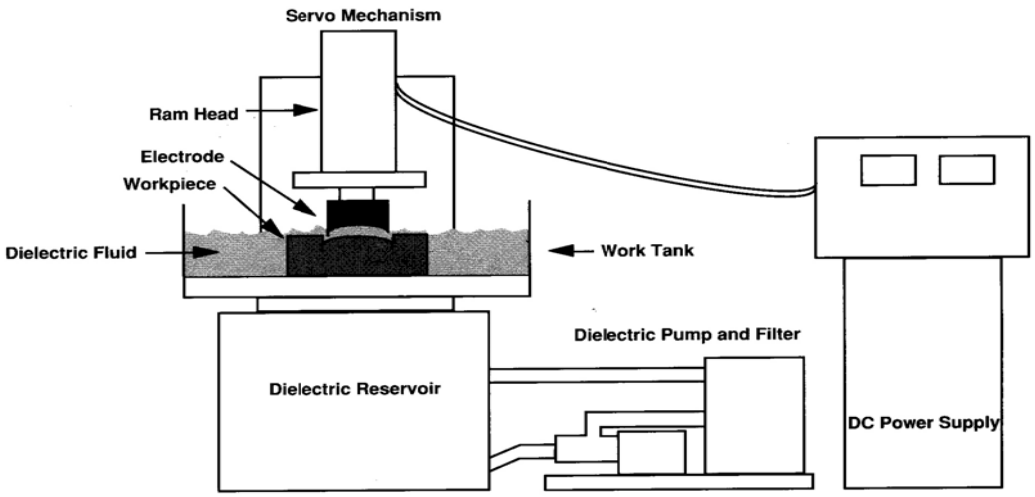

Figure 1.7: Sinker EDM system [7]

1.7 EDM PROCESS PARAMETERS

1.7.1 Polarity

Polarity, in EDM process determines the direction of current flow relative to electrode. Polarity of electrode can be either positive or negative depending on applications.

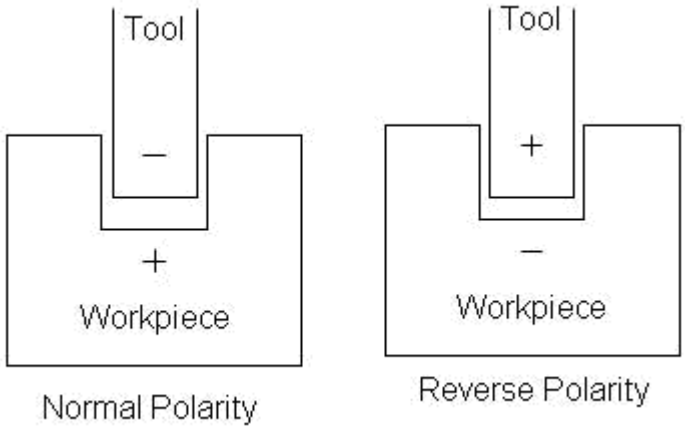

Figure 1.8: Concept of normal polarity and reverse polarity

In normal polarity workpiece is positive and tool electrode is negative. In negative polarity workpiece is negative and tool is positive (Figure 1.8). With the discharge taking place between workpiece and tool, electriferous particles and electrons from the cathode in the dielectric arouse the ionization which produced ionized channel. The particles with positive charge bombard the cathode while electrons bombard the anode in ionized channel. In this process, electrons, which are smaller and lighter, thus accelerate faster and reach higher speed, whereas the particles with positive charge accelerate more slowly and do not reach high speeds. As a result, electrons transfer more energy to anode than positive charged particles to transfer to the cathode. This difference leads to material removal in anode that is greater than material removal in the cathode. Polarity is determined by tool material, work material, current density and pulse length.

1.7.2 Pulse on time

Pulse on time is the time period during which machining is takes place. Material removal rate (MRR) is directly proportional to amount of energy applied during pulse on time. When the

pulses with small on time are used, material removal by electron bombardment is predominant due to higher response rate of less massive electrons. However, when the longer pulses are used, energy sharing by positive ions is predominant and material removal rate decreases. When the electrode polarities are reversed, longer pulses are found to produce higher MRR.

1.7.3 Pulse off time

Pulse off time is the time during which re-ionization of dielectric takes place. More pulse off time means greater machining time. A non-zero pulse off time is a necessary requirement for EDM operation. Discharge between the electrodes leads to ionization of the spark gap. Before another spark can take place, the medium must de-ionize and regain its dielectric strength. This takes some finite time and power must be switched off during this time. Too low values of pulse off time may lead to short-circuits and arcing. A large value on other hand increases the overall machining time since no machining can take place during the off-time. The surface roughness is found to depend strongly on the spark frequency. When high frequency sparks are used lower values of roughness average (R_a) are observed, because the energy available in given amount of time is shared by large number of sparks leading to shallower discharge craters. Each cycle has an on-time and off-time that is expressed in units of microseconds. Concept of pulse on-time and pulse off-time is shown in Figure 1.3.

1.7.4 Discharge current

The discharge current (I_d) is a measure of the power supplied to the discharge gap. A higher current leads to a higher pulse energy and formation of deeper discharge craters. This increases the material removal rate (MRR) and the surface roughness (R_a) value. Similar effect on MRR and R_a is produced when the gap voltage (V_g) is increased. Once the current starts to flow, voltage drops and stabilizes at the working gap level. The preset voltage determines the width of the spark gap between the leading edge of the electrode tool and workpiece. Higher voltage settings increase the gap, which improves the flushing conditions and helps to stabilize the cut.

1.7.5 Peak current

It is most important parameter in EDM process and it is amount of power used in discharge machining. Peak current is measured in units of amperage. During each pulse on-time, the

current increases until it reaches a preset level, which is expressed as the peak current. An increase in current, results in increased MRR as well as increased surface roughness (SR) and tool wear rate (TWR). In die-sinking and wire EDM applications, the maximum amount of amperage is governed by the surface of the cut.

1.7.6 Pulse wave form

Different wave forms are supplied by different generators. In case of rotating impulse generators the rectified sinusoidal voltage wave form is given across the spark gap to produce the spark. Due to the inductive circuitry there is a spark oscillation even after the pulse is withdrawn give rise to extremely high tool wear and arcing become frequent if the second pulse comes before complete dampening of the oscillation. In relaxation generator, the spark oscillation is reduced. TWR will be less and charging time is equal to ignition delay, so the ionization process is slower and depends on charging time. Pulse wave form, generated by the square pulse generators, is much more defined and easily controllable. Using a generator, which can produce trapezoidal pulses, one can reduce relative tool wear to very low values.

1.7.7 Types of dielectric fluid

Selection of dielectric medium is an important consideration for EDM performance. Mineral oils are commonly used as the dielectric medium for die-sinking EDM operations. Mineral oils are exhibit high dielectric strength and a low viscosity is preferred because of their better performance. For safety reasons, oils with a high flash point are normally used. Kerosene is one such oil which is used commonly for EDM process. Water based dielectric are used almost extensively for wire EDM operations. Water has a high specific heat capacity which leads to better cooling effect required for wire cut operations. To prevent chemical reactions, deionized water is used in such applications. In comparison to mineral oils and water, air has the lowest dielectric strength, viscosity, thermal capacity. A low viscosity air medium favors higher cutting accuracy and better surface finish. Low dielectric constant suggests a lower MRR with air medium. Low thermal capacity and thermal conductivity suggests higher thermal damage of workpiece. For a complete analysis of thermal damage an opposing effect caused by the expansion of plasma channel due to low viscosity must also be accounted. Air is the better

dielectric for surface finish and accuracy at the expanse of the MRR. In EDM process, dielectric fluid has following requirements:

1. Provide effective cooling during operation.
2. Breakdown electrically in the shortest possible time once the breakdown voltage has been reached.
3. Good degree of fluidity.
4. Remain electrically non-conducting until the required breakdown voltage has been reached.
5. Deionize the gap immediately after the spark has occurred.

1.7.8 Types of flushing

Flushing is the proper circulation of the dielectric fluid between electrode tool and workpiece during operation. During the machining operation debris are produced in the gap and reduces the dielectric strength. If the amount of debris in the gap becomes too many, the particles can form an electrically conducting path between the electrodes, causing unwanted discharge which becomes arcs, with consequential damage to both tool and workpiece. To obtain highest machining efficiency, proper flushing is necessary. When deep and complex shapes have to be produced, flushing plays a significant part in EDM. Filtration of dielectric fluid before re-circulation is highly essential. In EDM, flushing can be achieved by the following method:

1.7.8.1 Suction flushing

In this, dielectric is sucked through either the workpiece or the tool. This technique is employed to avoid any tapering effect due to sparking between machining debris and the side walls of the electrodes. Suction flushing through the tool rather than through the workpiece is more effective.

1.7.8.2 Injection flushing

In this technique, dielectric is fed through either the workpiece or the tool which are pre-drilled to accommodate the flow. With the injection method, tapering of components arises due to the lateral discharge action occurring as a result of particles being flushed up the sides of electrodes.

1.7.8.3 Side flushing

When the flushing holes cannot be drilled either in the workpiece or the tool, side flushing is employed. If there is need of flushing of entire working area, special precautions have to taken for the pumping of dielectric.

1.7.8.4 Flushing by dielectric pumping

This method has been found particularly suitable in deep hole drilling. Flushing is obtained by using the electrode pulsation movement. When the electrode is raised, clean dielectric is sucked into mixed with contaminated fluid, and as the electrode is lowered the particles are flushed out [4,6].

1.7.9 The electrode tool

The shape of electrode tool will be basically same as that of the product is desired. Metals with a high melting-point and good electrically conductivity are usually chosen as tool materials for EDM. They should be cheap and readily shaped by conventional methods. The electrode materials are classified as metallic material (copper, brass, tungsten, aluminum), non-metallic material (graphite), combined metallic and non-metallic (copper-graphite), and metallic coating as insulators (copper on moulded plastic, copper on ceramic) etc. High density graphite is used in pulsed EDM equipment, although the material does not perform satisfactorily in RC EDM work. It gives low wear due to its high melting temperature. Copper has the qualities for high stock metal removal. It is a stable material under sparking conditions. Brass as a tool material has high wear. Copper-boron and silver tungsten both exhibit extremely low wear. Sometimes copper tungsten is employed as the cathode metal. Its use yields high machining rates and very low wear. Due to its high cost and not so readily shaped, its applications are limited.

1.7.10 Electrode gap

Electro-mechanical and electro-hydraulic systems are used to respond to average gap voltage. During operation, the feed control must maintain a movement of electrode towards the workpiece at such speed that working gap, the sparking voltage remains unaltered. Rapid response of the mechanism is essential and this implies a low inertia drive and it is essential to

have rapid reversing speed with no backlash. Typically values of gap size range between 0.005 to 0.05 mm.

1.8 ORGANIZATION OF THESIS

The thesis has been organized in nine chapters. Brief description of the contents of each chapter is given below:

Chapter 1 highlights the brief introduction with non-conventional machining processes. Working principle and various discharge phases (preparation phase, discharge phase and interval phase) in EDM process has been discussed. Different EDM process parameters have been discussed in the brief, which can effects the performance of EDM process.

Chapter 2 presents an available literature of EDM process for surface modification. The available literature has been categorized in two broad classifications such as surface modification with powder mixing fluid and surface modification with electrode materials. Summary of the literature and gap in literature also discussed.

Chapter 3 presents the area of research work to be undertaken has been identified. Objective and work plan also discussed. Methodology to be adopted also described in brief.

Chapter 4 presents the analysis and results of the MRR. Results after the Analysis of Variance (ANOVA) and Taguchi Signal-to-Noise ratio are outlined in this chapter. Main effect plot and interaction plots for MRR are discussed in this chapter. Optimal design conditions have been discussed.

Chapter 5 presents the analysis and results of the TWR. Results after the Analysis of Variance (ANOVA) and Taguchi Signal-to-Noise ratio are outlined in this chapter. Main effect plot and interaction plots for TWR are discussed in this chapter. Optimal design conditions have been discussed.

Chapter 6 presents the analysis and results of the micro hardness at non-deposited and deposited region. Results after the Analysis of Variance (ANOVA) and Taguchi Signal-to-Noise ratio are outlined in this chapter. Main effect plot and interaction plots for non-deposited and deposited region are discussed in this chapter. Optimal design conditions have been discussed.

Chapter 7 presents the analysis and results of the surface roughness (R_a). Results after the Analysis of Variance (ANOVA) and Taguchi Signal-to-Noise ratio are outlined in this chapter. Main effect plot and interaction plots for surface roughness (R_a) are discussed in this chapter. Optimal design conditions have been discussed.

Chapter 8 presents the analysis of surface properties. XRD and microstructure analysis has been completed to understand the form and amount of deposition on the surface of the workpiece material.

Chapter 9 presents the results, conclusions and recommendations from the experimental work.

CHAPTER 2

LITERATURE REVIEW

2.1 REVIEW OF LITERATURE

Electrical discharge machining has been widely used for manufacturing various components such as moulds, dies and complex shapes on the hard materials with higher surface finish. A lot of work has been carried out on the different aspects of EDM such material removal rate, tool wear rate, surface modification with or without mixing of powder particles in the dielectric fluid. This chapter presents review of available literature on the aspects of surface modification.

2.2 CATEGORIZATION OF LITERATURE

The available literature has been divided into following categories:

1. Surface Modification with Powder Mixing.
2. Surface Modification with Electrode Material.

2.2.1 Surface Modification with Powder Mixing

Kansal et al. [9] investigated the effect of silicon powder mixing into the dielectric fluid of EDM on machining characteristics of AISI D2 die steel. Six parameters, peak current, pulse on-time, pulse off-time, concentration of powder, gain and nozzle flushing have been considered. The process performance is measured in the terms of machining rate. In the presence of suspended silicon powder in a kerosene dielectric of EDM, identify the important parameters and their effect on machining rate of AISI D2. All the selected parameter, except nozzle flushing has a significant effect on the mean and variation in machining rate (S/N ratio). Optimization to maximize to machining rate has been undertaken using the Taguchi method. The ANOVA analysis indicated that the percentage contribution of peak current and powder concentration toward machining rate is maximum among all the parameters. They showed that the setting of peak current at a high level (16 A), pulse on-time at medium level (100μs), pulse off-time at low level (15μs), powder concentration at high level (4 g/l), gain at a low level (0.83

mm/s) produced optimum machining rate from AISI D2 surface when the machined by silicon powder mixed.

Uno et al. [10] proposed a surface modification technique to obtain high surface wear resistance using EDM with powder mixed fluid. First, a coating application of nickel layer on aluminum bronze for plastic molds and shell molds and then formation of a hard titanium carbide layer on alloy steel is carried out by using carbon powder mixed fluid with titanium electrodes. They investigated that EDMed surface with nickel powder mixed fluid has smaller surface roughness than that in EDM with kerosene type fluid. The resolidified layer can nickel can be generated on EDMed surface and the thickness of the layer becomes larger and more uniform with increase of nickel powder concentration in the machining fluid. By mixing the carbon with dielectric kerosene, thick hard layer with small surface roughness values can be obtained. The hardness of the layer containing TiC is much higher than that of base material which leads to higher surface wear resistance.

Pecas and Henriques [11] suggested that powder particles to the EDM dielectric fluid modifies some process variables and creates the conditions to achieve a higher surface quality in large machined area. They studied the improvement in the polishing performance of conventional EDM when used with powder mixed dielectric. The analysis was carried out varying the silicon powder concentration and flushing flow rate over a set of different processing areas and the effects in the final surface is evaluated. The evaluation was done surface morphologic analysis and measured through some quality surface indicators. The result showed the positive influence of silicon powder in the reduction of crater dimensions, white layer thickness and surface roughness. It was demonstrated that an accurate control of powder concentration and flushing flow is a requirement for achieving an improvement in the process polishing capability.

Simao et al. [12] reviewed the published on the deliberate alloying of various workpiece materials using EDM. Experiments carried out by powder metallurgy tool electrodes and the use of powders suspended in the dielectric fluid, typically aluminum, nickel, titanium etc. Results have been presented on the surface alloying of AISIH 13 hot work tool steel during a die sink operation using partially sintered WC/Co electrodes operating hydrocarbon oil dielectric. An L_8 fractional factorial Taguchi experiment was used to identify the effect of key operating factors on the output measures viz., electrode wear, workpiece surface hardness, etc. With respect to

microhardness, the percentage contribution ratio for peak current, electrode polarity and pulse on-time were approximately 24, 20 and 19% respectively. Typically changes in surface metallurgy were measured upto a depth of about 30μm (with a higher than normal voltage of 270V) and an increase in the surface hardness of the recast layer varying from 620 HK 0.025 to1350 HK 0.025approximately.

Furutani et al. [13] attempted to make thick titanium carbide (TiC) or WC layer and investigated a surface modification method by EDM with a green impact electrode. Titanium alloy powder or tungsten powder was supplied from the green compact electrode and it adhered on a workpiece by the heat caused by the discharge. They proposed a surface modification method by EDM with powder suspended in working fluid in order to avoid the production process of green compact electrode. According to the investigators, the use of thin electrode and a rotating disk electrode were expected to keep the powder concentration high in the gap between an electrode and workpiece and to accrete powder material on workpiece. Titanium powder is suspended kerosene working oil. TiC layer developed a thickness of 150 μm with hardness of 1600 HV on carbon steel with electrode of 1mm in diameter. When a disk placed near a plate rotates in viscous fluid, the disk dragged into the gap between disk and the plate. Powder concentration in the gap between a workpiece and a rotational disk electrode could be kept high. A wider area of the accretion could be obtained by using the rotational electrode with gear shape.

Wong et al. [14] proposed a near mirror finish phenomena in electrical discharge machining when powder is introduced into dielectric fluid as a suspension at the tool-workpiece or inter-electrode gap during machining. The dielectric flushing system of conventional die sinking EDM machine was specially modified to inject and distribute the powder into the dielectric fluid, especially at the gap between the tool and the workpiece. Machining was performed on various types of steel with different types of powder suspension at a peak current of around 1A. Particular combination of powder mixed dielectric and workpiece have been found to produce mirror surface or glossy machined surface. Close scrutiny of mirror finish surface reveals shallow overlapping resoldified discs with smooth rims, unlike typically EDMed surfaces, which are typically covered with deep craters, pock marks and globules. The various factors affecting the generation of mirror like surfaces were studied. The appropriate settings of

electrode polarity and pulse parameters and correct combination of workpiece material and powder characteristics have a significant influence on the mirror finish condition. The use of negative electrode polarity (i.e. with tool as negative electrode, which condition is normally used for finishing EDM) is necessary to achieve the mirror finish condition. Other features of powder mixed dielectric EDM shorter machining time, more uniform dispersion of electrical discharge, and stable machining. Based on the results of the experimental investigation, types of material composition, powder properties and machine setting in bringing the near mirror condition were discussed.

Wu et al. [15] investigated the effect of surfactant and Al powder added in the dielectric on the surface status of workpiece after EDM. It was found that the best distribution effect was produced when the concentration of Al powder and surfactant in the dielectric were 0.1 and 0.25 g/l, respectively. An optimal surface roughness (R_a) value of 0.172 μm was achieved under positive polarity, discharge current 0.3A, pulse duration time 1.5 μs, open circuit potential 140V, gap voltage 90V, and surfactant concentration 0.25 g/l. the surface roughness of workpiece is improved upto 60% as compared to that EDMed under pure dielectric with high surface roughness (R_a) 0.434 μm.

Pecas and Henriques [16] studied the performance improvement of conventional EDM when used with powder mixed dielectric fluid. A silicon powder was used and the improvement is assessed through quality surface indicators and process time measurement, over a set of different processing areas. The result showed the positive influence of the silicon powder in the reduction of the operating time, required to achieve a specific surface quality, and in the decrease of the surface roughness, allowing the generation of mirror like surfaces.

Jeswani [17] used graphite powder in kerosene dielectric fluid. Experimental results revealed that the addition of about 4g of fine graphite powder (10μm in average size) per litre of kerosene increases the metal removal rate (MRR) by 60% and tool wear rate (TWR) by 15% in electrical discharge machining. The wear ratio TWR/MRR is reduced by about 28%. This effect may be attributed to the reduction in the breakdown voltage of kerosene dielectric caused by the addition of the graphite powder. A scheme of in-process of graphite contamination, based on measuring the clarity of the kerosene with a photodiode, is proposed.

Furutani and Shimizu [18] investigated the deposition process of lubricant surface by EDM with Molybdenum disulfide (MoS_2) powder suspended in working oil. They also studied the influence of some machining condition through the friction test. It was found that Molybdenum disulfide could be deposited on the metals which melting point lowers than MoS_2. The expansion of the gap length caused the improvement of the roughness.

Prihandana et al. [19] proposed a new method that consists of suspending micro-MoS_2 powder in dielectric fluid and using ultrasonic vibration during micro-electrical discharge machining (μ-EDM) processes. The Taguchi method is adopted to ascertain the optimal process parameters to increase the material removal rate of dielectric fluid containing micro-powder in μ-EDM using a L_{18} orthogonal array. Pareto analysis of variance is employed to analyze the four machining process parameters: ultrasonic vibration of dielectric fluid, concentration of micro powder, tool electrode material and workpiece materials. They showed that the introduction of MoS_2 micro-powder in dielectric fluid and using ultrasonic vibration significantly increase the material removal rate and improves the surface quality by providing a flat surface free from black carbon spots.

Zhao et al. [20] performed experimental research on machining efficiency and surface roughness of powder mixed EDM (PMEDM) in rough machining. They showed that PMEDM machining can clearly improve the machining efficiency at the same time surface roughness by selecting proper discharging parameters.

Ming and Liu [21] studied the effects of additives in kerosene used as dielectric fluid for EDM. They showed that additives can increase the MRR and decrease the TWR and improve the surface quality of work, especially in mid-finish machining and finish machining.

Kozak et al. [22] reported investigation of electrical discharge machining using powder suspended working fluid instead of pure dielectric. The EDM characteristics obtained using hydrocarbon dielectric and mixtures of deionized water with abrasive powder have been compared. The relationships between surface roughness parameters, material removal rate and operating parameters of EDM have determined for different kinds of powder and concentration in kerosene/water.

Kansal et al. [23] optimized the process parameters of powder mixed electrical discharge machining. Response surface methodology has been used to plan and analyze the experiments. Pulse on-time, duty cycle, peak current and concentration of silicon powder added into dielectric fluid of EDM were chosen as variables to study the process performance in terms of material removal rate and surface roughness. The silicon powder effect both material removal rate and surface roughness. MRR increases with the increase in the concentration of silicon powder. Peak current and powder concentration are the most influential parameters on MRR and SR.

Tzeng and Chen [24] conducted experiment on SKD-11 steel with aluminum, chromium, copper and silicon carbide powder. They found that aluminum powder gave the best surface finish followed by chromium; whereas copper powder generated worst surface characteristics. Particle size, concentration as well as its properties such thermal conductivity, density and electrical resistivity affected performance.

Chow et al. [25] used kerosene, kerosene with aluminum powder, kerosene with silicon carbide powder in EDM as a dielectric fluid. The addition of both aluminum and silicon carbide powder to the kerosene permit an extension of the gap between electrode and workpiece. The extended gap increases the debris removal rate and material removal depth. Several discharging trajectories formed within a single input impulse and several discharging spots created within a discharging impulse. The effects due to discrete discharging pulse were, minimizing of machined debris, increases the material removal depth and surface roughness.

Chen and Lin [26] proposed a combined process that integrates the electrical discharge machining and ultrasonic machining to investigate the machining performance and surface modification on Al-Zn-Mg alloy. Titanium carbide particles added in dielectric fluid. The elemental distribution of titanium and carbon on the cross-section were quantitatively determined using an electron probe micro-analyzer. They showed that combined process improve the hardness and wear resistance of the machined surface.

2.2.2 Surface Modification with Electrode Materials

Tsai et al. [27] proposed a new method of blending the copper powders contained resin with chromium powders to form tool electrodes. Such electrodes made at low pressure (20Mpa) and

temperature (200ºC) in ho mounting machine. They showed that using such electrodes facilitated the formation of modified surface layer on the workpiece with corrosion resistant properties. The optimal mixing ratio and proper machining parameters (polarity, peak current, and pulse duration) were used to investigate the effect of material removal rate, electrode wear rate, surface roughness and thickness of recast layer on the usability of these electrodes. Composite electrodes obtained higher MRR than copper electrodes; the recast layer was thinner and fewer cracks were present on the machined surface. Chromium elements in the composite electrode migrated to workpiece, resulting in good corrosion resistance of the machined surface.

Mohri et al. [28] proposed a new method of surface modification by EDM using composite electrodes on workpieces of carbon steel or aluminum were carried out in hydrocarbon oil. Copper, aluminum, tungsten carbide and titanium were used for the materials of electrodes, it was revealed that there existed the electrode material in the work surface layer and the characteristics of the surface of material are changed. Surfaces have lesser cracks, high corrosion resistance and wear resistance.

Koshy et al. [29] used a rotating disk electrode which is more productive and accurate technique than use conventional electrode. Material removal rate, tool wear rate, relative electrode wear, corner reproduction accuracy and surface finish aspects of rotary electrode were compared with those of a stationary one. The effective flushing of the working gap improves material removal rate and machines surface with better finish. Despite the prevalent high tool wear rate, the reproduction accuracy is least affected as the wear gets uniformly distributed over the entire circumference of the disk. Machining of the sharp corner is possible even with aluminum electrode, whose relative electrode wear is greater than unity.

Singh et al. [30] investigated the effects of machining parameters such as pulsed current on the material removal rate, diameteral overcut, electrode wear, and surface roughness in the electric discharge machining of EN-31 tool steel hardened and tempered to 55 HRc. The work material machined with copper, copper tungsten, brass and aluminum electrodes by varying the pulsed current at reverse polarity. They showed that the output parameters of EDM increase with increase in pulsed current and beat machining rate were achieved with copper and aluminum electrodes.

Khanra et al. [31] developed a metal matrix composite (ZrB_2-Cu) to get an optimum combination of wear resistance, electrical and thermal conductivity. The ZrB_2-Cu composite have been developed by adding different amounts of Cu and tested as a tool material at different process parameters of EDM during machining of mild steel. The ZrB_2-40 wt% Cu composite showed more material removal rate with less tool wear rate than commonly used Cu tool. But the diameteral overcut and average surface roughness found to be lesser in the case Cu tool than composite tool. The tools and workpiece surfaces were analyzed by scanning electron microscope (SEM)/EDS and X-RD technique.

Erden and Bilgin [32] observed that there is practically no change in machining rate during machining of mild steel with copper electrode when the dielectric is artificially contaminated with metallic powder. But when the brass electrode was used, there was a significant increase in machining rate. This is due to short time lag in case of copper electrodes and long time lags in case of brass electrodes. The impurities decrease the time lag and some of open circuit pulses replaced by erosive electrical discharge.

Curodeau et al. [33] used an electrically conductive polymer electrode made of styrene-carbonaceous composite. Water was used as dielectric medium in the projected EDM processes, a preliminary evaluation of water as dielectric medium, in conjunction with graphite electrode, was performed. Tool steel workpiece with a macro-level 0.35 mm Peak-Valley milled surface roughness is smoothed down to a 0.25 mm Peak-Valley in a single EDM iteration step in deionised water.

Marafona and Wykes [34] used 75/25 tungsten copper electrode and D2 tool steel workpieces. They optimized the parameters such MRR, TWR and surface roughness. It was found that a black layer of carbon was deposited on the tool when low current intensity and long pulse duration was used. This layer inhibits further tool wear and a higher current intensity can then be used to improve the MRR without increase the TWR. SEM showed that a layer was formed on the surface of tool with high carbon content as well as D2 steel elements such as iron and chromium. Energy dispersive X-ray analysis was used to measure the composition of tool.

Muttamara et al. [35] used a graphite electrode for machining of alumina. They showed that, machining with graphite electrode gave a significantly higher MRR and low electrode wear than copper electrode. The value of MRR was found to increase by 60% with positive electrode wear. No element of copper was observed on the conductive layer when investigated with energy dispersive spectroscopy. Surface roughness was improved by 12% with positive polarity.

Haron et al. [36] investigated the machining characteristics when machining XW42 tool steel at two current setting (3A and 6A), three diameter sizes (10, 15, and 20mm) of copper and graphite electrodes with kerosene as dielectric. They showed that material removal rate is higher and the relative electrode wear ratio is lower with copper electrode than graphite electrode. The increase in current and electrode diameter reduced tool wear rate as well as material removal rate. Combination of both electrodes will improve surface finish.

Mohan et al. [37] analyzed the effects of EDM parameters (polarity, current, electrode material, pulse duration, rotation of electrode on MRR TWR and surface roughness) in machining of Al-SiC metal matrix composite with 20 and 25 volume% Sic. Electrode material, polarity of electrode and volume percentage of SiC, the MRR increased with increase in the discharge current and for a specific current it decreased with increase in pulse duration. Increase in the volume percentage of SiC had an inverse effect on MRR and Positive effect on TWR and surface finish. Increasing the speed of rotating electrode resulted in a positive effect with MRR, TWR and better surface roughness than at stationary.

Mohri et al. [38] used 0.1 mm diameters wires of tungsten, copper and brass as electrode on AISI-1049 steel workpiece material to observe the effects of electrode materials on material accretion process using EDM. Under the same machining conditions, tungsten was the deposited on the workpiece, while the workpiece drilled with copper and brass electrode.

Li et al. [39] investigated the effects of titanium carbide (TiC) in sintered copper-tungsten (Cu-W) electrodes. Six batches of specimens with TiC content varying from 5 to 40% were fabricated by mixing, ball milling, pressing and liquid phase sintering. A uniform dispersion of fine particles of TiC in Cu-W system and a narrower particle size distribution provide possibility for obtaining the dense electrodes. The relative density first increased then decreased

with increasing TiC while the electrical resistivity correspondingly first decreased then increased. The surface roughness decreased with increase of relative density and vice-versa. The highest relative density, lowest electrical resistivity, and best EDM could be obtained by 15% TiC addition, i.e. the lowest TWR, highest MRR and best surface finish.

Roethel and Garbajs [40] observed that the properties of machined surfaces depended on the properties of alloys which were formed in the surface layers due to diffusion of the tool electrode material and breakdown of the dielectric. By microprobe analysis, it was possible to study the phase changes of the material in the surface layers. The working conditions in the gap played a highly significant role in deciding the chemical structure and he properties of method and consequently solidify layer.

Jeswani and Basu [41] carried out electron microprobe analysis for surface deposition and diffusion of tool material on mild steel, high carbon steel and high speed steel with copper and brass tool electrodes using kerosene and distilled water as dielectric medium. They observed that high energy machining results in lower surface deposition but more depth of diffusion. High speed steel had best deposition followed by the high carbon steel and mild steel showed the least deposition. Machining in distilled water high pulse energy resulted in lower surface deposition and depth of diffusion as compared to machining in kerosene. Pulse energy was found to be the most important factor aiding surface deposition as compared to tool material, work material and dielectric.

2.3 SUMMARY OF THE LITERATURE REVIEW

A lot of work has been done in surface modification with electrical discharge machining. Surface modification has been done either with electrode material or with powder mixing in the dielectric medium. From the literature survey, it is observed that the field of surface modification using EDM process is still at the experimental stage. Many researchers [9], [11], [16], [23], [25] used silicon metal powder in the kerosene dielectric fluid and investigated the various effects on the machining parameters such as surface roughness, tool wear rate, material removal rate. Some [10], [12], [15], [24] studied effects on material removal rate and surface roughness value with adding aluminum powder in the kerosene dielectric fluid. Effects of MoS2

powders [18], [19] also carried out. Graphite powder [17] reduced the wear ratio TWR/ MRR about 28%. Material removal rate is increased by 60%.

Surface modification by electrode materials also carried out. Many researchers [28], [30], [32], [34], [36], [38], [41] used copper electrode for machining of different materials and observed that a layer of electrode material has taken place on the surface of workpiece material which improve the surface properties. Some of researchers [29], [37] showed that aluminum electrode has positive effect on tool wear rate and surface finish. Graphite electrode [35], [36] reduce tool wear rate and increase the material removal rate than copper electrode. Tungsten copper electrode [34] improves the MRR without increase the TWR.

2.4 PROBLEM FORMULATION

The field of surface modification using EDM process is still in at the experimental stage. A number of research studies have been carried out and feasibility of the process is well established. From the literature review, it is observed that no research work has been carried out on surface modification using tungsten powder in EDM oil dielectric fluid. Analysis of material transfer from tungsten and copper electrode and material transfer from powder suspend in dielectric medium is missing. No work has been reported on effects of copper powder on high carbon high chromium, hot die steel, EN31 with graphite and tungsten-copper electrode in kerosene oil and EDM oil. So in the thesis work it is proposed to study the effect of different input parameters, namely, current, workpiece material, electrode material, dielectric medium, pulse on time, pulse off time and powder and some their interactions on the MRR, TWR, micro hardness and surface roughness. The effect of various input parameters on output responses have been analyzed using Analysis of Variance (ANOVA). Deposition of the powder material either in pure form or in compound form was also proposed to studied. XRD and microstructure analysis was to understand the form and amount of deposition on the surface of the workpiece material.

CHAPTER 3

PILOT EXPERIMENT &DESIGN OF STUDY

3.1 PILOT EXPERIMENTATION

The effect of various input parameters i.e. pulse on time, pulse off time, current, electrode, workpiece material and powder were investigated through the pilot experimentation. Two responses were selected for pilot experimentation namely material removal rate (MRR) and tool wear rate (TWR). The assignment of factors was carried out using statistical software MINITAB. All the factors were varied at three levels except workpiece material, which was varied at two levels. The degrees of freedom required for the experiment was calculated to be 11, thus the orthogonal array that can be used should have degrees of freedom (dof) greater than 11. L18 which can accommodate a combination of 2-level and 3-level factors was thus used for conduct of experiments to measures two response values namely, MRR and TWR. After the conduct of the 18 trials the mean values for MRR and TWR are tabulated in Table 3.1. For the analysis of the result, Analysis of Variance (ANOVA) was performed.

Table 3.1: L18 Orthogonal Array along with results for powder mixed EDM process during pilot experimentation

Trial No.	Workpiece	Pulse on time (μs)	Current (Amp)	Pulse off time (μs)	Electrode	Powder	MRR (mm^3/min)	TWR (mm^3/min)
1	HCHCr	10	2	38	Copper	Copper	2.98	0.011
2	HCHCr	10	5	57	Graphite	Graphite	11.92	5.024
3	HCHCr	10	8	85	W-Cu	Mix	37.26	0.616
4	HCHCr	50	2	38	Graphite	Graphite	0.99	1.256
5	HCHCr	50	5	57	W-Cu	Mix	14.03	0.136
6	HCHCr	50	8	85	Copper	Copper	14.03	0.449
7	HCHCr	100	2	57	Copper	Mix	1.36	0.112
8	HCHCr	100	5	85	Graphite	Copper	15.65	3.14
9	HCHCr	100	8	38	W-Cu	Graphite	1.61	1.57

10	H13	10	2	85	W-Cu	Graphite	4.91	0.205
11	H13	10	5	38	Copper	Mix	10.89	0.449
12	H13	10	8	57	Graphite	Copper	34.97	3.14
13	H13	50	2	57	W-Cu	Copper	3.89	0.068
14	H13	50	5	85	Copper	Graphite	9.87	0.112
15	H13	50	8	38	Graphite	Mix	1.43	4.71
16	H13	100	2	85	Graphite	Mix	3.35	0.628
17	H13	100	5	38	W-Cu	Copper	8.5	0.068
18	H13	100	8	57	Copper	Graphite	11.49	0.157

Table 3.2: ANOVA for MRR

Source	SS	v	V	F	F critical at 95% confidence level	P
Workpiece	6.16	1	6.160	0.10		0.766
Pulse off time	398.17	2	199.085	3.15		0.116
Current	593.65	2	296.827	5.22	5.14	0.049
Pulse on time	340.26	2	170.130	2.69		0.147
Electrode	38.88	2	19.441	0.31		0.746
Powder	135.21	2	67.605	1.07		0.401
Residual error	379.42	6	63.237			
Total	1891.76	17				

The relationship of MRR with current, pulse on time and pulse off time during the machining using copper, graphite and tungsten- copper electrode in powder mixed dielectric is shown in the Figure 3.1. It was observed that at low current, MRR is low but increases sharply with increased current. ANOVA for MRR is given in Table 3.2. The current was observed to be most significant factor affecting MRR. The MRR increased with increase in the pulse on time and decreased with increase in pulse off time. The workpiece material and the electrode material had insignificant effect on MRR. Further, the MRR was observed to increase when copper powder was suspended in dielectric and reduce with graphite powder.

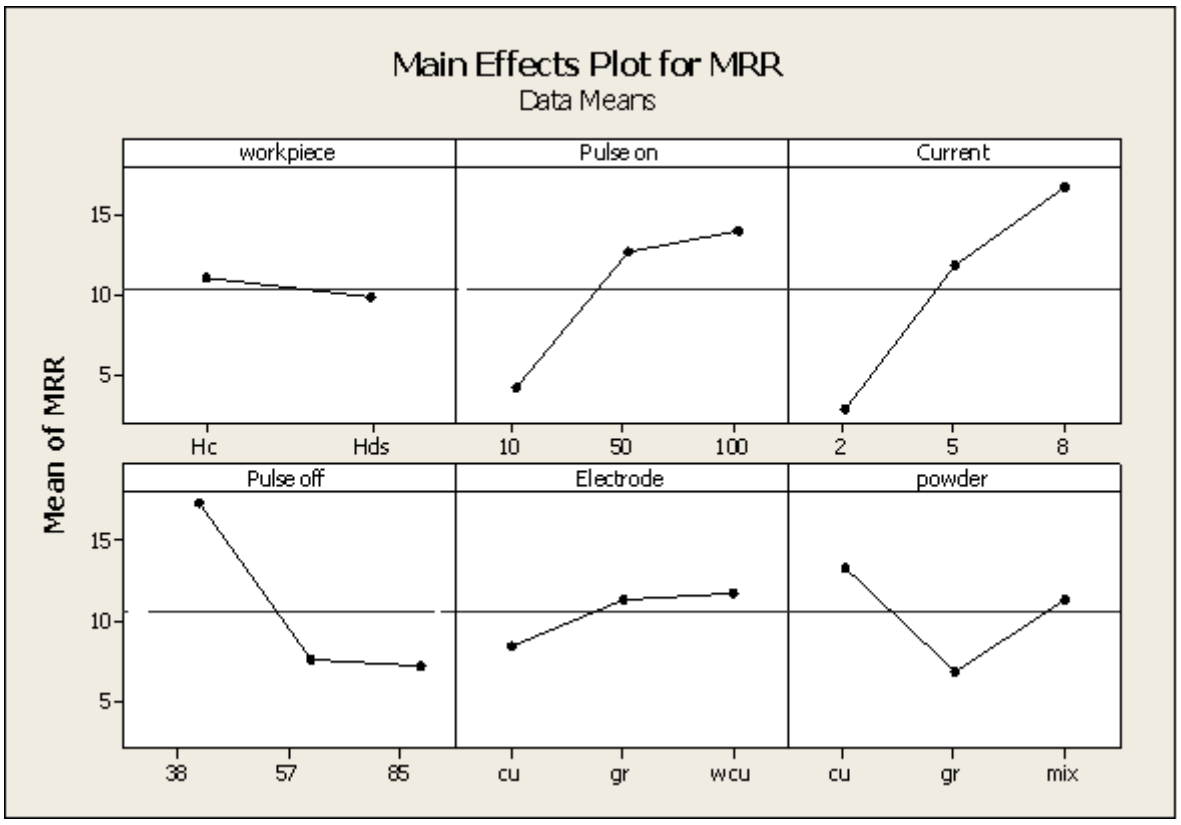

Figure 3.1: Main effect plot for MRR during pilot experimentation

Table 3.3: ANOVA for TWR

Source	SS	v	V	F	F critical at 95% confidence level	P
Workpiece	0.4284	1	0.4284	0.32		0.591
Pulse off time	1.2608	2	0.6304	0.47		0.645
Current	6.5037	2	3.2519	2.44		0.168
Pulse on time	1.1655	2	0.5827	0.44		0.665
Electrode	28.3231	2	14.1616	10.62	5.14	0.011
Powder	0.2748	2	0.1374	0.10		0.904
Residual error	8.0008	6	1.3335			
Total	45.9571	17				

The relationship of TWR with the current, pulse on and pulse off during the machining with copper, graphite and tungsten- copper electrode in powder mixed dielectric is shown in the

Figure 3.2. The electrode material was found to be most significant factor effecting TWR. With copper electrode showing least TWR while graphite electrode has maximum TWR. Also, increase in current caused high tool wear, while all other factors had insignificant effect on TWR.

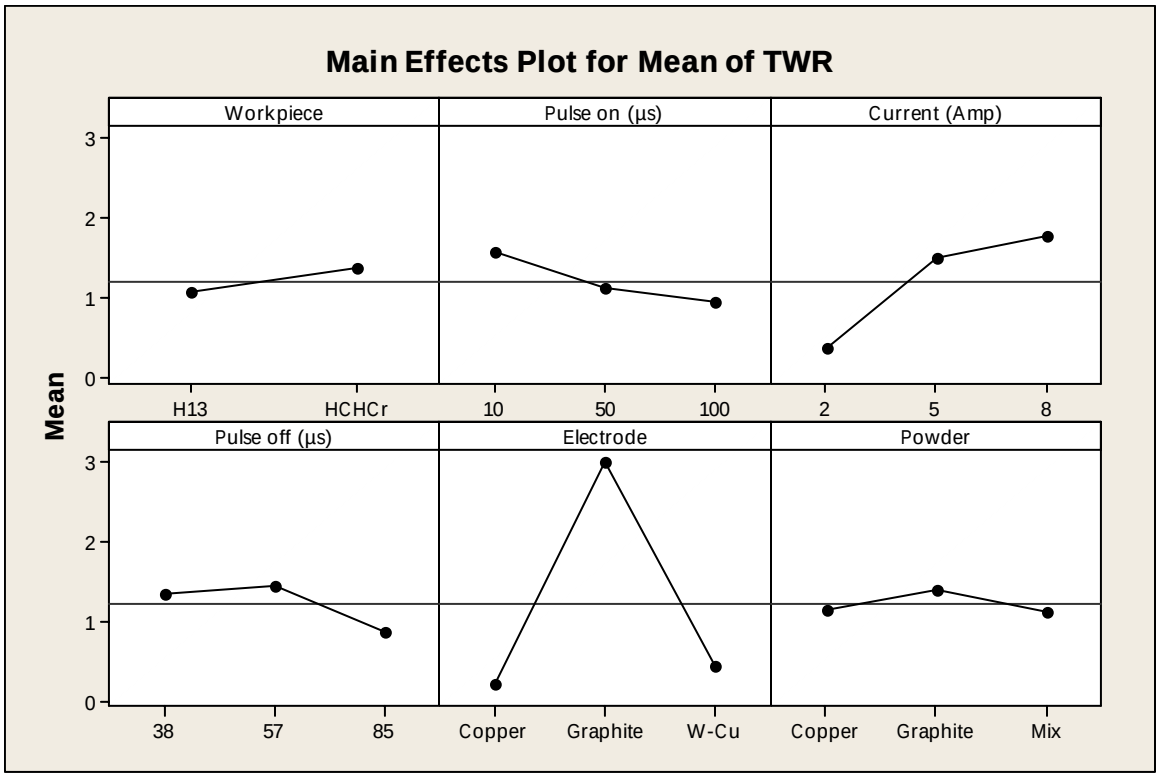

Figure 3.2: Main effect plot for TWR during pilot experimentation

3.2 METHODOLOGY

The full factorial design is referred as the technique of defining and investigating all possible conditions in an experiment involving multiple factors while the fractional factorial design investigates only a fraction of all the combinations. Although these approaches are widely used, they have certain limitations: they are inefficient in time and cost when the number of the variables is large; they require strict mathematical treatment in the design of the experiment and in the analysis of results; the same experiment may have different designs thus produce different results; further, determination of contribution of each factors is normally not permitted in this kind of design. The Taguchi method has been proposed to overcome these limitations by simplifying and standardizing the fractional factorial design. The methodology involves

identification of controllable and uncontrollable parameters and the establishment of a series of experiments to find out the optimum combination of the parameters which has greatest influence on the performance and the least variation from the target of the design. The effect of various parameters (workpiece material, electrode, dielectric, pulse on time, pulse off time, current and powder) and some of the effects of interactions between the main factors were also be studied using parameterization approach developed by Taguchi [42].

3.3 PROCEDURE OF EXPERIMENTAL DESIGN

The whole procedure of Taguchi method is as under. [43]

1. Establishment of objective function.
2. Selection of factors and/or interactions to be evaluated.
3. Identifications of uncontrollable factors and test conditions.
4. Selection of number of levels for the controllable and uncontrollable factors.
5. Calculation total degree of freedom needed
6. Select the appropriate Orthogonal Array (OA).
7. Assignment of factors and/or interactions to columns.
8. Execution of experiments according to trial conditions in the array.
9. Analyze results.
10. Confirmation experiments

3.4 ESTABLISHMENT OF OBJECTIVE FUNCTION

The objective of the study is to evaluate the main effects of workpiece material, dielectric, electrode, pulse off time, pulse on time, current and powder on the MRR, TWR, surface roughness and micro hardness. Deposition of the powder material either in pure form or in compound form was also studied. XRD and microstructure analysis was completed to understand the form and amount of deposition on the surface of the workpiece material.

3.5 DEGREE OF FREEDOM (dof)

The number of factors and their interactions and level for factors determine the total degree of freedom required for the entire experimentation. The degree of freedom for each factor is given by the number of levels minus one.

dof for each factor : k-1

where k is the number of level for each factor

dof for interactions between factors : $(k_A-1) \times (k_B-1)$

where k_A and k_B are number of level for factor A and B

3.6 DUMMY TREATMENT

The dummy treatment accommodates 2-level factor in a basic 3-level orthogonal array by using only two of possible levels for the factor and simply repeating one level from the previous of two levels for the indicated third level. Any one of the two levels for the factor can be repeated, so whichever is easiest, cheapest, or makes more sense should be repeated.

3.7 SELECTION OF FACTORS AND INTERACTION

The determination of which factors to investigate depends on the responses of interest. The factors affects the responses were identified using cause and effect analysis, brainstorming and pilot experimentation. The lists of factors studied with their levels are given in the Table 3.4.

Table 3.4: Factors interested and their levels

S. No	Factors	Factor designation	Levels		
			Level-1	Level-2	Level-3
1	Worpiece material	A	HCHCr	HDS	EN 31
2	Dielectric	B	Kerosene oil	EDM oil	Kerosene oil**
3	Electrode	C	Graphite	Tungsten-copper	Graphite**
4	Pulse off time (µs)	D	38	57	85
5	Pulse on time (µs)	E	10	50	100
6	Current (Amp)	F	2	5	8
7	Powder	G	No	Copper	Tungsten

**= Dummy treated

Some of interactions between the main factors were believed to be of interest. The interaction identified for detailed statistical analysis is as under:

(i) Workpiece v/s Electrode, A × C
(ii) Workpiece v/s Powder, A × G
(iii) Electrode v/s Powder, C × G

The minimum dof required in the experiment are the sum of all the degrees of freedom of factors and interactions. In the present experiment setup, there are five 3-level factor and two, electrode and dielectric are 2-level factor. The number of dof for factors A, D, E, F and G are two and for factor B and C is one. The total dof for the experiment including the interaction is given in Table 3.5. As the dof required for the experiment is 20, the orthogonal array (OA) to be used should have more than 20 dof. The most suitable orthogonal array that can be used for this experiment is L27, which has 26 dof assigned to its various columns. The additional six dof were used to measure the random error.

Table 3.5: Degree of freedom

Factor	A	B	C	D	E	F	G	Ax C	A x G	C x G	Total
Degree of Freedom	2	1	1	2	2	2	2	$2\times1 = 2$	$2\times2 = 4$	$1\times2 = 2$	20

3.8 ORTHOGONAL ARRAY

OA plays a critical part in achieving the high efficiency of the Taguchi method. OA is derived from factorial design of experiment by a series of very sophisticated mathematical algorithms including combinatorics, finite fields, geometry and error- correcting codes. The algorithms ensure that the OA to be constructed in a statistically independent manner that each level has an equal number of occurrences within each column; and for each level within one column, each level within any other column will occurs an equal number of times as well. Then, the columns are called orthogonal to each other. OAs are available with a variety of factors and levels in the Taguchi method. Since each column is orthogonal to the others, if the results associated with one level of a specific factor are much different at another level, it is because changing that factor

from one level to the next has strong impact on the quality characteristic being measured. Since the levels of the other factors are occurring an equal number of times for each level of the strong factor, any effect by these other factors will be ruled out. The Taguchi method apparently has the following strengths:

1. Consistency in experimental design and analysis.
2. Reduction of time and cost of experiments.
3. Robustness of performance without removing the noise factors.

The selection of orthogonal array depends on:

- The number of factors and interactions of interest
- The number of levels for the factors of interest

Taguchi's orthogonal arrays are experimental designs that usually require only a fraction of the full factorial combinations. The arrays are designed to handle as many factors as possible in a certain number of runs compared to those dictated by full factorial design. The columns of the arrays are balanced and orthogonal. This means that in each pair of columns, all factor combinations occur same number of times. Orthogonal designs allow estimating the effect of each factor on the response independently of all other factors. Once the degrees of freedom are known, the next step, selecting the orthogonal array (OA) is easy. The number of treatment conditions is equal to the number of rows in the orthogonal array and it must be equal to or greater than the degrees of freedom. The interactions to be evaluated will require an even larger orthogonal array. Once the appropriate orthogonal array has been selected, the factors and interactions can be assigned to the various columns. [42]

The linear graph used for assignment of factors in L27 array is shown in Figure 3.3. The L27 array has 13 columns and each column has two dof associated with it. In the linear graph, each vertex of the triangle represents a column in L27 array. Factor A has been assigned to column 1, factor B to column 2 and factor G to column 5. Each connecting line of the triangle represents interaction and also the column merged for the purpose. Column 3 and 4 were merged to measure the interaction of factor A×C, column 6 and 7 and column 8 and 11 were merged to measure the interaction of factor A×G and C×G respectively. The remaining factors B, D, E and F were assigned to columns 9, 10, 12 and 13 respectively. Two factors, dielectric fluid and

electrode material, were varied at two levels each and the third level was dummy treated. To calculate the variation due to error a comparison of average response value of level 1 and 1** (repeated dummy treatment experiment) was calculated.

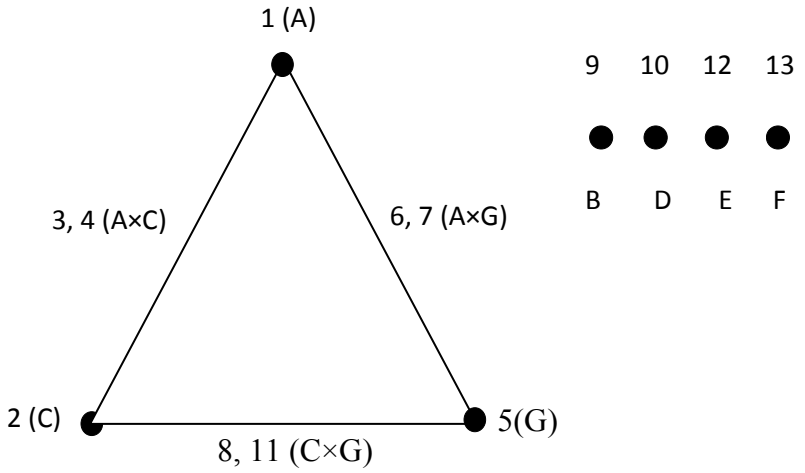

Figure 3.3: L27 Linear Graph

The 27 trial conditions represented by Taguchi's L27 are given in Table 3.6. The dummy treated levels are marked by using ** against the repeated level.

Table 3.6: L27 Experimental design

Trial no	Workpiece	Dielectric	Electrode	Pulse off time (μs)	Pulse on time (μs)	Current (Amp)	Powder
1	HCHCr	Kerosene	Gr	38	10	2	No
2	HCHCr	EDM oil	Gr	57	50	5	Cu
3	HCHCr	Kerosene**	Gr	85	100	8	W
4	HCHCr	EDM oil	W-Cu	57	100	8	No
5	HCHCr	Kerosene**	W-Cu	85	10	2	Cu
6	HCHCr	Kerosene	W-Cu	38	50	5	W
7	HCHCr	Kerosene**	Gr**	85	50	5	No
8	HCHCr	Kerosene	Gr**	38	100	8	Cu
9	HCHCr	EDM oil	Gr**	57	10	2	W
10	HDS	EDM oil	Gr	85	50	8	No
11	HDS	Kerosene**	Gr	38	100	2	Cu
12	HDS	Kerosene	Gr	57	10	5	W

13	HDS	Kerosene**	W-Cu	38	10	5	No
14	HDS	Kerosene	W-Cu	57	50	8	Cu
15	HDS	EDM oil	W-Cu	85	100	2	W
16	HDS	Kerosene	Gr**	57	100	2	No
17	HDS	EDM oil	Gr**	85	10	5	Cu
18	HDS	Kerosene**	Gr**	38	50	8	W
19	EN31	Kerosene**	Gr	57	100	5	No
20	EN31	Kerosene	Gr	85	10	8	Cu
21	EN31	EDM oil	Gr	38	50	2	W
22	EN31	Kerosene	W-Cu	85	50	2	No
23	EN31	EDM oil	W-Cu	38	100	5	Cu
24	EN31	Kerosene**	W-Cu	57	10	8	W
25	EN31	EDM oil	Gr**	38	10	8	No
26	EN31	Kerosene**	Gr**	57	50	2	Cu
27	EN31	Kerosene	Gr**	85	100	5	W

** = Dummy Treated

Each of the 27 experimental design represents the set of values of input process parameters with which particular experiment is to be conducted. Thus the total 27 experiment were, thus performed with repetition to minimize the effect of uncontrollable factors for each combination of all input parameters. Machining time during each experiment was 10 minutes.

3.9 EXPERIMENTAL SET UP

The experiments have been conducted on the Electrical Discharge Machine model T-3822 (Figure 3.4) of victory electromech available at Thapar University, Patiala in the Machine Tool lab. Many input parameters can be varied in EDM process, like discharge voltage, pulse on time, pulse off time, polarity, peak current, electrode gap and type of flushing, each factor has its own effect on the output parameters such as tool wear rate (TWR), material removal rate (MRR), surface roughness (SR) and hardness of the machined surface. The ranges of the parameters varied for the experimental work were selected on the basis of results of pilot experiments. The input parameters, which were kept constant during the experimentation, are given in the Table 3.7.

Table 3.7: Constant input parameters

S.No	Parameter	Value set as
1	Open circuit voltage	135±5%
2	Polarity	Positive
3	Machining time	10 minutes
4	Spark energy	Low
5	Powder concentration	10 gm/l

To ensure that the suspended powder particles do not clog the filtering system special mild steel tank was designed for the conducting experiments. This tank of size 330 × 180 × 187 mm was made of 3mm thick mild steel and had capacity of 9 litre. The tank was installed in EDM machine as shown in Figure 3.6. A stirrer rotating at 1400 rpm was used in the tank for proper mixing of the powder in the dielectric.

Figure 3.4: Electrical Discharge Machine

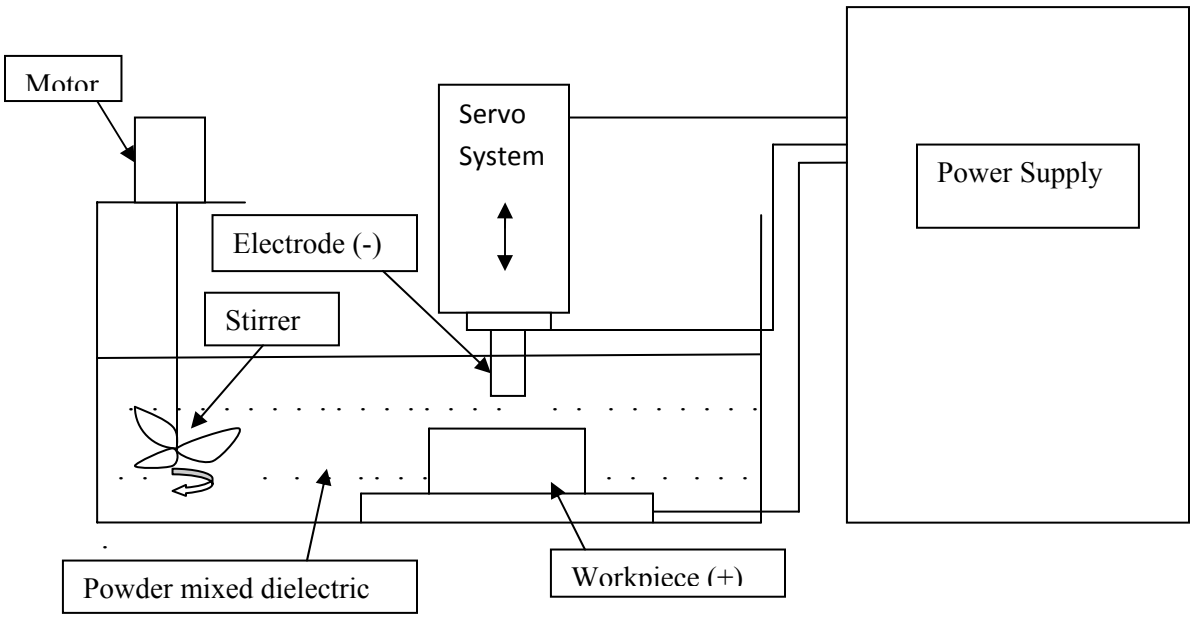

Figure 3.5: Schematic diagram of set up

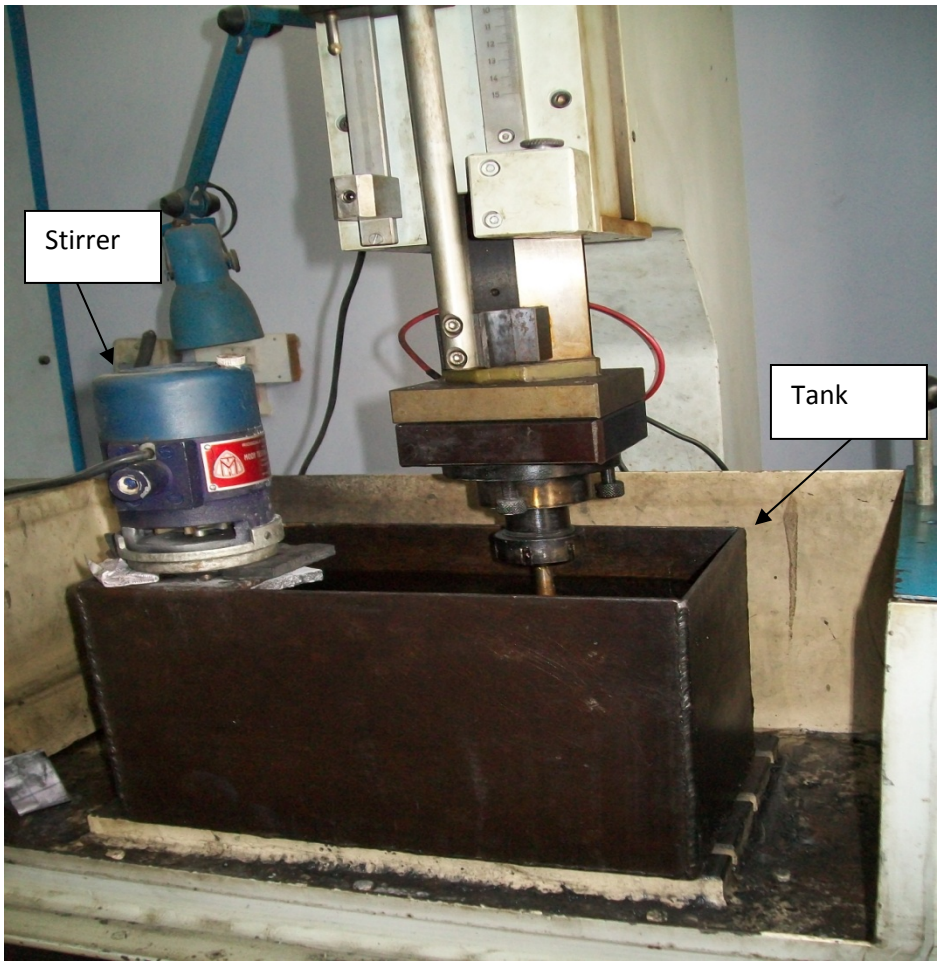

Figure 3.6: Dielectric Tank with stirrer attachments

3.10 MEASURING AND TEST EQUIPMENT USED

Micro hardness and surface roughness tests were conducted on all the samples, produced after each of the 27 trials. Also, MRR was measured using a weighing machine, while TWR was measured using a Vernier Calliper. The details of important test equipment used in experimental study are given below:

3.10.1 Surface Roughness Tester

Surface roughness was measured using the Perthometer, model M4Pi of Mahr, Germany available in the Metrology lab of Thapar University, Patiala. The equipment uses the stylus method of measurement, has profile resolution of 12 nm and measure roughness up to 100µm. A tracing length of 4.8 mm was used for analysis. Surface roughness of each sample was measured

at three different positions namely, centre, left and right of each machined sample. The left and right positions were taken at 7mm form center on each side.

3.10.2 Micro Hardness Tester

Micro hardness was measured on a computer interfaced Micro Hardness Tester, (model MVH-2) Metatech industries, Pune, India, available at Thapar University, Patiala. The micro hardness measurement is dependent on the diameter of indentation on the samples. The indents formed in the pyramid shaped indenter were measured with Quantimet software using a load of 1 kg for 20 seconds. The micro hardness was measured at deposition as well as non deposition region.

3.10.3 X-Ray Diffraction Machine

XRD analysis was carried out on X-Ray Diffraction machine, (model ME 210 LA 2) of Rigaku corporation, Japan, available in Material Testing lab of Thapar University, Patiala. The range of 2θ from the 5^0 to 100^0 was used at a scan speed of 5^0/minute for each test.

3.10.4 Scanning Electron Microscope (SEM) Machine

Microstructure was carried out of some selected samples on Scanning Electron Microscope, (model JSM-840A) of Joel, Japan, available in Material Testing lab of Thapar University, Patiala. The range of magnification from 10× to 3,00,000×. SEM of samples was carried out on three ranges, namely, 200×, 500× and 1000×.

3.11 ANALYSIS OF RESULTS

Signal-to-noise ratio

The parameters that influence the output can be categorized into two classes, namely controllable (or design) factors and uncontrollable (or noise) factors. Controllable factors are those factors whose values can be set and easily adjusted by the designer. Uncontrollable factors are the sources of variation often associated with operational environment. The best settings of control factors as they influence the output parameters are determined through experiments. From the analysis point of view, there are three possible categories of the response characteristics explained below.

r is the number of tests in a trial (noise of repetitions regardless of noise levels)

$\sum_{i=1}^{r} y^2{}_i$ = summation of all response values under each trial

MSD = Mean square deviation

y_j= Observed value of the response characteristic

y_o= nominal or target value of the results

The three different response characteristics are given by the following.

1) Higher is Better. The S/N for higher the better is given by:

$(S/N)_{HB} = -10 \log (MSD_{HB})$

Where $MSD_{HB} = \frac{1}{r}\sum_{j=1}^{r}\left(\frac{1}{y_j^{\,2}}\right)$ (Equation 3.1)

MSD_{HB}= Mean Square Deviation for higher-the-better response.

2) Nominal is Better. The S/N for nominal is better is:

$(S/N)_{NB} = -10 \log (MSD_{NB})$

Where $MSD_{NB} = \frac{1}{r}\sum_{j=1}^{r}\left(y_j - y_0\right)^2$ (Equation 3.2)

3) Lower is Better. In this design situation, TWR and surface roughness is the type of ‘‘lower is better’’, which is a logarithmic function based on the mean square deviation (MSD), given by

$$S/N_{LB} = -10\log(MSD) = -10\log[(\frac{1}{r}\sum_{i=1}^{r} y^2{}_i)$$

Where $MSD_{LB} = \frac{1}{r}\sum_{j=1}^{r}\left(y_j^{\,2}\right)$ (Equation 3.3)

Signal to noise ratio for response characteristics

The parameters that influence the output can be categorized in two categories, controllable factors and uncontrollable factors. The control factors that may contribute to reduced variation can be quickly identified by looking at the amount of variation present in response. The uncontrollable factors are the sources of variation often associated with operational environment. For this experimental work, response characteristics have given in the Table 3.8.

Table 3.8: Response Characteristics

Response name	Response type	Units
Material Removal Rate (MRR)	Higher the better	mm^3/min
Tool Wear Rate (TWR)	Lower the better	mm^3/min
Micro Hardness	Higher the better	Hvn
Surface Roughness	Lower the better	Microns

Measurement of F-value of Fisher's F ratio

The principle of the *F* test is that the larger the *F* value for a particular parameter, the greater the effect on the performance characteristic due to the change in that process parameter. F value is defined as:

$$F=\frac{MS\ for\ the\ term}{MS\ for\ the\ error\ term}$$

Depending on F-value, percentage contribution is calculated of each factor and interaction.

Computation of average performance:

Average performance of a factor at certain level is the influence of the factor at this level on the mean response of the experiments.

Analysis of variance

The knowledge of the contribution of individual factors is critically important for the control of the final response. The analysis of variance (ANOVA) is a common statistical technique to determine the percent contribution of each factor for results of the experiment. It calculates parameters known as sum of squares (*SS*), pure *SS*, degree of freedom (dof), variance, F-ratio

and percentage contribution of each factor. Since the procedure of ANOVA is a very complicated and employs a considerable of statistical formula, only a brief description of is given as following.

The Sum of Squares (SS) is a measure of the deviation of the experimental data from the mean value of the data.

Let '*A*' be a factor under investigation

$$SS_T = \sum_{i=1}^{N} (y_i - \overline{T})^2$$

Where N = Number of response observations, $\overline{T}$ is the mean of all observations y_i is the i, *th* response

Factor Sum of Squares (SS_A) - Squared deviations of factor (*A*) averages from overall average

$$SS_A = \left[\sum_{i=1}^{k_A} \left(\frac{A_i^2}{n_{Ai}} \right) \right] - \frac{T^2}{N} \qquad \text{(Equation 3.4)}$$

Where

A_i =Average of all obseravtions under A_i level = A_i / n_{Ai}

T = sum of all observations

$\overline{T}$ = Average of all observations = T / N

n_{Ai} = Number of obsernations under A_i level

Error Sum of Squares (SS_e) - Squared deviations of observations from factor (A) averages

$$SS_e = \sum_{j=1}^{k_A} \sum_{i=1}^{n_{Ai}} \left(y_i - \overline{A}_j \right)^2$$ (Equation 3.5)

Sum of Squares ($SS_{A\times B}$) for interactions

$$SS_{A\times B} = \left[\sum_{i=1}^{c} \left(\frac{(A\times B)_i^2}{n_{(A\times B)i}} \right) \right] - \frac{T^2}{N} - SS_A - SS_B$$ (Equation 3.6)

Sum of Squares of factors for dummy treatment level

The level symbols for A_1 & A_1^{**} , both indicate the same test condition w.r.t. factor A. Therefore

$$SS_A = \frac{(A_1 + A_1^{**})^2}{n_{A1} + n_{A1^{**}}} + \frac{A_2^2}{n_{A2}} - \frac{T^2}{N}$$ (Equation 3.7)

$$SS_e = \frac{(A_1 - A_1^{**})^2}{n_{A1} + n_{A1^{**}}}$$ (Equation 3.8.)

$$SS_{A\times B} = \left[\sum_{i=1}^{c} \left(\frac{(A\times B)_i^2}{n_{(A\times B)i}} \right) \right] - \frac{T^2}{N} - SS_A - SS_B - SS_e$$ (Equation 3.9)

$$SS'_A = SS_A - (V_e)(v_A)$$

SS'_A is expected sum of squares due to factor A, and the percent contribution to the total variation can be calculated as:

$$P = \frac{SS'_A}{SS_T} \times 100$$

3.12 TEST RESULTS FOR WORKPIECE & ELECTRODE MATERIAL

Three workpiece materials High-Carbon High-Chromium (HCHCr), Hot Die Steel (H13) and EN31 and two electrode materials Graphite and Tungsten-Copper were used. Before the start of experimentation, the chemical composition of workpiece and electrode material was measured on an Optical Emission Spectrometer DV-6. The percentage composition of the workpiece and electrode material is provided in Table 3.9 and 3.10 respectively. The dimension of each workpiece 100× 50× 10 mm was selected. The worpieces are shown in the Figure 3.7 and Figure 3.8 before and after machining respectively. The diameter of each electrode was 20mm and pictorial view of electrode are shown in the Figure 3.9.

Table 3.9: Chemical composition of workpiece materials

Workpiece	% composition													
	Fe	C	Si	Mn	P	S	Cr	Mo	Ni	Co	Cu	Ti	V	W
HDS	90.6	0.4	1.0	0.39	0.03	0.02	5.32	1.1	0.36	0.01	0.01	0.01	0.3	0.1
HCHCr	83.5	1.6	0.5	0.55	0.03	0.03	13.3	0.05	0.07	0.01	0.05	0.02	-	0.02
EN31	92.3	0.35	1.0	0.40	0.04	0.02	5.0		0.09	0.01	0.03		1.0	

Table 3.10: Chemical composition of electrode materials

Electrode	% composition					
	W	Cu	Ni	Z	Ti	Pb
Tungsten-copper	79.36	19.462	0.121	0.047	0.014	0.026
Graphite	More than 99% purity					

Figure 3.7: Workpiece materials before machining

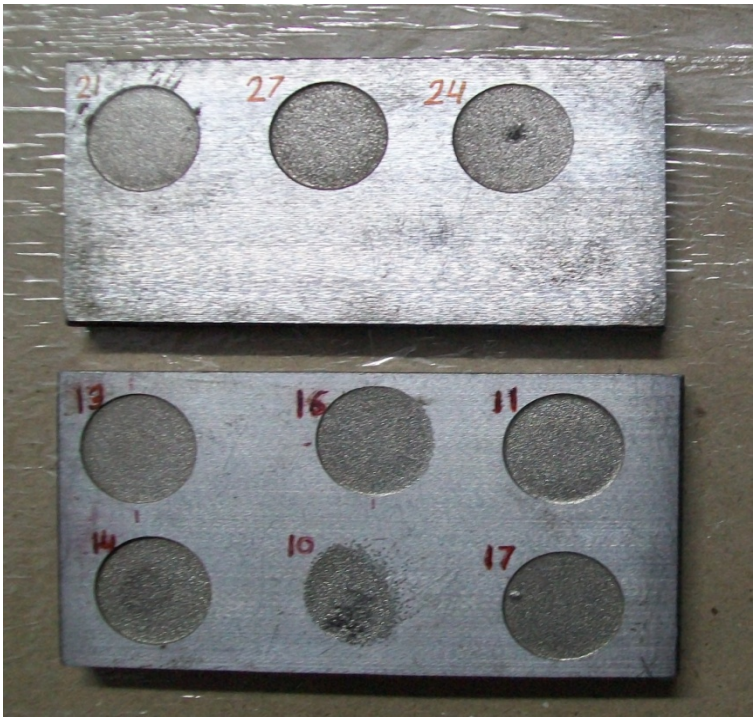

Figure 3.8: Workpiece materials after machining

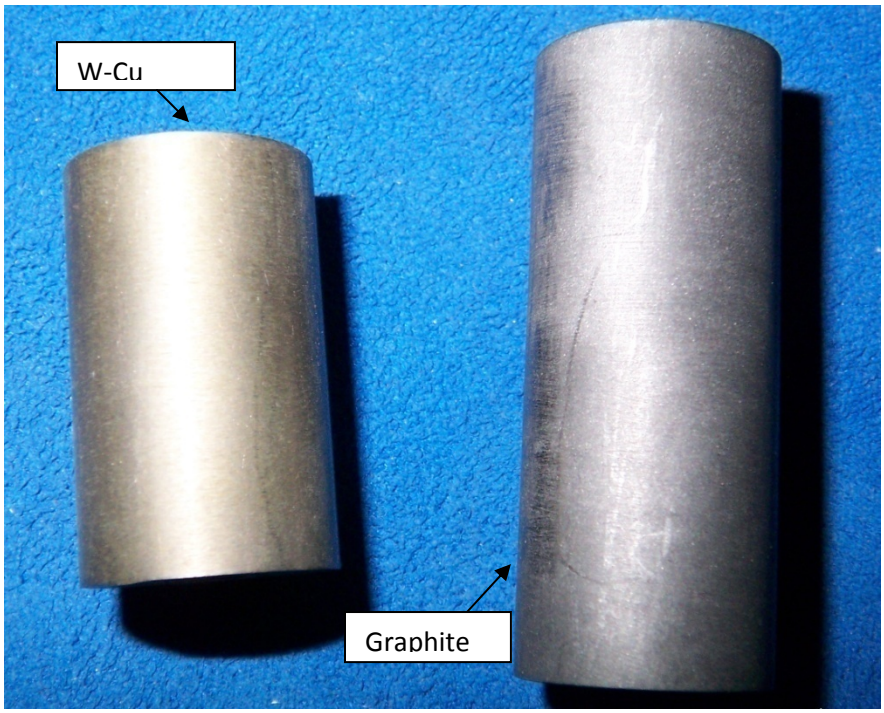

Figure 3.9: Electrodes

The surface of workpiece was ground on the surface grinder to remove any scaling. Micro hardness of workpiece was measured at three different positions before machining and is given in the Table 3.11.

Table 3.11: Micro hardness of worpiece materials before machining

Workpiece material	HCHCr	HDS (H13)	EN31
Micro hardness (hvn)	576	534	552

CHAPTER 4

RESULTS AND ANALYSIS OF MRR

4.1 INTRODUCTION

The effect of parameters i.e. workpiece, dielectric, electrode, pulse on time, pulse off time, current, powder and some of their interactions were evaluated using ANOVA and factorial design analysis. A confidence interval of 99% has been used for the analysis. One repetition for each of 27 trials was completed so as to measure Signal to Noise ratio (S/N ratio).

4.2 RESULTS FOR MRR

The results for MRR for each of the 27 treatment conditions with repetition are given in Table 4.1. MRR of each sample was calculated from weight difference of workpiece before and after the performance trial:

$$\text{MRR} = \frac{(\text{Wi} - \text{Wf})}{\rho \times \text{t}} \times 1000 \text{ mm}^3/\text{min}$$

Where Wi = Initial weight of workpiece material (gms)

Wf = Final weight of workpiece material (gms)

t = Time period of trails in minutes

ρ = Density of workpiece in gms/cc

Table 4.1: Results for MRR

Trial no.	Workpiece	Dielectric	Electrode	Pulse off (µs)	Pulse on (µs)	Current (Amp)	Powder	MRR (mm^3/min)		Mean MRR (mm^3/min)	S/N ratio
								I	II		
1	HCHCr	Kerosene	Gr	38	10	2	No	3.75	4.06	3.90	11.81
2	HCHCr	EDM oil	Gr	57	50	5	Cu	18.05	17.52	17.78	25.00
3	HCHCr	Kerosene**	Gr	85	100	8	W	10.17	10.12	10.14	20.12
4	HCHCr	EDM oil	W-Cu	57	100	8	No	26.69	26.84	26.77	28.55

5	HCHCr	Kerosene**	W-Cu	85	10	2	Cu	6.51	6.85	6.68	16.49
6	HCHCr	Kerosene	W-Cu	38	50	5	W	26.86	26.86	26.86	28.58
7	HCHCr	Kerosene**	Gr**	85	50	5	No	14.46	14.00	14.23	23.06
8	HCHCr	Kerosene	Gr**	38	100	8	Cu	32.01	32.74	32.37	30.20
9	HCHCr	EDM oil	Gr**	57	10	2	W	8.46	8.60	8.53	18.62
10	HDS	EDM oil	Gr	85	50	8	No	2.42	2.06	2.24	6.92
11	HDS	Kerosene**	Gr	38	100	2	Cu	7.51	8.48	7.99	18.01
12	HDS	Kerosene	Gr	57	10	5	W	7.69	7.93	7.81	17.85
13	HDS	Kerosene**	W-Cu	38	10	5	No	10.51	10.51	10.51	20.43
14	HDS	Kerosene	W-Cu	57	50	8	Cu	26.30	25.90	26.10	28.33
15	HDS	EDM oil	W-Cu	85	100	2	W	10.86	11.31	11.08	20.89
16	HDS	Kerosene	Gr**	57	100	2	No	3.18	3.16	3.17	10.02
17	HDS	EDM oil	Gr**	85	10	5	Cu	10.42	10.90	10.66	20.55
18	HDS	Kerosene**	Gr**	38	50	8	W	12.68	13.45	13.06	22.31
19	EN31	Kerosene**	Gr	57	100	5	No	14.47	13.54	14.00	22.91
20	EN31	Kerosene	Gr	85	10	8	Cu	4.11	4.28	4.20	12.46
21	EN31	EDM oil	Gr	38	50	2	W	12.53	12.13	12.33	21.82
22	EN31	Kerosene	W-Cu	85	50	2	No	3.67	3.98	3.82	11.63
23	EN31	EDM oil	W-Cu	38	100	5	Cu	20.04	20.78	20.41	26.19
24	EN31	Kerosene**	W-Cu	57	10	8	W	17.31	17.84	17.58	24.89
25	EN31	EDM oil	Gr**	38	10	8	No	1.05	1.45	1.25	1.66
26	EN31	Kerosene**	Gr**	57	50	2	Cu	5.37	5.97	5.67	15.03
27	EN31	Kerosene	Gr**	85	100	5	W	20.821	21.08	20.95	26.42

4.3 ANALYSIS OF VARIANCE - MRR

The results were analyzed using ANOVA for identifying the significant factors affecting the performance measures. The Analysis of Variance (ANOVA) for the mean MRR at 99% confidence interval is given in Table 4.2. The variation data for each factor and their interactions were F-tested to find significance of each. The principle of the F-test is that the larger the F value for a particular parameter, the greater the effect on the performance characteristic due to the change in that process parameter. ANOVA table shows that electrode (F value 60.22), current (F value 41.03), pulse on time (F value 26.75), powder (F value16.05), pulse off time (F value11.73) are the factors that significantly affect the MRR. All others factors, namely, dielectric and workpiece material and interactions were found to be insignificant. Table 4.3 shows the ranks of various factors in the terms of their relative significance. Current has the highest rank, signifying highest contribution to MRR and dielectric has the lowest rank and was observed to be insignificant in affecting MRR. Main effect plot for the mean MRR is shown in the Figure 4.1 which shows the variation of MRR with the input parameters. As can be seen MRR increases with increase in current from 2Amp to 5Amp. It, however, shows no significant change in MRR when current is further increased from 5Amp to 8Amp. MRR is high with tungsten-copper electrode as compared to graphite electrode and the MRR increases with addition of powder in dielectric. The interaction plot is shown in the Figure 4.2 which shows that none of the interactions are significant for the MRR.

Table 4.2: ANOVA for MRR

Sources	SS	v	V	F	F (critical)	SS'	% contribution
Workpiece (A)	102.11	2	51.06	10.87			
Dielectric (B)	1.01	1	1.01	0.22			
Electrode (C)	282.98	1	282.98	60.22	13.7	262.53	17.172
Pulse off time (D)	110.26	2	55.13	11.73	10.9	69.36	4.537
Pulse on time (E)	251.42	2	125.71	26.75	10.9	210.52	13.770
Current (F)	385.60	2	192.80	41.03	10.9	344.70	22.547

Powder (G)	150.87	2	75.43	16.05	10.9	109.96	7.193
(A × C)	38.80	2	19.40	4.13			
(A × G)	162.56	4	40.64	8.65			
(C × G)	14.99	2	7.49	1.59			
Error	28.19	6	4.70				
TOTAL	1528.79	26	58.80			1528.79	100
e pooled	347.66	17	20.45			531.72	34.780

Table 4.3: Response table for means of MRR

Level	Workpiece (A)	Dielectric (B)	Electrode (C)	Pulse off time (D)	Pulse on time (E)	Current (F)	Powder (G)
1	11.13	12.34	10.55	14.30	7.90	7.02	14.65
2	16.36	12.72	16.64	14.16	13.57	15.91	8.88
3	10.29			9.33	16.32	14.86	14.26
Delta	6.07	0.38	6.07	4.96	8.41	8.89	5.77
Rank	4	7	3	6	2	1	5

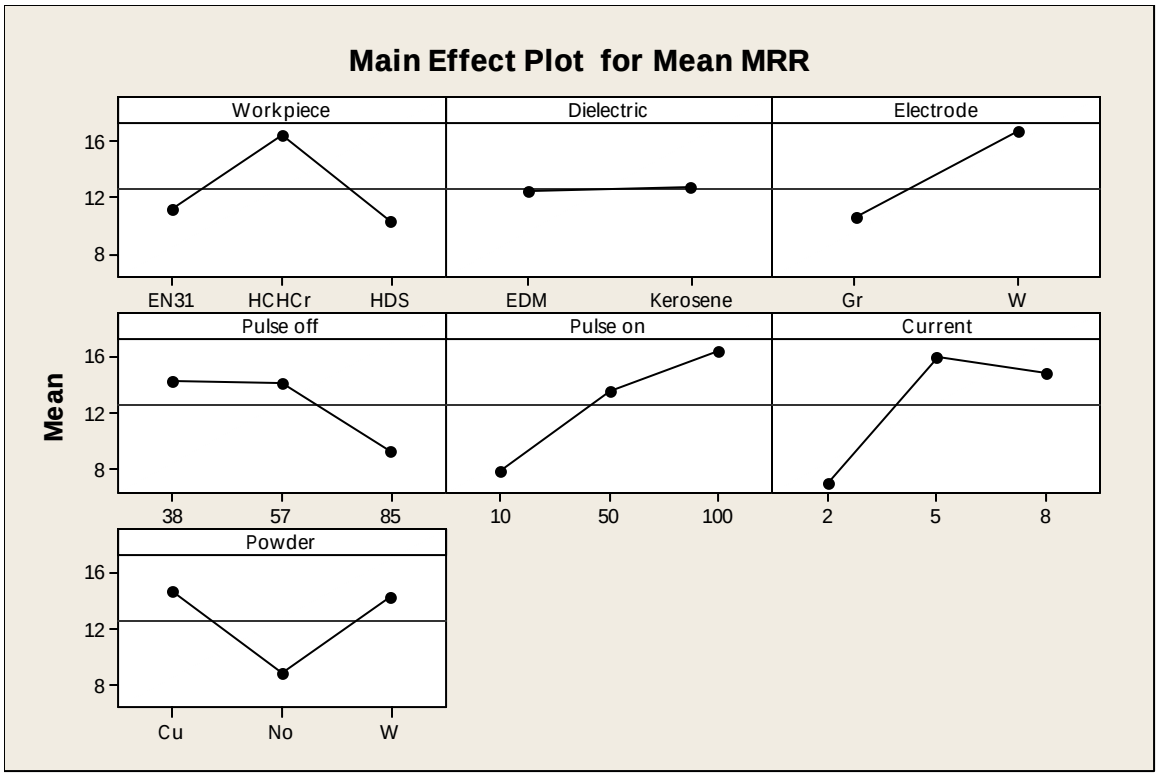

Figure 4.1: Main effect plot for Mean MRR

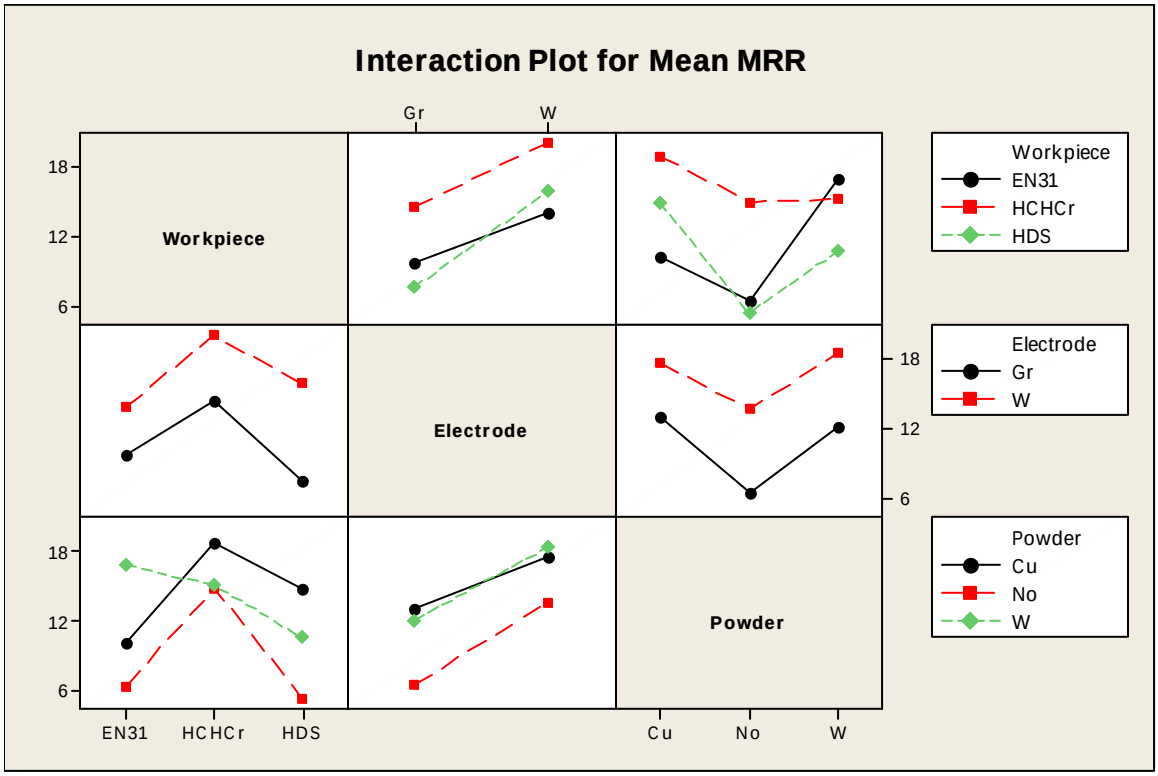

Figure 4.2: Interaction plot for MRR

4.4 RESULTS FOR S/N RATIO - MRR

The S/N ratio consolidated several repetitions into one value and is an indication of the amount of variation present in the process. The S/N ratios have been calculated to identify the major contributing factors and interactions that cause variation in MRR. MRR is a "Higher the better" type response is given by a logarithmic function based on the mean square deviation:

$(S/N)_{HB} = -10 \log (MSD_{HB})$

Where $MSD_{HB} = \frac{1}{r}\sum_{j=1}^{r}\left(\frac{1}{y_j^{\,2}}\right)$

MSD_{HB} = Mean Square Deviation for higher-the-better response.

Table 4.4 shows the ANOVA results for S/N ratio of MRR at 99% confidence interval. Other than the dielectric, all other factors are significant. According to F-test powder was observed to be the most significant factor affecting the MRR, followed by current, pulse on time, electrode, workpiece according to F-test. All the interactions studied during the trials were found to be significant. Main effect plot and interaction plot of S/N ratio for MRR are shown in the figure 4.3 and 4.4 respectively. Table 4.5 shows the ranks of various factors in the terms of their relative significance. Current has the highest rank, signifying highest contribution to MRR and dielectric has the lowest rank and was observed to be insignificant in affecting MRR.

Table 4.4: ANOVA for S/N ratio of MRR

Sources	SS	v	V	F	F (critical)	SS'	% contribution
Workpiece (A)	108.77	2	54.38	37.72	10.9	104.14	7.880
Dielectric (B)	7.53	1	7.53	5.22			
Electrode (C)	140.74	1	140.74	97.63	13.7	138.43	10.474
Pulse off time (D)	62.07	2	31.03	21.53	10.9	57.44	4.346
Pulse on time (E)	195.92	2	97.96	67.95	10.9	191.30	14.474
Current (F)	247.32	2	123.66	85.78	10.9	242.69	18.363
Powder (G)	270.53	2	135.27	93.83	10.9	265.91	20.119

(A × C)	99.45	2	49.72	34.49	10.9	94.83	7.175
A × G)	131.42	4	32.85	22.79	9.15	122.17	9.244
(C × G)	49.27	2	24.64	17.09	10.9	44.65	3.378
Error	8.65	6	1.44				
TOTAL	1321.66	26	50.83			1321.66	100
e pooled	16.18	7	2.31			60.09	4.547

Table 4.5: Response table for S/N ratio of MRR

Level	Workpiece (A)	Dielectric (B)	Electrode (C)	Pulse off time (D)	Pulse on time (E)	Current (F)	Powder (G)
1	18.12	18.91	18.05	20.12	16.09	16.04	21.37
2	22.50	20.03	22.89	21.25	20.30	23.45	15.22
3	18.37			17.62	22.59	19.50	22.39
Delta	4.38	1.12	4.84	3.63	6.50	7.41	7.17
Rank	5	7	4	6	3	1	2

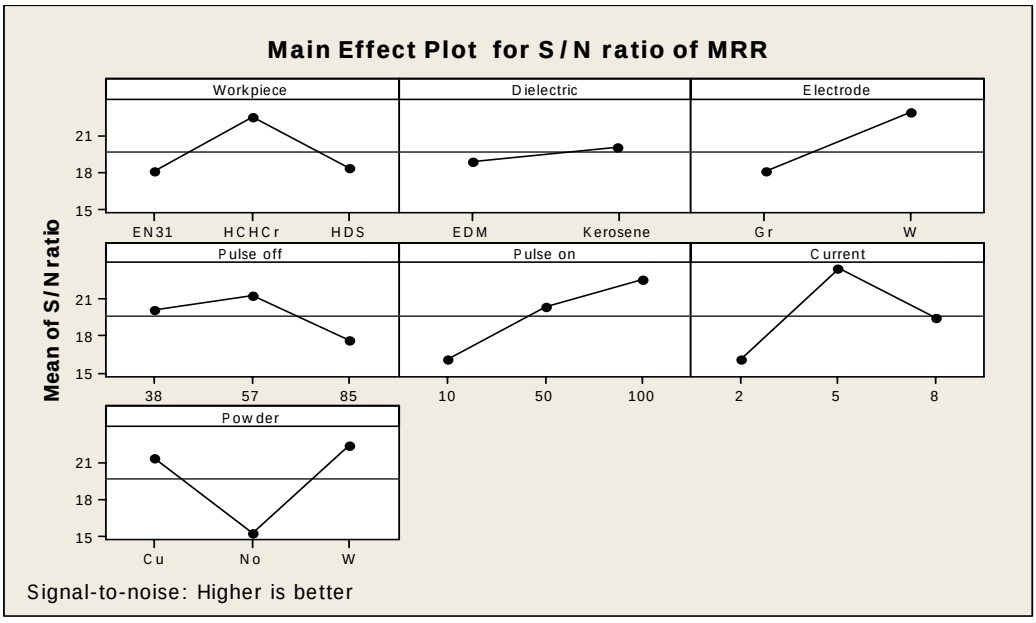

Figure 4.3: Main effects plot for of S/N ratio of MRR

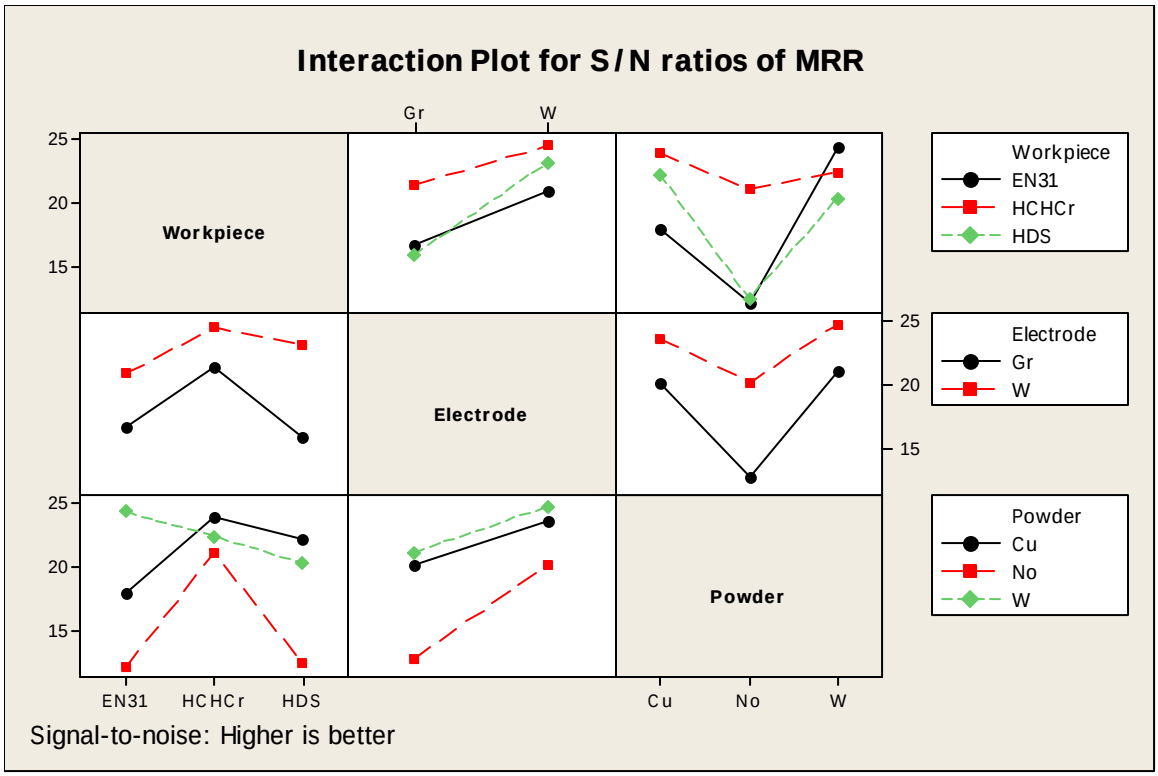

Figure 4.4: Interaction plot for S/N ratio of MRR

4.5 OPTIMAL DESIGN

In this experimental analysis, the main effect plot and interaction plot in Figure 4.1 and Figure 4.2 used to estimate the mean MRR with optimal design conditions. From the, Table 4.6 it is concluded that highest MRR was observed when tugsten-copper electrode, pulse off time 38µs, pulse on time 100 µs, current 5Amp and tungsten powder was selected in the treatment conditions. In S/N ratio highest MRR was observed when workpiece material HCHCr, tugsten-copper electrode, pulse off time 57µs, pulse on time 100 µs, current 5Amp and tungsten powder was selected in treatment condition. In this case, the same levels of the significant factors and interactions provide the higher average and reduced variability so nothing has to be compromised. In some situations, the levels of factors which improve the average and improve the uniformity may conflict, so a compromise may have to be reached. Also, a compromise may have to occur when multiple responses are considered and the same factor level may cause one response to improve and another to deteriorate.

Table 4.6: Significant factors and interactions for MRR

Factors	Affecting mean		Affecting variation (S/N ratio)	
	Contribution	Best level	Contribution	Best level
Workpiece (A)	Insignificant	-	Significant	Level 1- HCHCr
Dielectric (B)	Insignificant	-	Insignificant	-
Electrode (C)	Significant	Level 2- W-Cu	Significant	Level 2- W-Cu
Pulse off time (D)	Significant	Level 1- 38µs	Significant	Level 2- 57 µs
Pulse on time(E)	Significant	Level 3-100 µs	Significant	Level 3- 100 µs
Current (F)	Significant	Level 2- 5 Amp	Significant	Level 2- 5 Amp
Powder (G)	Significant	Level 3- W	Significant	Level 3-W
(A × C)	Insignificant	-	Significant	A_1C_2
(A × G)	Insignificant	-	Significant	A_1G_3
(C × G)	Insignificant	-	Significant	C_2G_3

Estimating the mean

In experimental analysis, the MRR is a higher average response is better (HB) characteristic. Depending on the characteristic, different treatment combinations has chosen to obtain satisfactory results. After conducting the experiments the optimum treatment condition within the experiments determined on the basis of prescribed combination of factor levels is determined to one of those in the experiment.

Mean value of MRR

$$\mu_{A_1\times C_2\ A_1\times A_1A_1\times A_1,D_2,E_3,F_2} = \overline{A_1 \times C_2} + \overline{A_1 \times G_3} + \overline{C_2 \times G_3} + \overline{D_2} + \overline{E_3} + \overline{F_2} - 5\overline{T}$$

$$\mu_{A_1\times C_2\ A_1\times A_1A_1\times A_1,D_2,E_3,F_2} = 20.18+15.18+18.51+14.16+14.82+15.91-5\times 12.07=38.33\ mm^3/min$$

Confidence Interval around the Estimated Mean

The confidence interval is a maximum and minimum value between which the true average should fall at some stated percentage of confidence. The estimate of the mean µ is only a point estimate based on the averages of results obtained from the experiment. Statistically this provides

a 50% chance of the true averages being greater than μ and a 50% chance of the true average being less than μ [43].

Confidence Interval around the estimated MRR

$$CI_1 = \sqrt{\frac{F_{\alpha,\nu_1,\nu_2} V_e}{n_{eff}}} \quad \text{Where} \quad F_{\alpha\nu_1\nu_2} = F\ ratio$$

$\alpha = risk\ (0.01)$ $\qquad$ $confidence\ = 1-\alpha$

$\nu_1 = dof\ \ for\, mean\, which\, is\ always = 1$

$\nu_2 = dof\ \ for\, error = \nu_e$

$n_{eff}\ =$ Number of tests under that condition using the participating factors

$$n_{eff} = \frac{N}{1 + dof_{A\times C, A\times G, C\times G, D, E, F}} = \frac{27}{1+2+4+2+2+2+2} = 1.8$$

$$CI_1 = \sqrt{\frac{F_{\alpha,\nu_1,\nu_2} V_e}{n_{eff}}} = \sqrt{\frac{0.17 \times 20.45}{1.8}} = 1.38$$

So the confidence interval around the estimated mean of MRR is given by 38.33±1.38 mm^3/min.

CHAPTER 5

RESULTS AND ANALYSIS OF TWR

5.1 INTRODUCTION

The effect of parameters i.e. workpiece, dielectric, electrode, pulse on time, pulse off time, current, powder and some of their interactions were evaluated using ANOVA and factorial design analysis. A confidence interval of 99% has been used for the analysis. One repetition for each of 27 trials was completed so as to measure Signal to Noise ratio (S/N ratio).

5.2 RESULTS FOR TWR

The results for TWR for each of the 27 treatment conditions with repetition are given in Table 5.1. The TWR is calculated from the loss in length in electrode during performance trial:

$$\text{TWR} = \frac{A \times L}{\text{t}} \ \text{mm}^3/\text{min}$$

Where A = front area of electrode (mm^2)

L = Loss in length of electrode (mm)

t = time period of trial (minutes)

Table 5.1: Results for TWR

Trial no.	Workpiece	Dielectric	Electrode	Pulse off (μs)	Pulse on (μs)	Current (Amp)	Powder	TWR mm^3/min		Mean TWR mm^3/min	S/N ratio
								I	II		
1	HCHCr	Kerosene	Gr	38	10	2	No	0.356	0.356	0.356	-8.97
2	HCHCr	EDM oil	Gr	57	50	5	Cu	2.512	2.512	2.512	-8.00
3	HCHCr	Kerosene**	Gr	85	100	8	W	2.134	2.043	2.0885	-6.39
4	HCHCr	EDM oil	W-Cu	57	100	8	No	2.567	2.567	2.567	-8.18
5	HCHCr	Kerosene**	W-Cu	85	10	2	Cu	0.314	0.314	0.314	10.06
6	HCHCr	Kerosene	W-Cu	38	50	5	W	0.836	0.836	0.836	1.55

7	HCHCr	Kerosene**	Gr**	85	50	5	No	3.65	3.65	3.65	-11.24
8	HCHCr	Kerosene	Gr**	38	100	8	Cu	2.124	2.512	2.318	-7.33
9	HCHCr	EDM oil	Gr**	57	10	2	W	0.628	0.628	0.628	4.04
10	HDS	EDM oil	Gr	85	50	8	No	2.512	2.512	2.512	-8.00
11	HDS	Kerosene**	Gr	38	100	2	Cu	1.768	1.768	1.768	-4.94
12	HDS	Kerosene	Gr	57	10	5	W	1.256	1.57	1.413	-3.05
13	HDS	Kerosene**	W-Cu	38	10	5	No	1.057	1.057	1.057	-0.48
14	HDS	Kerosene	W-Cu	57	50	8	Cu	1.456	1.456	1.456	-3.26
15	HDS	EDM oil	W-Cu	85	100	2	W	0.523	0.523	0.523	5.63
16	HDS	Kerosene	Gr**	57	100	2	No	1.125	1.125	1.125	-1.02
17	HDS	EDM oil	Gr**	85	10	5	Cu	3.14	3.14	3.14	-9.93
18	HDS	Kerosene**	Gr**	38	50	8	W	1.256	1.256	1.256	-1.97
19	EN31	Kerosene**	Gr	57	100	5	No	3.16	3.16	3.16	-9.99
20	EN31	Kerosene	Gr	85	10	8	Cu	2.512	2.512	2.512	-8.00
21	EN31	EDM oil	Gr	38	50	2	W	0.314	0.314	0.314	10.06
22	EN31	Kerosene	W-Cu	85	50	2	No	0.954	0.954	0.954	0.40
23	EN31	EDM oil	W-Cu	38	100	5	Cu	0.828	0.828	0.828	1.63
24	EN31	Kerosene**	W-Cu	57	10	8	W	1.256	1.256	1.256	-1.97
25	EN31	EDM oil	Gr**	38	10	8	No	2.225	2.225	2.225	-6.94
26	EN31	Kerosene**	Gr**	57	50	2	Cu	1.256	1.256	1.256	-1.97
27	EN31	Kerosene	Gr**	85	100	5	W	1.256	1.256	1.256	-1.97

5.3 ANALYSIS OF VARIANCE - TWR

The results were analyzed using ANOVA for identifying the significant factors affecting the performance measures. The ANOVA results for the mean TWR at 99% confidence interval is given in Table 5.2. ANOVA table shows that current (F value 7.79), powder (F value 3.22) and electrode (F value 3.17) are the factors that significantly affecting the TWR. All other factors,

namely, workpiece material, dielectric, pulse on time, pulse off time and interactions were found to be insignificant. The rank of importance for various factors in the terms of their relative significance is given in the Table 5.3. Current has the highest rank, signifying highest contribution to TWR and dielectric has the lowest rank and was observed to have insignificant affect on TWR. Main effect plot for mean TWR is shown in the Figure 5.1 which shows the variation of TWR with the input parameters. As can be seen TWR increases with increase in current and pulse on. TWR in tungsten-copper electrode as compared to graphite electrode is low. Also, TWR decreased with addition of powder in dielectric and significantly affected the TWR when tungsten powder has mixed in the dielectric. The interaction plots are shown in the Figure 5.2 which shows that none of interaction was significant for the TWR.

Table 5.2: ANOVA for TWR

Sources	SS	v	V	F	F (critical)	SS'	% contribution
Workpiece (A)	0.13	2	0.07	0.55			
Dielectric (B)	0.11	1	0.11	0.95			
Electrode (C)	3.58	1	3.58	30.08	13.7	3.25	14.000
Pulse off time (D)	2.14	2	1.07	9.00			
Pulse on time (E)	0.43	2	0.22	1.81			
Current (F)	8.62	2	4.31	36.19	10.9	7.96	34.271
Powder (G)	4.06	2	2.03	17.03	10.9	3.39	14.615
(A × C)	0.74	2	0.37	3.10			
(A × G)	1.20	4	0.30	2.52			
(C × G)	1.48	2	0.74	6.23			
Error	0.71	6	0.12				
TOTAL	23.22	26	0.89			23.22	100
e pooled	6.96	21	0.33			8.62	37.114

Table 5.3: Response table for means of TWR

Level	Workpiece (A)	Dielectric (B)	Electrode (C)	Pulse off time(D)	Pulse on time (E)	Current (F)	Powder (G)
1	1.52	1.69	1.86	1.21	1.43	0.80	1.78
2	1.69	1.55	1.08	1.70	1.63	1.98	1.95
3	1.58			1.88	1.73	2.02	1.06
Delta	0.16	0.13	0.77	0.66	0.30	1.21	0.89
Rank	6	7	3	4	5	1	2

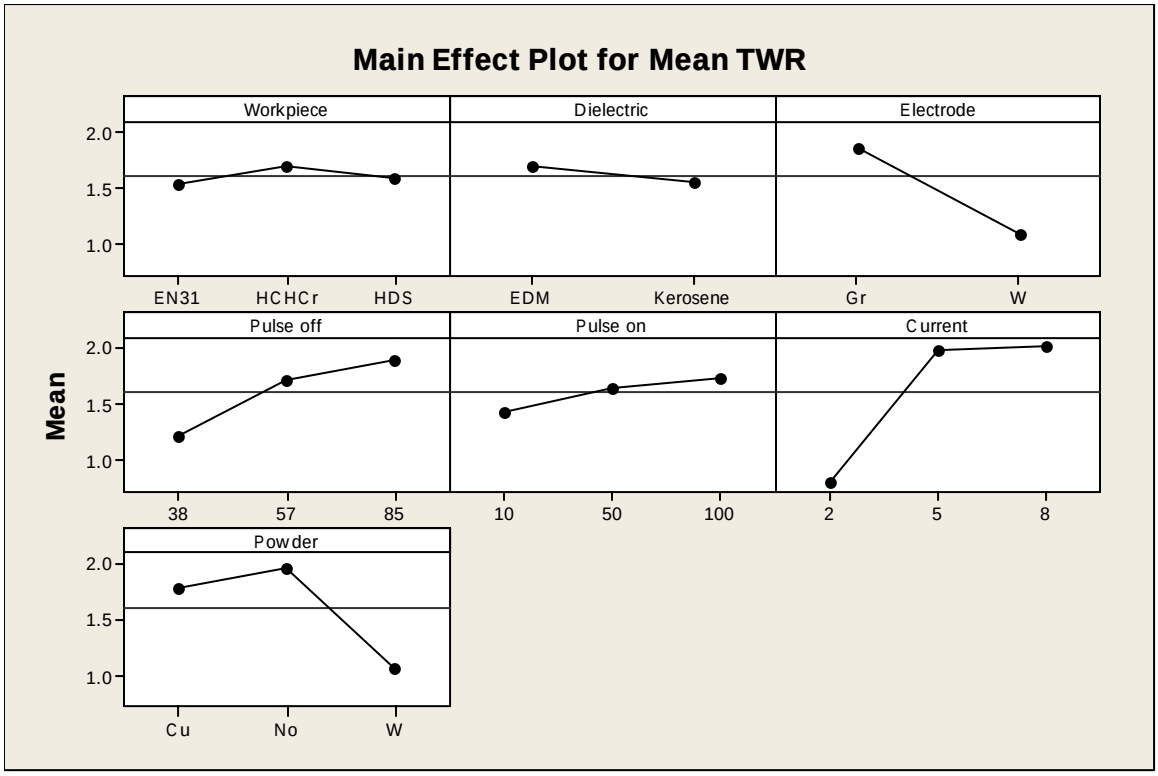

Figure 5.1: Main effects plot for mean TWR

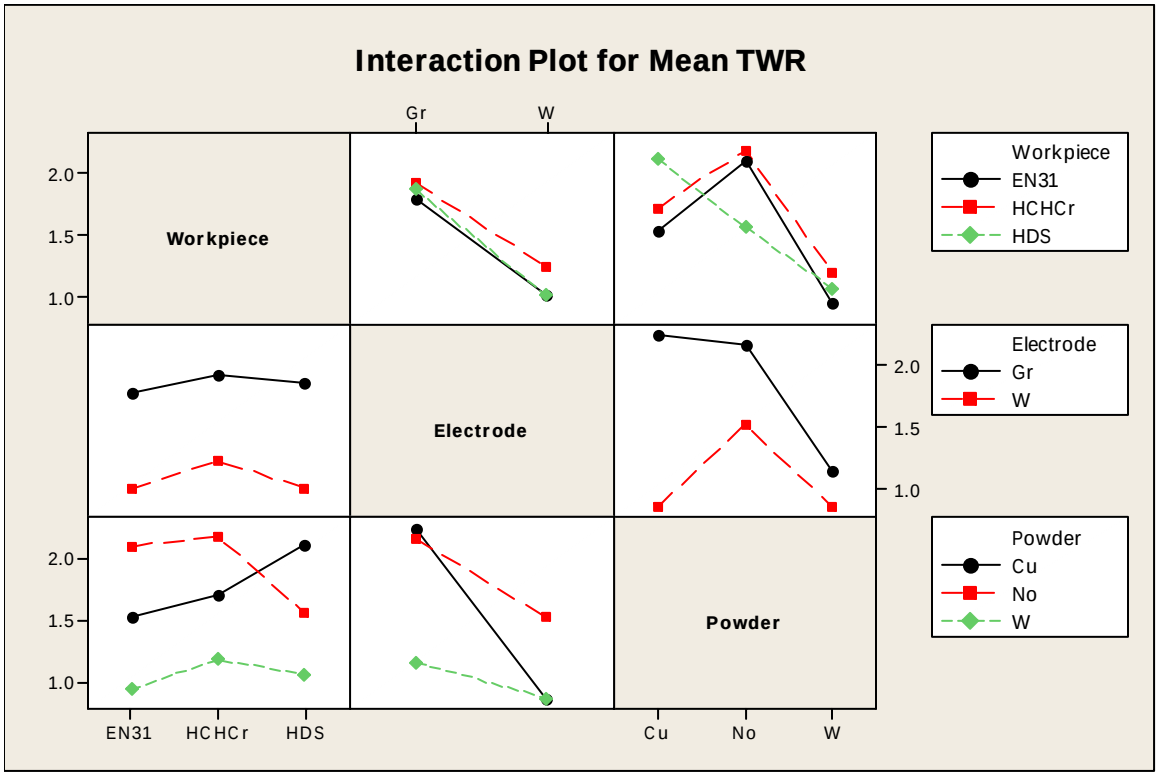

Figure 5.2: Interaction plot for mean TWR

5.4 RESULTS FOR S/N RATIO - TWR

The S/N ratios have been calculated to identify the major contributing factors and interactions that cause variation in TWR. TWR is a "Lower is better", type response and is given by a logarithmic function based on the mean square deviation (MSD) given by:

$$S/N_{LB} = -10\log(MSD) = -10\log[(\frac{1}{r}\sum_{i=1}^{r} y^2{}_i)$$

Table 5.4 shows the ANOVA results for S/N ratio of TWR at 99% confidence interval. According the F test, current was observed to be the most significant factor affecting the TWR, followed by electrode, powder and pulse off time. Interaction between electrode and powder is the significant for TWR. The rank of importance of various factors in the terms of their relative significance is given in the Table 5.5. The current has the highest rank, signifying highest contribution to TWR and dielectric has the lowest rank and was observed be insignificant in affecting TWR. Main effect plot and interaction plot of S/N ratio for TWR are shown in the Figure 5.3 and Figure 5.4 respectively.

Table 5.4: ANOVA for S/N of TWR

Sources	SS	v	V	F	F (critical)	SS'	% contribution
Workpiece (A)	6.83	2	3.42	1.18			
Dielectric (B)	0.20	1	0.20	0.07			
Electrode (C)	114.17	1	114.17	39.36	13.7	107.12	10.922
Pulse off time (D)	76.69	2	38.35	13.22	10.9	62.59	6.381
Pulse on time (E)	35.92	2	17.96	6.19			
Current (F)	457.09	2	228.54	78.80	10.9	442.98	45.167
Powder (G)	119.92	2	59.96	20.67	10.9	105.81	10.789
(A × C)	17.63	2	8.82	3.04			
(A × G)	41.90	4	10.48	3.61			
(C × G)	93.02	2	46.51	16.04	10.9	78.92	8.046
Error	17.40	6	2.90				
TOTAL	980.77	26	37.72			980.77	100
e pooled	119.89	17	7.05			183.36	18.695

Table 5.5: Response table for S/N ratio of TWR

Level	Workpiece (A)	Dielectric (B)	Electrode (C)	Pulse off time (D)	Pulse on time (E)	Current (F)	Powder (G)
1	-2.08	-2.18	-3.76	0.05	-0.81	3.46	-3.52
2	-1.83	-2.37	0.59	-3.71	-2.49	-4.61	-4.05
3	-3.00			-3.27	-3.62	-5.78	0.65
Delta	1.16	0.18	3.89	3.77	2.80	9.25	4.71
Rank	6	7	3	4	5	1	2

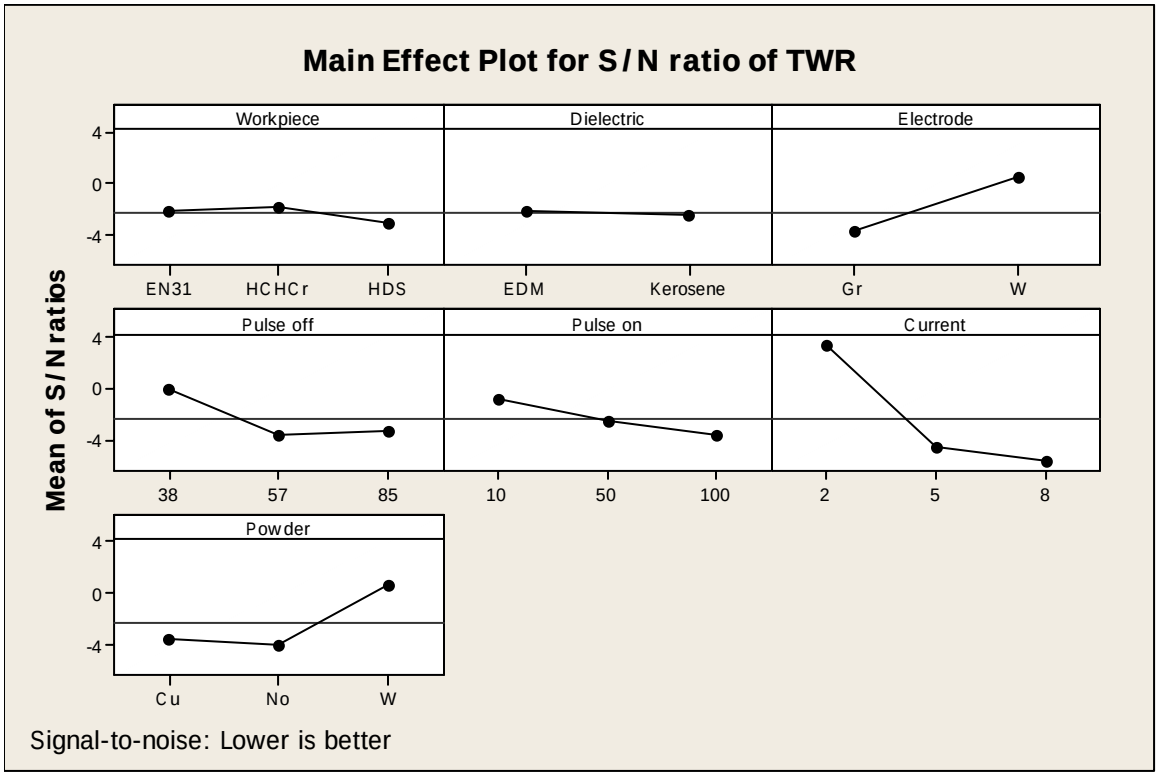

Figure 5.3: Main effects plot of TWR for S/N ratio

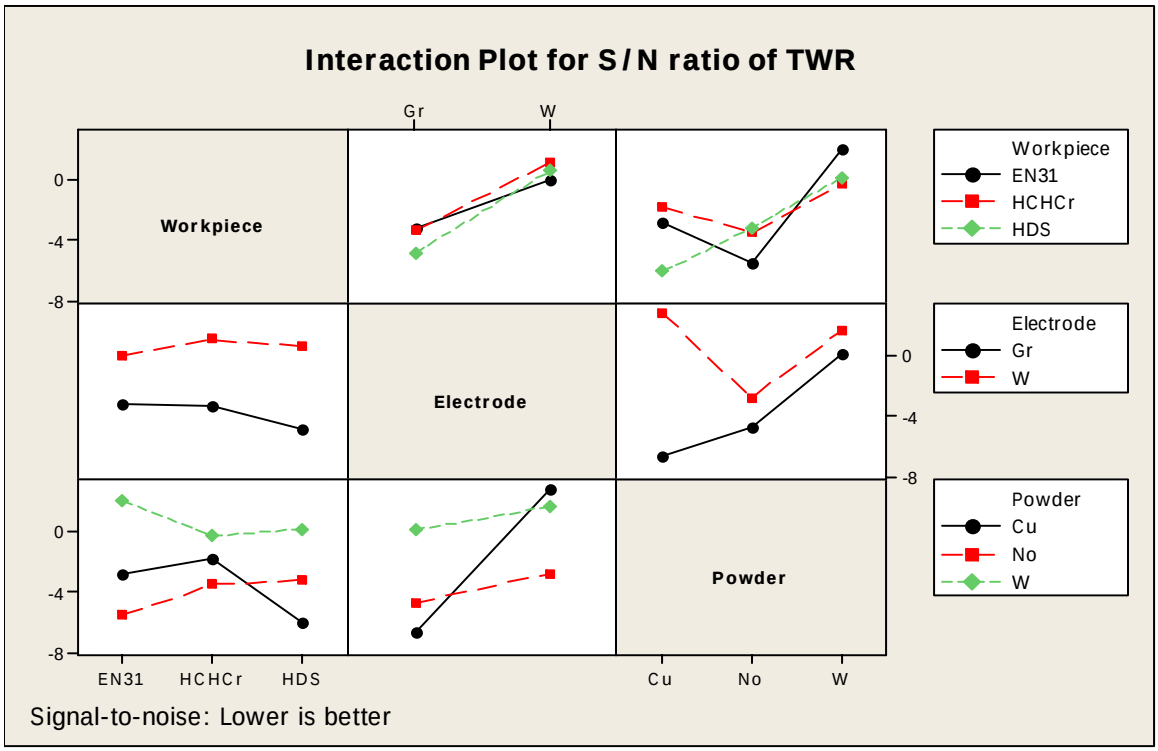

Figure 5.4: Interaction plot for S/N ratio of TWR

5.5 OPTIMAL DESIGN

In this experimental analysis, the main effect plot and interaction plot in Figure 5.1 and Figure 5.2 used to estimate the mean TWR with optimal design conditions. From the, Table 5.6 it is concluded that least TWR was observed when tugsten-copper electrode, current 2Amp and tungsten powder was selected in the treatment conditions. In S/N ratio least TWR was observed when tugsten-copper electrode, pulse off time 57µs, current 5Amp and tungsten powder was selected in treatment condition. In this case, the same levels of the significant factors provide the higher average and reduced variability so nothing has to be compromised. In some situations, the levels of factors which improve the average and improve the uniformity may conflict, so a compromise may have to be reached. Also, a compromise may have to occur when multiple responses are considered and the same factor level may cause one response to improve and another to deteriorate.

Table 5.6: Significant factors and interactions for TWR

Factors	Affecting mean		Affecting variation (S/N ratio)	
	Contribution	Best level	Contribution	Best level
Workpiece (A)	Insignificant	-	Insignificant	-
Dielectric (B)	Insignificant	-	Insignificant	-
Electrode (C)	Significant	Level 2- W-Cu	Significant	Level 2- W-Cu
Pulse off (D)	Insignificant	-	Significant	Level 2- 57µs
Pulse on (E)	Insignificant	-	Insignificant	-
Current (F)	Significant	Level 1- 2 Amp	Significant	Level 2- 5 Amp
Powder (G)	Significant	Level 3- W	Significant	Level 3-W
(A × C)	Insignificant	-	Insignificant	-
(A × G)	Insignificant	-	Insignificant	-
(C × G)	Insignificant	-	Significant	C_2G_3

Estimating the mean

In experimental analysis, the TWR is a lower average response is better (LB) characteristic. Depending on the characteristic, different treatment combinations has chosen to obtain

satisfactory results. After conducting the experiments the optimum treatment condition within the experiments determined on the basis of prescribed combination of factor levels is determined to one of those in the experiment.

Mean value of TWR

$$\mu_{C_2\times G_3,D_2,F_2} = \overline{C_2 \times G_3} + \overline{D_2} + \overline{F_2} - 2\overline{T}$$

$$\mu_{C_2D_2F_2G_3} = 0.87+1.70+1.98-2\times1.60 = 1.35 \text{ mm}^3/\text{min}$$

Confidence Interval around the Estimated Mean

The confidence interval is a maximum and minimum value between which the true average should fall at some stated percentage of confidence. The estimate of the mean μ is only a point estimate based on the averages of results obtained from the experiment.

Confidence Interval around the estimated TWR

$$CI_1 = \sqrt{\frac{F_{\alpha,\nu_1,\nu_2} V_e}{n_{eff}}} \quad \text{Where} \quad F_{\alpha\nu_1\nu_2} = F \text{ ratio}$$

$\alpha = risk$ (0.01) $\qquad$ $confidence = 1-\alpha$

$\nu_1 = dof$ for mean which is always $= 1$

$\nu_2 = dof$ for error $= \nu_e$

n_{eff} = Number of tests under that condition using the participating factors

$$n_{eff} = \frac{N}{1 + dof_{C\times G,D,F}} = \frac{27}{1+2+2+2} = 3.85$$

$$CI_1 = \sqrt{\frac{F_{\alpha,\nu_1,\nu_2} V_e}{n_{eff}}} = \sqrt{\frac{0.21 \times 0.33}{3.85}} = 0.134$$

So the confidence interval around the estimated mean of TWR is given by 1.35±0.134mm^3/min.

CHAPTER 6

RESULTS AND ANALYSIS OF MICRO HARDNESS

6.1 INTRODUCTION

The effect of parameters i.e. workpiece, dielectric, electrode, pulse on time, pulse off time, current, powder and some of their interactions were evaluated using ANOVA and factorial design analysis. A confidence interval of 99% has been used for the analysis. One repetition for each of 27 trials was completed so as to measure Signal to Noise ratio (S/N ratio).

6.2 RESULTS FOR MICRO HARDNESS

The results for micro hardness at deposited region and non-deposited region for each of the 27 treatment conditions with repetition are given in Table 6.1. The micro hardness measurement is dependent on the diameter of indentation on the samples. The indents formed in the pyramid shaped indenter were measured with Quantimet software using a load of 1 kg for 20 seconds.

Table 6.1: Results for micro hardness at non-deposited and deposited region

Trial no.	Micro hardness at non-deposited region (hvn)		Mean Micro hardness	S/N ratio		Micro hardness at deposited region (hvn)		Mean Micro hardness	S/N ratio
	I	II				I	II		
1	635	632	634	56.03		733	723	728	57.24
2	672	678	675	56.58		835	829	832	58.40
3	832	840	836	58.44		1175	1181	1178	61.42
4	774	779	777	57.80		978	971	975	59.77
5	729	735	732	57.29		934	935	935	59.41
6	812	821	817	58.23		1156	1162	1159	61.28
7	671	672	672	56.54		845	838	842	58.50

8	826	820	823	58.30		1012	1018	1015	60.12
9	763	771	767	57.69		1045	1040	1043	60.36
10	745	751	748	57.47		912	920	916	59.23
11	682	687	685	56.70		856	851	854	58.62
12	758	763	761	57.62		1188	1185	1187	61.48
13	724	731	728	57.23		1022	1030	1026	60.22
14	782	776	779	57.83		1047	1053	1050	60.42
15	745	740	743	57.41		1092	1089	1091	60.75
16	687	690	689	56.75		863	871	867	58.76
17	743	750	747	57.46		924	931	928	59.34
18	842	838	840	58.48		1174	1165	1170	61.35
19	731	735	733	57.30		745	738	742	57.40
20	765	758	762	57.63		826	835	831	58.38
21	739	730	735	57.31		1098	1089	1094	60.77
22	768	774	771	57.74		832	840	836	58.44
23	792	798	795	58.00		874	869	872	58.80
24	856	848	852	58.60		1126	1125	1126	61.02
25	774	770	772	57.75		843	839	841	58.49
26	756	761	759	57.599		824	831	828	58.35
27	792	785	789	57.935		1189	1193	1191	61.51

6.3 ANALYSIS OF VARIANCE- MICRO HARDNESS AT NON-DEPOSITED REGION

The results for micro hardness at non deposited region for each of the 27 treatment conditions with repetition are given in Table 6.1. The results were analyzed using ANOVA for identifying the significant factors affecting the performance at 99% confidence interval. ANOVA Table 6.2

shows that factors, namely workpiece material, dielectric, electrode material, pulse on time, pulse off time and interactions studied in trials were found to be insignificant. Table 6.3 shows ranks of various factors in terms of their relative significance. Current has the highest rank, signifying the highest contribution in micro hardness and pulse off has the lowest rank and was observed to be insignificant in micro hardness at non-deposited region. Main effect plots are shown in the Figure 6.1 which shows that micro hardness increases with addition of powder in dielectric medium. The tungsten powder increased the micro hardness as compared to copper powder. The micro hardness increases with increase in current. The micro hardness was found to be high when machined with tungsten electrode as compared to graphite electrode. The interaction plots for micro hardness are shown in Figure 6.2.

Table 6.2: ANOVA for micro hardness at non-deposited region

Sources	SS	v	V	F	F (critical)	SS'	% contribution
Workpiece (A)	4348.96	2	2174.48	2.81			
Dielectric (B)	378.69	1	378.69	0.49			
Electrode (C)	5848.96	1	5848.96	7.55			
Pulse off time(D)	82.57	2	41.29	0.05			
Pulse on time (E)	753.69	2	376.84	0.49			
Current (F)	26757.63	2	13378.81	17.27	10.9	24225.93	31.835
Powder (G)	21492.02	2	10746.01	13.87	10.9	18960.32	24.916
(A × C)	2228.70	2	1114.35	1.44			
(A × G)	5060.70	4	1265.18	1.63			
(C × G)	4496.98	2	2248.49	2.90			
Error	4649.44	6	774.91				
TOTAL	76098.35	26	2926.86			76098.35	100
e pooled	27848.70	22	1265.85			32912.10	43.249

Table 6.3: Response table for means of micro hardness at non-deposited region

Level	Workpiece (A)	Dielectric (B)	Electrode (C)	Pulse off time (D)	Pulse on time (E)	Current (F)	Powder (G)
1	774	750.8	745.7	758.5	750.3	723.6	750.6
2	747.9	758.7	776.9	754.4	754.9	746	724.6
3	746.3			755.3	763.1	798.7	793.1
Delta	27.7	7.9	31.2	4.1	12.8	75.1	68.4
Rank	4	6	3	7	5	1	2

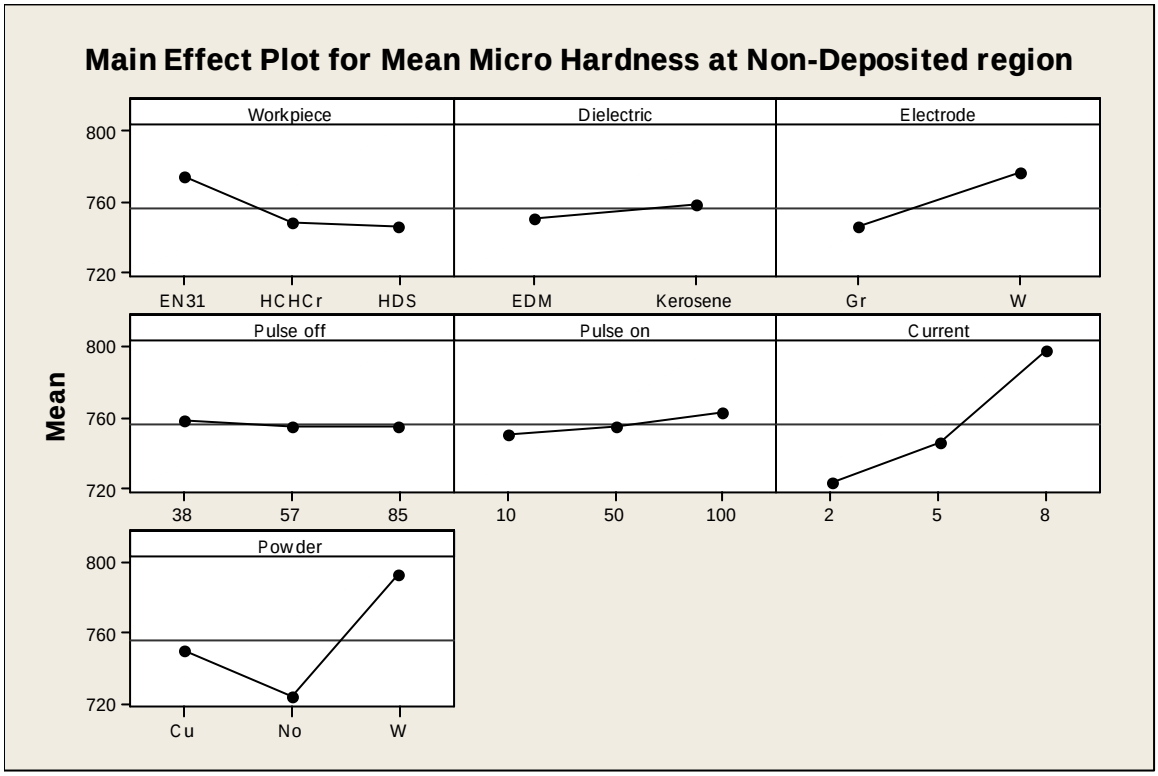

Figure 6.1: Main effect plots for mean micro hardness at non-deposited region

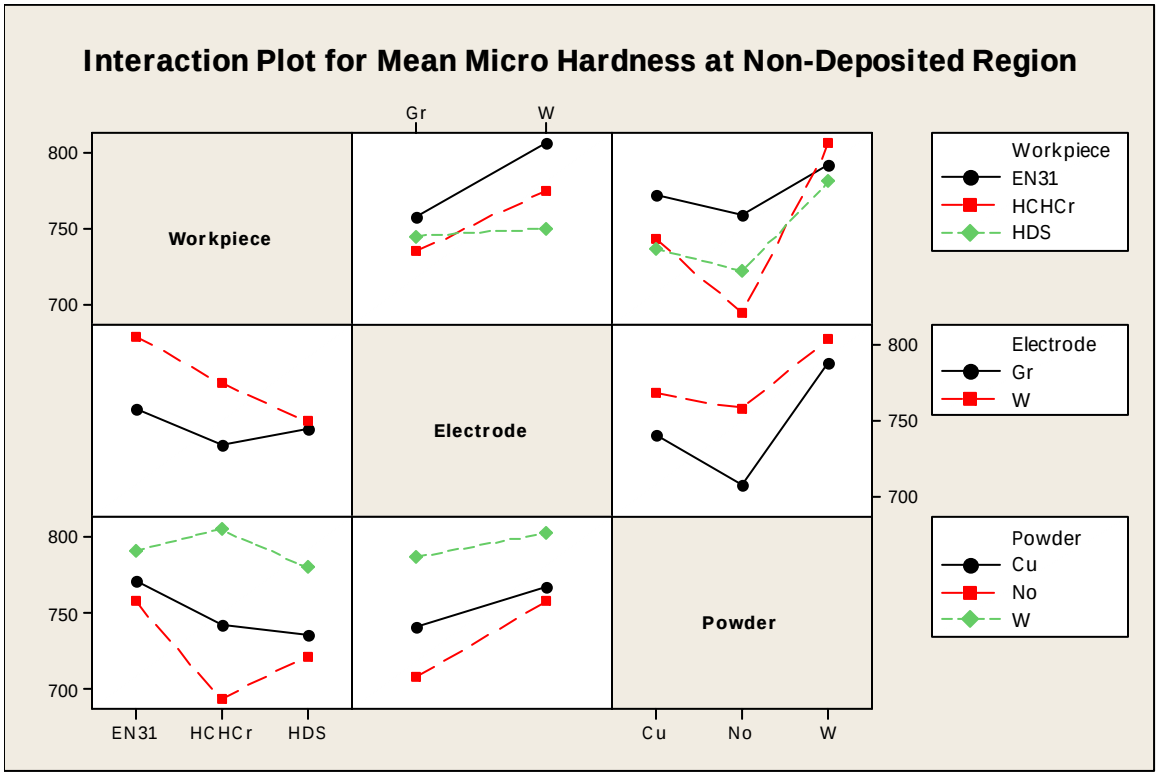

Figure 6.2: Interaction plot for micro hardness at non deposited region

6.4 RESULTS FOR S/N RATIO – MICRO HARDNESS AT NON-DEPOSITED REGION

The S/N ratio consolidated several repetitions into one value and is an indication of the amount of variation present in the process. The S/N ratios have been calculated to identify the major contributing factors and interactions that cause variation in micro hardness at non-deposited region. Micro hardness is a "Higher the better" type response is given by a logarithmic function based on the mean square deviation:

$(S/N)_{HB} = -10 \log (MSD_{HB})$

Where $MSD_{HB} = \frac{1}{r}\sum_{j=1}^{r}\left(\frac{1}{y_j^{\,2}}\right)$

MSD_{HB} = Mean Square Deviation for higher-the-better response.

Table 6.4 shows the ANOVA results for S/N ratio of micro hardness at non-deposited region at 99% confidence interval. The factors, namely, workpiece material, dielectric, electrode material, pulse off time, pulse on time, and interactions studied in trials powder were found to

insignificant for micro hardness at non-deposited region. Table 6.5 shows rank importance to various factors in terms of their relative significance. The highest rank to current signifying the highest contribution to micro hardness and pulse off time has the lowest rank and was observed to be insignificant for micro hardness. Main effect plots and interaction plots of S/N ratio for micro hardness at non-deposited region are shown in the Figure 6.3 and Figure 6.4 respectively.

Table 6.4: ANOVA for S/N ratio of micro hardness at non-deposited region

Sources	SS	v	V	F	F (critical)	SS'	% contribution
Workpiece (A)	0.64	2	0.32	2.96			
Dielectric (B)	0.03	1	0.03	0.28			
Electrode (C)	0.83	1	0.83	7.66			
Pulse off time(D)	0.00	2	0.00	0.02			
Pulse on time (E)	0.10	2	0.05	0.48			
Current (F)	3.54	2	1.77	16.41	10.9	3.14	30.355
Powder (G)	2.86	2	1.43	13.27	10.9	2.46	23.807
(A × C)	0.29	2	0.15	1.36			
(A × G)	0.76	4	0.19	1.77			
(C × G)	0.65	2	0.33	3.02			
Error	0.65	6	0.11				
TOTAL	10.35	26	0.40			10.35	100
e pooled	3.95	20	0.20			4.74	45.838

Table 6.5: Response table for S/N ratio of micro hardness at non-deposited region

Level	Workpiece (A)	Dielectric (B)	Electrode (C)	Pulse off time (D)	Pulse on time (E)	Current (F)	Powder (G)
1	57.77	57.50	57.43	57.57	57.48	57.17	57.49
2	57.44	57.57	57.80	57.53	57.54	57.44	57.18
3	57.44			57.55	57.63	58.04	57.97
Delta	0.33	0.07	0.37	0.03	0.15	0.86	0.79
Rank	4	6	3	7	5	1	2

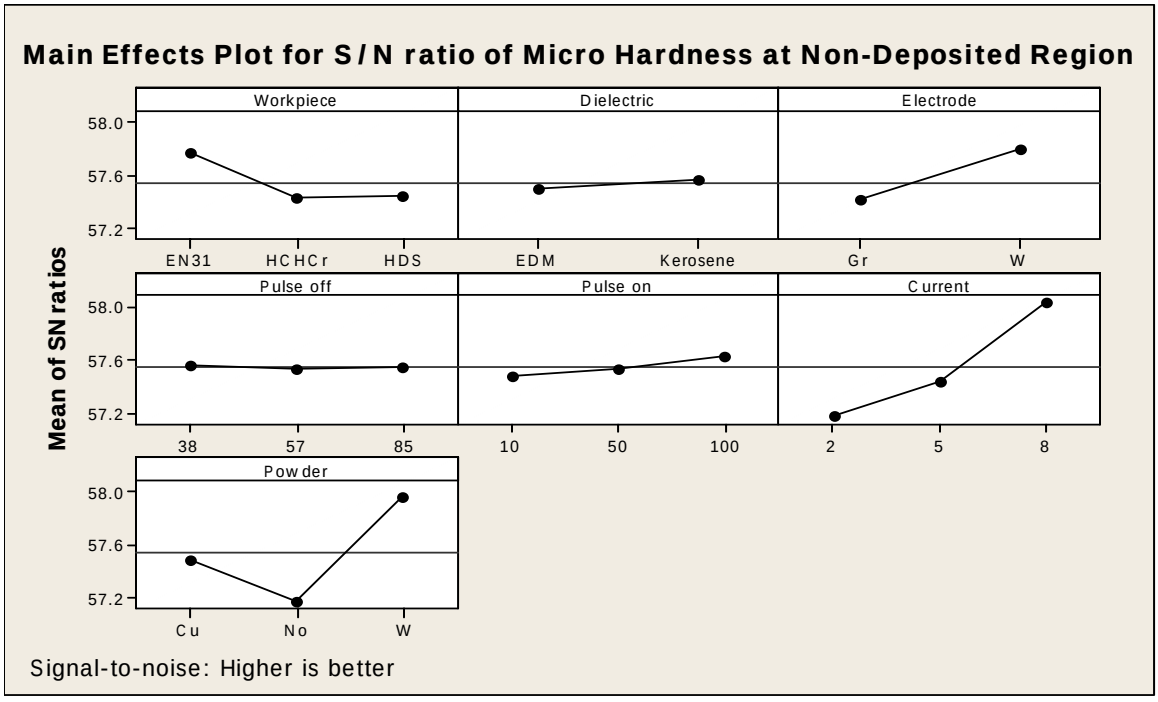

Figure 6.3: Main effect plot for S/N ratio of micro hardness at non-deposited region

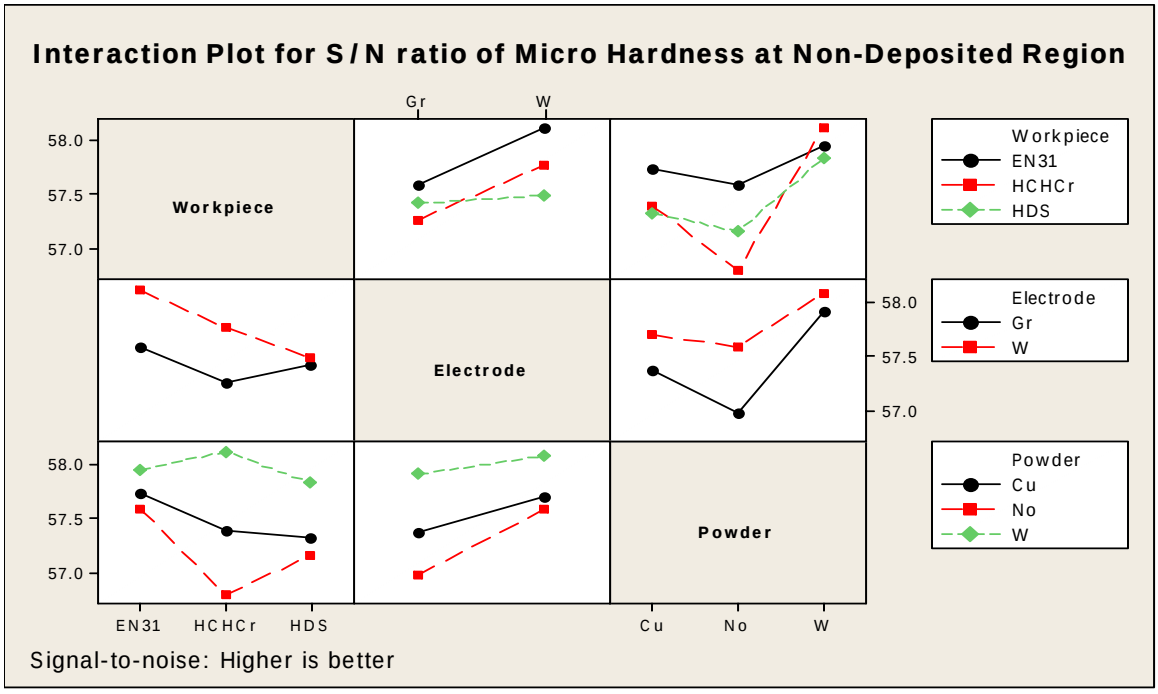

Figure 6.4: Interaction plot for S/N ratio of micro hardness at non-deposited region

6.5 OPTIMAL DESIGN

In this experimental analysis, the main effect plot in Figure 6.1 used to estimate the mean micro hardness at non-deposited region with optimal design coditions. From the, Table 6.6 it is concluded that the highest micro hardness at non-deposited was observed when current 8Amp and tungsten powder was selected in the treatment conditions. In S/N ratio the highest micro hardness was to be observed at same treatment conditions.

Table 6.6 Significant factors and interactions for micro hardness at non-deposited region

Factors	Affecting mean		Affecting variation (S/N ratio)	
	Contribution	Best level	Contribution	Best level
Workpiece (A)	Insignificant	-	Insignificant	-
Dielectric (B)	Insignificant	-	Insignificant	-
Electrode (C)	Insignificant	-	Insignificant	-
Pulse off time (D)	Insignificant	-	Insignificant	-
Pulse on time(E)	Insignificant	-	Insignificant	-
Current (F)	Significant	Level3-8 Amp	Significant	Level 3-8 Amp

Powder (G)	Significant	Level 3- W	Significant	Level 3- W
(A × C)	Insignificant	-	Insignificant	-
(A × G)	Insignificant	-	Insignificant	-
(C × G)	Insignificant	-	Insignificant	-

Estimating the mean

In experimental analysis, the micro hardness is a higher average response is better (HB) characteristic. Depending on the characteristic, different treatment combinations has chosen to obtain satisfactory results. After conducting the experiments the optimum treatment condition within the experiments determined on the basis of prescribed combination of factor levels is determined to one of those in the experiment.

Mean value of micro hardness at non-deposited region

$$\mu_{F_3G_3} = \overline{F_2} + \overline{G_3} - \overline{T}$$

$$\mu_{F_3G_3} = 798+793-756 = 835 \text{ hvn}$$

Confidence Interval around the Estimated Mean

The confidence interval is a maximum and minimum value between which the true average should fall at some stated percentage of confidence. The estimate of the mean μ is only a point estimate based on the averages of results obtained from the experiment. Statistically this provides a 50% chance of the true averages being greater than μ and a 50% chance of the true average being less than μ.

Confidence Interval around the estimated micro hardness at non-deposited region

$$CI_1 = \sqrt{\frac{F_{\alpha,\nu_1,\nu_2} V_e}{n_{eff}}} \quad \text{Where} \quad F_{\alpha\nu_1\nu_2} = F \text{ ratio}$$

$$\alpha = risk \ (0.01) \qquad confidence = 1-\alpha$$

$$\nu_1 = dof \text{ for mean which is always} = 1$$

$\nu_2 = dof \ \ for error = \nu_e$

n_{eff} = Number of tests under that condition using the participating factors

$$n_{eff} = \frac{N}{1 + dof_{F,G}} = \frac{27}{1 + 2 + 2} = 5.4$$

$$CI_1 = \sqrt{\frac{F_{\alpha,\nu_1,\nu_2} V_e}{n_{eff}}} = \sqrt{\frac{0.22 \times 1265.85}{5.4}} = 7.18$$

So the confidence interval around the mean micro hardness at non-deposited region is given by 835±7.18 hvn.

6.6 ANALYSIS OF VARIANCE - MICRO HARDNESS AT DEPOSITED REGION

The results were analyzed using ANOVA for identifying the significant factors affecting the performance measures. The Analysis of Variance (ANOVA) for the mean micro hardness at 99% confidence interval is given in Table 6.7. ANOVA table shows that factors, namely, powder (F value 133.15), electrode material (F value 13.93) and current (F value 13.09) were found to be significant for micro hardness at deposited region. Table 6.8 shows rank of various factors in the terms their relative significance. The powder has the highest rank, signifying highest contribution in micro hardness and pulse off time has the lowest rank and was observed to be insignificant in affecting in micro hardness at deposited region. The interactions were found to be significant for the micro hardness at deposited region. Main effect plots for mean micro hardness at deposited region are shown in the Figure 6.5 which shows that micro hardness has increased with addition of powder in dielectric medium. It was observed that with tungsten powder micro hardness increased as compared to copper powder. The micro hardness increased with increase in current. The micro hardness was found to be more when machined with tungsten electrode as compared to graphite electrode. The interaction plots for micro hardness at deposited region are shown in Figure 6.6.

Table 6.7: ANOVA for micro hardness at deposited region

Sources	SS	v	V	F	F (critical)	SS'	% contribution
Workpiece (A)	29506.06	2	14753.03	10.01			
Dielectric (B)	2709.38	1	2709.38	1.84			
Electrode (C)	20533.50	1	20533.50	13.93	13.7	16046.79	2.940
Pulse off time (D)	812.39	2	406.19	0.28			
Pulse on time (E)	1108.72	2	554.36	0.38			
Current (F)	38596.06	2	19298.03	13.09	10.9	29622.63	5.427
Powder (G)	392439.5	2	196219.7	133.15	10.9	383466.08	70.259
(A × C)	7163.44	2	3581.72	2.43			
(A × G)	15168.78	4	3792.19	2.57			
(C × G)	28910.00	2	14455.00	9.81			
Error	8842.18	6	1473.70				
TOTAL	545790	26	20991.92			545790.00	100
e pooled	94220.94	21	4486.71			116654.50	21.374

Table 6.8: Response table for means of micro hardness at deposited region

Level	Workpiece (A)	Dielectric (B)	Electrode (C)	Pulse off time (D)	Pulse on time (E)	Current (F)	Powder (G)
1	928.7	954.3	949	973	960	919.2	904.7
2	967.2	975.6	1007.5	960.8	969.4	975.2	863.5
3				971.7	975.8	1011.1	1137.3
Delta	80.9	21.2	58.5	12.2	15.6	91.9	273.8
Rank	3	5	4	7	6	2	1

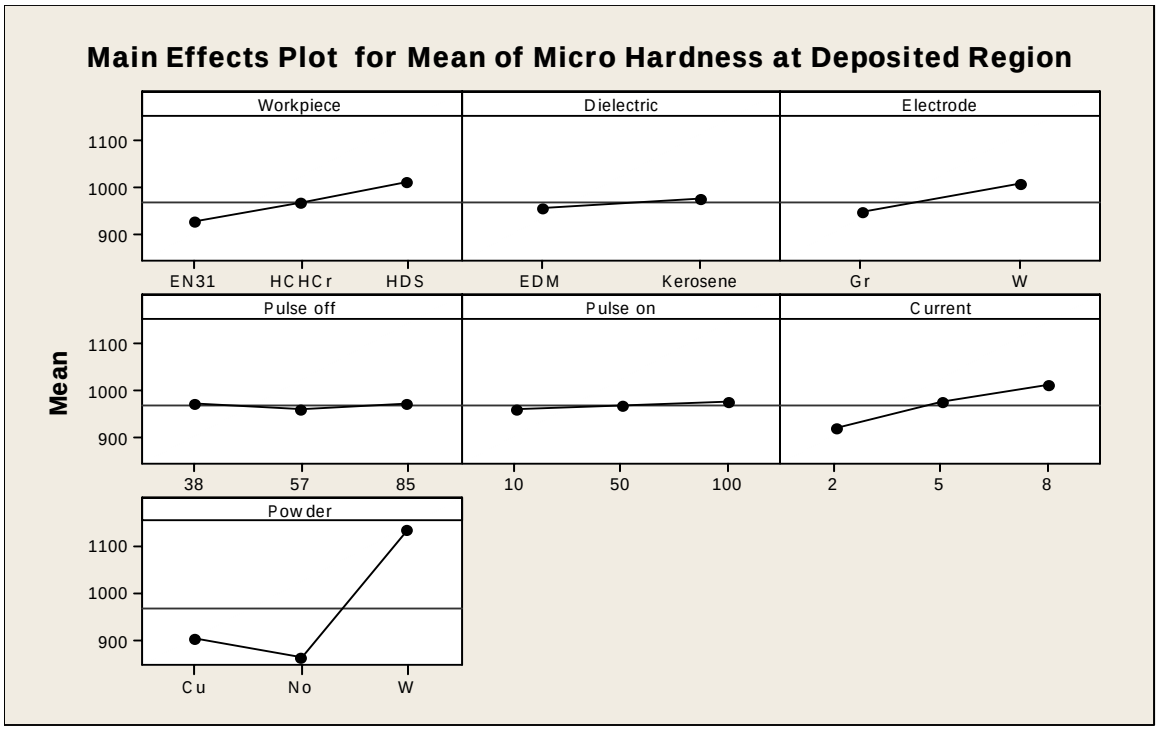

Figure 6.5: Main effect plot for mean micro hardness at deposited region

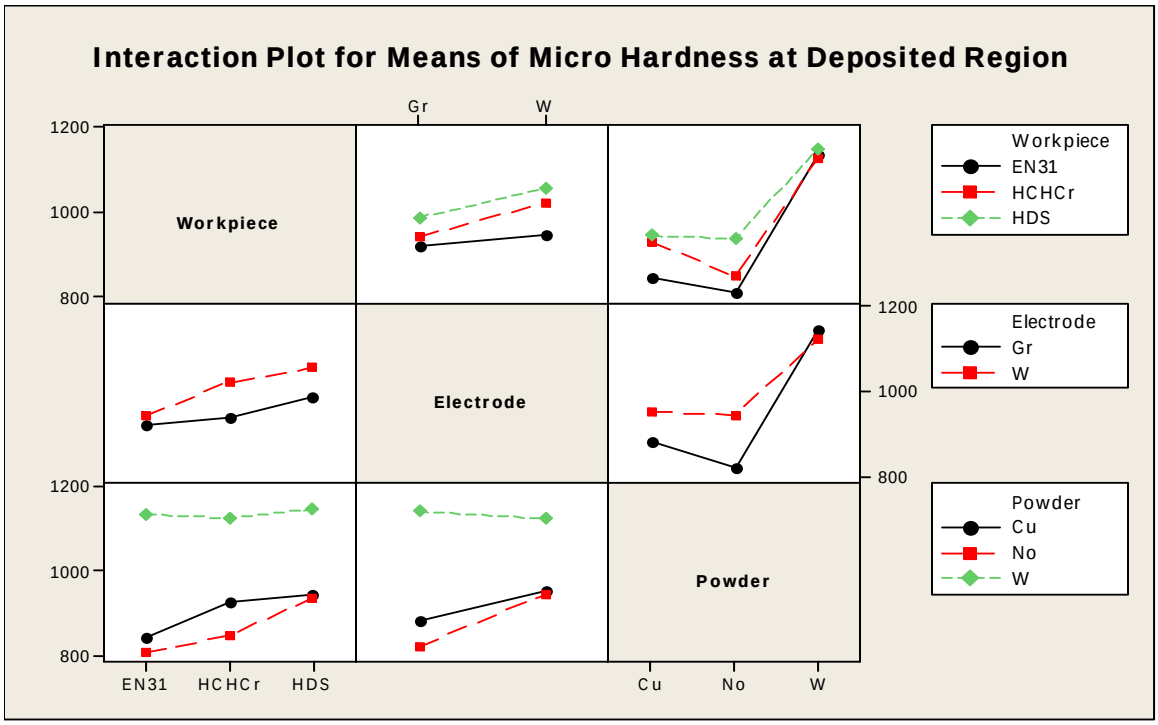

Figure 6.6: Interaction plot of mean micro hardness at deposited region

6.7 RESULTS FOR S/N RATIO – MICRO HARDNESS AT DEPOSITED REGION

The S/N ratio consolidated several repetitions into one value and is an indication of the amount of variation present in the process. The S/N ratios have been calculated to identify the major contributing factors and interactions that cause variation in micro hardness at deposited region. Micro hardness is a "Higher the better" type response is given by a logarithmic function based on the mean square deviation:

$(S/N)_{HB} = -10 \log (MSD_{HB})$

Where $MSD_{HB} = \frac{1}{r}\sum_{j=1}^{r}\left(\frac{1}{y_j^{\,2}}\right)$

MSD_{HB} = Mean Square Deviation for higher-the-better response.

Table 6.9 shows the ANOVA for S/N ratio for micro hardness at 99% confidence interval. Rather than the three factors, namely, electrode material, current and powder all other factors are found to be insignificant. According to F-test powder is the most significant factors which affecting the micro hardness at deposited followed by current, electrode. All interactions studied during the trails were found to be insignificant for micro hardness at deposited region. Main effect plots and interaction plots of S/N ratio for micro hardness at deposited region are shown in the Figure 6.7 and Figure 6.8 respectively.

Table 6.9: ANOVA for S/N ratio of micro hardness at deposited region

Sources	SS	v	V	F	F (critical)	SS'	% contribution
Workpiece (A)	2.73	2	1.36	8.86			
Dielectric (B)	0.08	1	0.08	0.53			
Electrode (C)	2.03	1	2.03	13.23	13.7	1.62	3.581
Pulse off time (D)	0.07	2	0.04	0.24			
Pulse on time (E)	0.08	2	0.04	0.27			
Current (F)	4.17	2	2.09	13.55	10.9	3.35	7.385
Powder (G)	30.44	2	15.22	98.94	10.9	29.62	65.377

(A × C)	0.66	2	0.33	2.13			
(A × G)	1.52	4	0.38	2.47			
(C × G)	2.59	2	1.30	8.43			
Error	0.92	6	0.15				
TOTAL	45.30	26	1.74			45.30	100
e pooled	8.66	21	0.41			10.72	23.656

Table 6.10: Response table for S/N ratio of micro hardness at deposited region

Level	Workpiece (A)	Dielectric (B)	Electrode (C)	Pulse off time (D)	Pulse on time (E)	Current (F)	Powder (G)
1	59.25	59.55	59.43	59.66	59.55	59.19	59.10
2	59.61	59.67	60.02	59.55	59.64	59.66	58.68
3	60.2			59.67	59.69	60.03	61.11
Delta	0.78	0.12	0.58	0.11	0.13	0.84	2.43
Rank	3	6	4	7	5	2	1

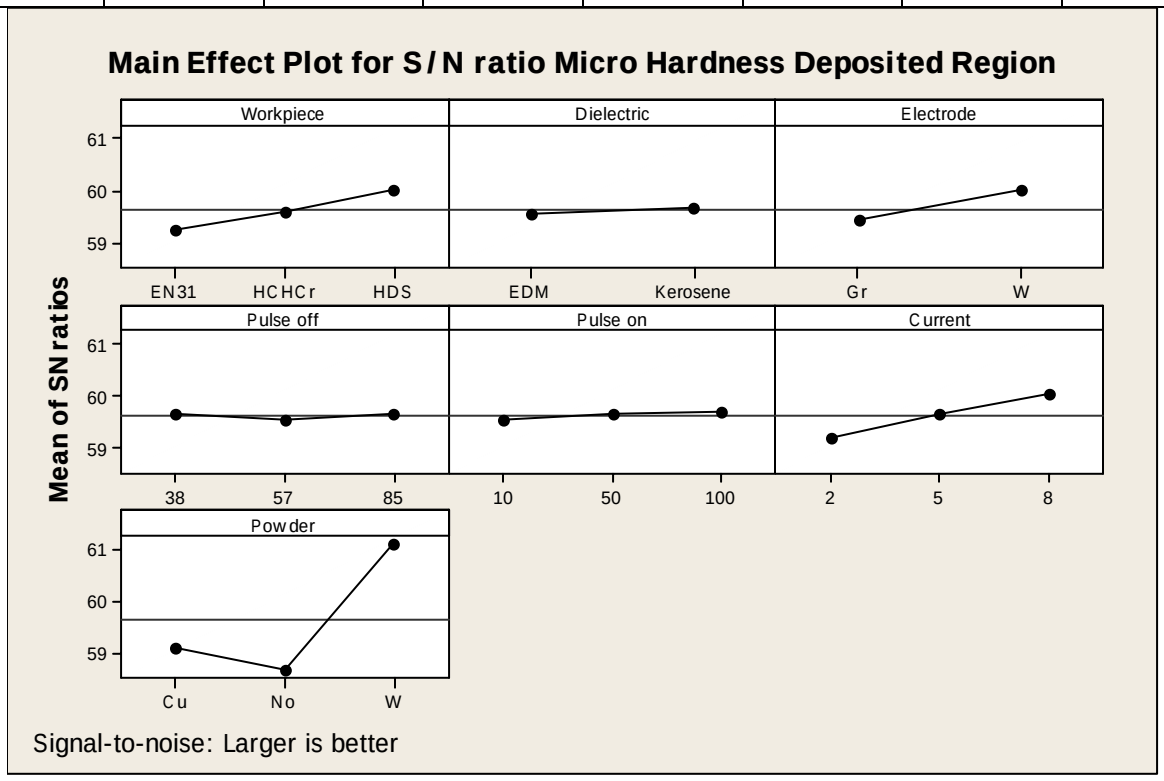

Figure 6.7: Main effect plot for S/N ratio of micro hardness at deposited region

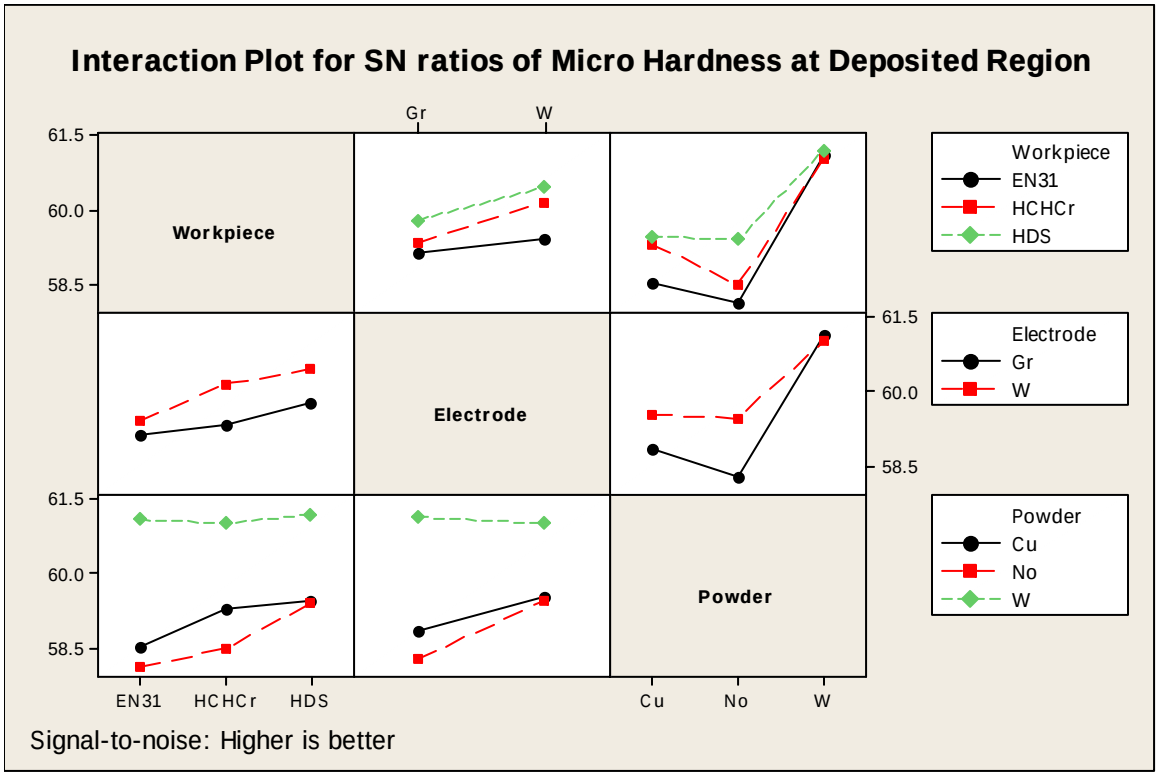

Figure 6.8: Interaction plot of SN ratio for micro hardness at deposited region

6.8 OPTIMAL DESIGN

In this experimental analysis, the main effect plot in Figure 6.5 used to estimate the mean micro hardness at deposited region. From the, Table 6.11 it is concluded that the highest micro hardness at deposited was observed when current 8Amp, tungsten-copper electrode and tungsten powder was selected in the treatment conditions. In S/N ratio the highest micro hardness was to be observed at same treatment conditions.

Table 6.11: Significant factors and interactions for micro hardness at deposited region

Factors	Affecting mean		Affecting variation (S/N ratio)	
	Contribution	Best level	Contribution	Best level
Workpiece (A)	Insignificant	-	Insignificant	-
Dielectric (B)	Insignificant	-	Insignificant	-
Electrode (C)	Significant	Level 2- W-Cu	Significant	Level 2- W-Cu
Pulse off time (D)	Insignificant	-	Insignificant	-
Pulse on time (E)	Insignificant	-	Insignificant	-

Current (F)	Significant	Level 3- 8 Amp	Significant	Level 3- 8 Amp
Powder (G)	Significant	Level 3- W	Significant	Level 3- W
(A × C)	Insignificant	-	Insignificant	-
(A × G)	Insignificant	-	Insignificant	-
(C × G)	Insignificant	-	Insignificant	-

Estimating the mean

Mean value of micro hardness at deposited region

$\mu_{C_2F_3G_3} = \overline{C_2} + \overline{F_3} + \overline{G_3} - 2\overline{T}$

$\mu_{C_2F_3G_3}$ = 1007.5+1011.11+1137.33-2×968.5 = 1218.94 HVN

Confidence Interval around the Estimated Mean

Confidence Interval around the estimated micro hardness at deposited region:

$CI_1 = \sqrt{\frac{F_{\alpha,\nu_1,\nu_2} V_e}{n_{eff}}}$ Where $F_{\alpha\nu_1\nu_2} = F\ ratio$

$\alpha = risk$ (0.01) $confidence = 1-\alpha$

$\nu_1 = dof\ for\ mean\ which\ is\ always = 1$

$\nu_2 = dof\ for\ error = \nu_e$

n_{eff} = Number of tests under that condition using the participating factors

$$n_{eff} = \frac{N}{1 + dof_{F,G}} = \frac{27}{1+2+2} = 5.4$$

$$CI_1 = \sqrt{\frac{F_{\alpha,v_1,v_2} V_e}{n_{eff}}} = \sqrt{\frac{0.21 \times 4486.71}{5.4}} = 13.20$$

So the confidence interval around the mean micro hardness at deposited region is given by 1218.94±13.20 hvn.

CHAPTER 7

RESULTS AND ANALYSIS OFSURFACE ROUGHNESS

7.1 INTRODUCTION

The effect of parameters i.e. workpiece, dielectric, electrode, pulse on time, pulse off time, current, powder and some of their interactions were evaluated using ANOVA and factorial design analysis. A confidence interval of 99% has been used for the analysis. One repetition for each of 27 trials was completed so as to measure Signal to Noise ratio (S/N ratio).

7.2 RESULTS FOR SURFACE ROUGHNESS (R_a)

In this experiment surface roughness of 27 treatment conditions with repetition are measured at three positions, namely, center, left and right of each sample. The left and right positions were taken 7 mm on each side of center. The results for surface roughness at center for each of the 27 treatment conditions with repetition are given in Table 7.1.

Table 7.1: Results for surface roughness at center, left and right position

Trial no.	Surface roughness at center position (microns)		Mean	S/N ratio	Surface roughness at left position (microns)		Mean	S/N ratio	Surface roughness at right position (microns)		Mean	S/N ratio
	I	II			I	II			I	II		
1	3.74	3.79	3.76	-11.52	3.51	3.43	3.47	-10.80	3.05	3.5	3.27	-10.33
2	6.43	5.92	6.17	-15.82	6.30	6.89	6.6	-16.39	6.04	5.85	5.95	-15.49
3	8.10	8.64	8.37	-18.46	10.52	9.28	9.90	-19.93	8.17	7.69	7.93	-17.98
4	8.72	8.79	8.75	-18.84	7.14	9.02	8.08	-18.20	7.9	8.67	8.28	-18.37
5	4.09	4.21	4.15	-12.36	3.95	3.99	3.97	-11.98	3.75	4.03	3.89	-11.81
6	5.55	6.12	5.84	-15.33	6.17	5.51	5.84	-15.34	6.52	6.22	6.37	-16.08
7	5.57	5.21	5.39	-14.64	5.87	5.67	5.77	-15.22	6.03	5.21	5.62	-15.02
8	6.36	6.87	6.61	-16.42	6.38	7.79	7.08	-17.05	6.95	7.9	7.42	-17.43

9	3.49	4.02	3.75	-11.51	4.11	3.85	3.98	-12.00	3.66	4.20	3.93	-11.91
10	6.77	8.17	7.47	-17.51	6.72	7.94	7.33	-17.33	6.49	7.00	6.75	-16.59
11	5.37	4.91	5.14	-14.22	5.55	4.72	5.13	-14.24	5.77	5.37	5.57	-14.92
12	6.29	5.96	6.12	-15.74	5.83	5.88	5.85	-15.35	5.75	5.83	5.79	-15.26
13	4.73	4.36	4.54	-13.15	5.03	5.3	5.16	-14.26	4.83	4.94	4.89	-13.78
14	6.85	7.50	7.17	-17.12	6.94	7.24	7.09	-17.01	6.95	7.15	7.05	-16.96
15	5.53	5.90	5.715	-15.14	5.75	6.08	5.91	-15.44	6.17	5.93	6.05	-15.64
16	4.51	4.79	4.65	-13.36	5.01	4.86	4.93	-13.86	4.67	4.57	4.62	-13.29
17	5.79	4.97	5.385	-14.64	5.63	5.34	5.48	-14.79	5.16	5.36	5.26	-14.42
18	8.38	8.15	8.26	-18.34	8.17	7.69	7.93	-17.98	8.29	8.38	8.34	-18.42
19	6.18	6.96	6.57	-16.36	6.83	6.70	6.77	-16.61	6.99	6.8	6.89	-16.77
20	6.43	6.44	6.43	-16.17	6.21	5.67	5.94	-15.48	6.1	6.2	6.15	-15.77
21	5.33	5.57	5.45	-14.73	4.69	5.57	5.13	-14.24	4.78	4.77	4.78	-13.58
22	5.79	5.58	5.68	-15.1	5.11	4.98	5.04	-14.06	5.42	4.88	5.15	-14.25
23	7.41	6.95	7.18	-17.13	7.44	7.55	7.49	-17.49	7.1	6.82	6.96	-16.85
24	6.75	5.68	6.21	-15.90	6.94	6.22	6.58	-16.38	6.86	6.35	6.61	-16.41
25	5.26	5.57	5.41	-14.67	5.27	5.2	5.24	-14.39	5.21	5.43	5.32	-14.52
26	3.80	3.38	3.59	-11.12	4.04	4.38	4.21	-12.49	4.13	3.93	4.03	-12.11
27	6.32	7.89	7.10	-17.08	6.48	6.93	6.71	-16.53	6.68	7.27	6.98	-16.88

7.3 ANALYSIS OF VARIANCE- SURFACE ROUGHNESS AT CENTER POSITION

The results were analyzed using ANOVA for identifying the significant factors affecting the performance measures. The Analysis of Variance (ANOVA) for the mean surface roughness at 99% confidence interval is given in Table 7.2. The two factors, namely, current (F value 52.63) and pulse on time (F value 21.27) were found to be significant in surface roughness at center position. All other factors, namely, workpiece, dielectric, electrode, pulse off time, powder and interactions studied during trials were found to be insignificant for surface roughness. Table 7.3 shows the ranks of various factors in terms of their relative significance. Current has the highest

rank, signifying the highest contribution to surface roughness and workpiece material has the lowest rank and was observed to be insignificant in affecting surface roughness. Main effect plot and interaction plot are shown in Figure 7.1 and Figure 7.2 respectively. As the current and pulse on time increases, surface roughness increased. With tungsten powder, surface roughness of machined surface increases and with copper powder surface roughness decreases.

Table 7.2: ANOVA for surface roughness at center position

Sources	SS	v	V	F	F (critical)	SS'	% contribution
Workpiece (A)	0.15	2	0.08	0.27			
Dielectric (B)	0.46	1	0.46	1.66			
Electrode (C)	0.43	1	0.43	1.57			
Pulse off time (D)	0.75	2	0.37	1.35			
Pulse on time(E)	11.72	2	5.86	21.27	10.9	10.78	21.146
Current (F)	28.99	2	14.50	52.63	10.9	28.06	55.024
Powder (G)	1.72	2	0.86	3.11			
(A × C)	1.65	2	0.82	2.99			
(A × G)	1.01	4	0.25	0.92			
(C × G)	2.47	2	1.23	4.48			
Error	1.65	6	0.28				
TOTAL	50.99	26	1.96			50.99	100
e pooled	10.28	22	0.47			12.15	23.83

Table 7.3: Response table for means of surface roughness at center position

Level	Workpiece (A)	Dielectric (B)	Electrode (C)	Pulse off time (D)	Pulse on time (E)	Current (F)	Powder (G)
1	5.963	6.146	5.873	5.803	5.089	4.658	5.762
2	5.871	5.870	6.141	5.892	6.118	6.036	5.808
3	6.054			6.192	6.680	7.193	6.318
Delta	0.183	0.276	0.269	0.389	1.591	2.535	0.556
Rank	7	5	6	4	2	1	3

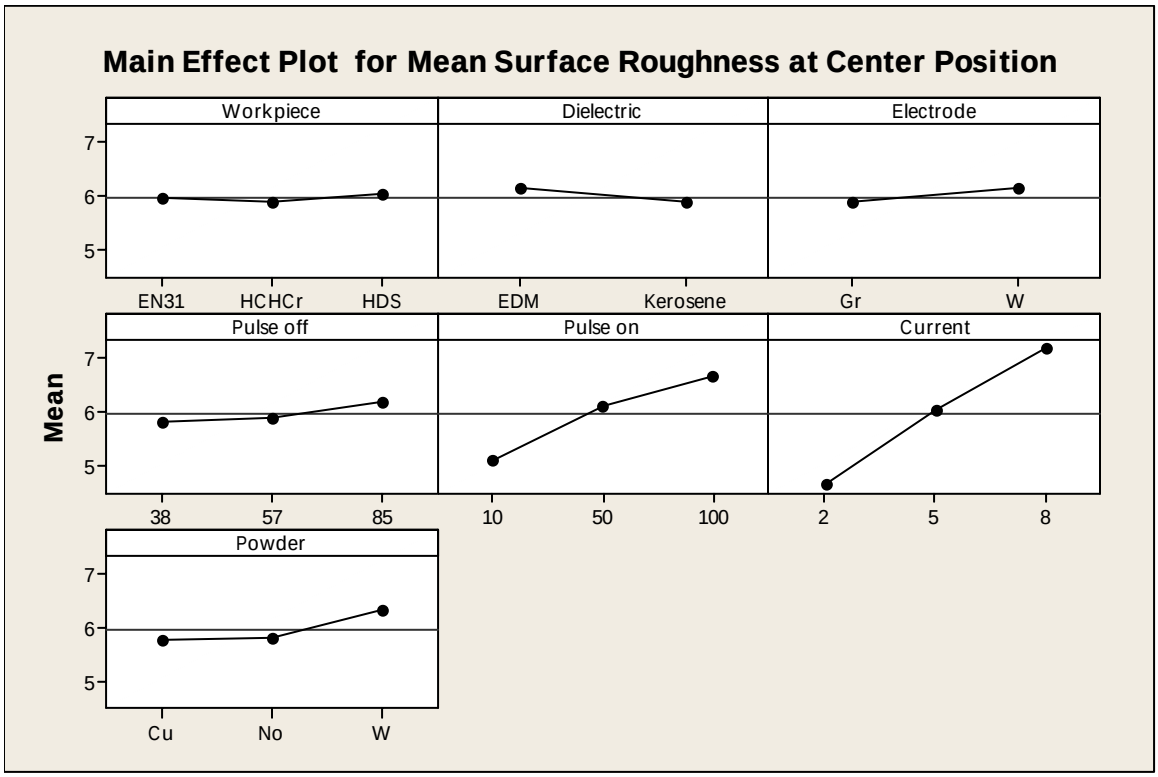

Figure 7.1: Main effect plot for mean surface roughness at center position

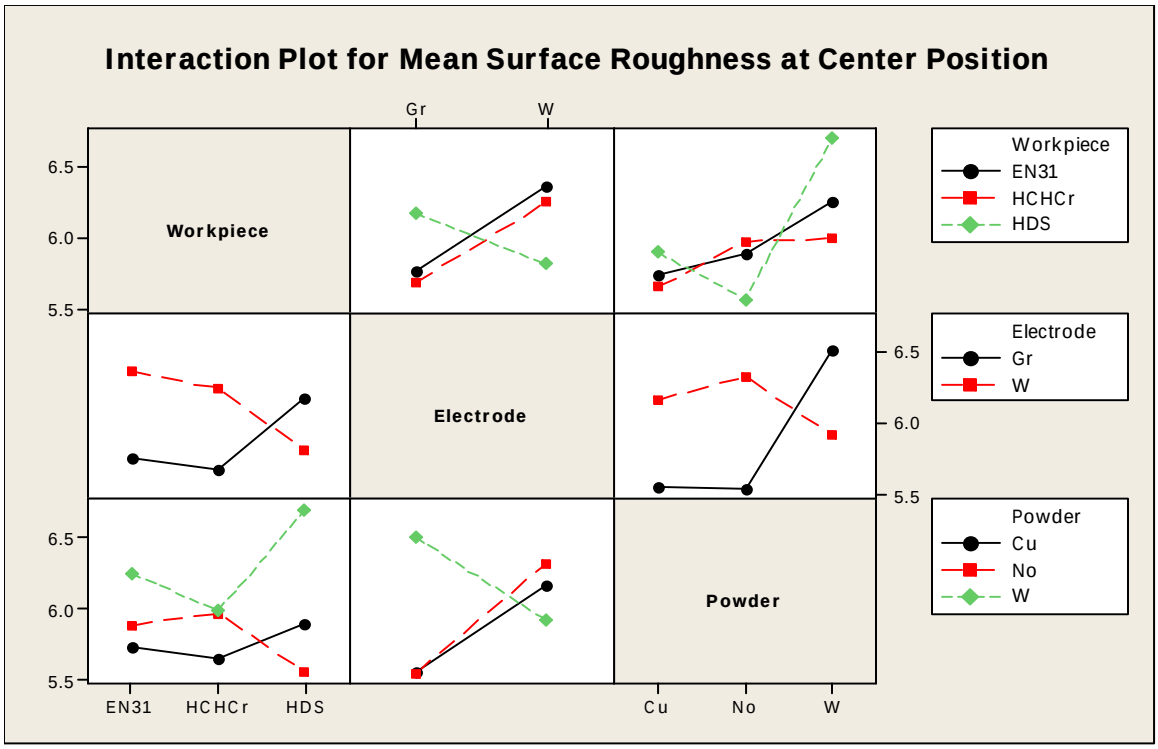

Figure 7.2: Interaction plot surface roughness at center position

7.4 RESUTLS FOR S/N RATIO - SURFACE ROUGHNESS AT CENTER POSITION

The S/N ratios have been calculated to identify the major contributing factors and interactions that cause variation in surface roughness. Surface roughness is a "Lower is better", type response and is given by a logarithmic function based on the mean square deviation (MSD) given by:

$$S/N_{LB} = -10\log(MSD) = -10\log[(\frac{1}{r}\sum_{i=1}^{r} y^2{}_i)$$

Table 7.4 shows the ANOVA for S/N ratio for roughness at 99% confidence interval. The two factors, namely, current and pulse on time were found to be significant in surface roughness. Remaining all other factors and all interactions studied during the trials were found to be insignificant. Table 7.5 shows the ranks to various factors in terms of their relative significance. Current has the highest rank, signifying the highest contribution to surface roughness and dielectric has the lowest rank and was observed to be insignificant in affecting surface roughness. Main effect plo and interaction plots for S/N ratio are shown in Figure 7.3 and Figure 7.4 respectively.

Table 7.4: ANOVA for S/N ratio of surface roughness at center position

Sources	SS	v	V	F	F (critical)	SS'	% contribution
Workpiece (A)	1.15	2	0.57	0.71			
Dielectric (B)	1.07	1	1.07	1.32			
Electrode (C)	1.14	1	1.14	1.41			
Pulse off time (D)	2.20	2	1.10	1.36			
Pulse on time (E)	26.13	2	13.07	16.20	10.9	23.99	20.612
Current (F)	66.62	2	33.31	41.30	10.9	64.47	55.399
Powder (G)	3.82	2	1.91	2.37			
(A × C)	3.57	2	1.78	2.21			
(A × G)	2.70	4	0.68	0.84			
(C × G)	3.14	2	1.57	1.95			
Error	4.84	6	0.81				
TOTAL	116.38	26	4.48			116.38	100
e pooled	23.62	22	1.07			27.92	23.98

Table 7.5: Response table for S/N ratio of roughness at center position

Level	Workpiece (A)	Dielectric (B)	Electrode (C)	Pulse off time (D)	Pulse on time (E)	Current (F)	Powder (G)
1	-15.37	-15.56	-15.13	-15.06	-13.97	-13.23	-15.00
2	-14.99	-15.14	-15.57	-15.09	-15.53	-15.55	-14.02
3	-15.47			-15.68	-16.34	-17.05	-15.81
Delta	0.37	0.42	0.44	0.62	2.37	3.82	0.81
Rank	5	7	6	4	2	1	3

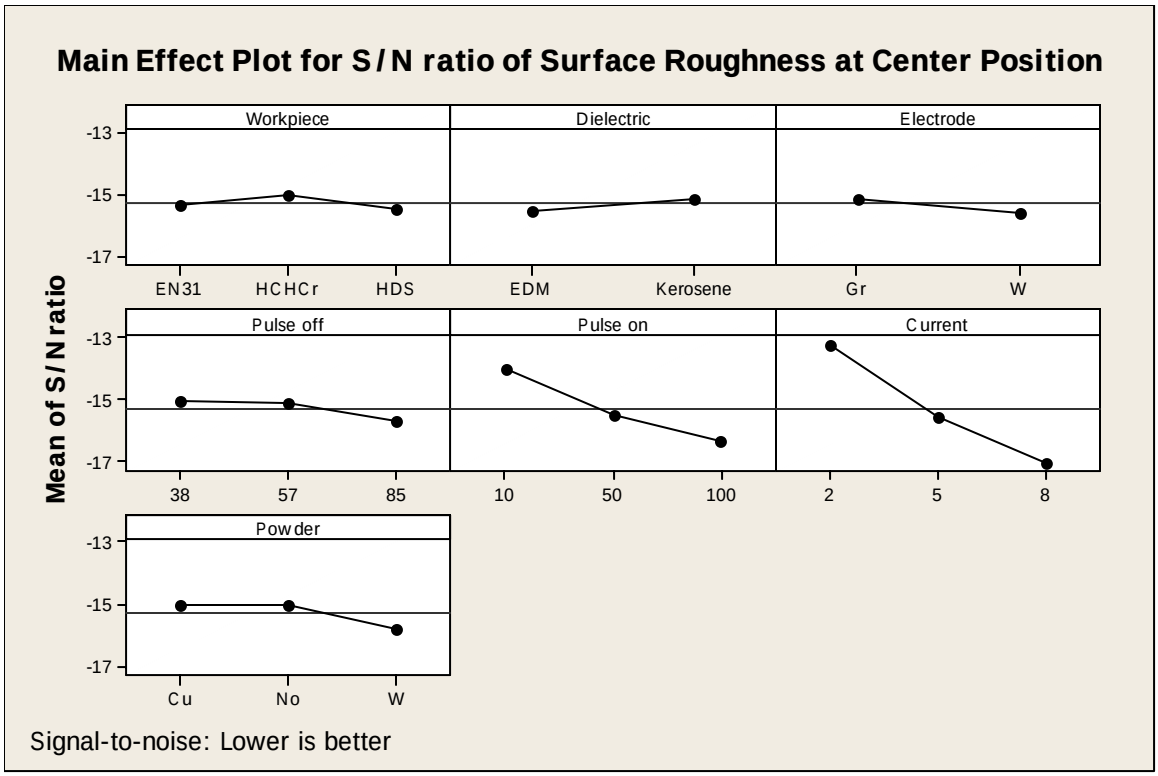

Figure 7.3: Main effect plot for S/N ratio of surface roughness at center position

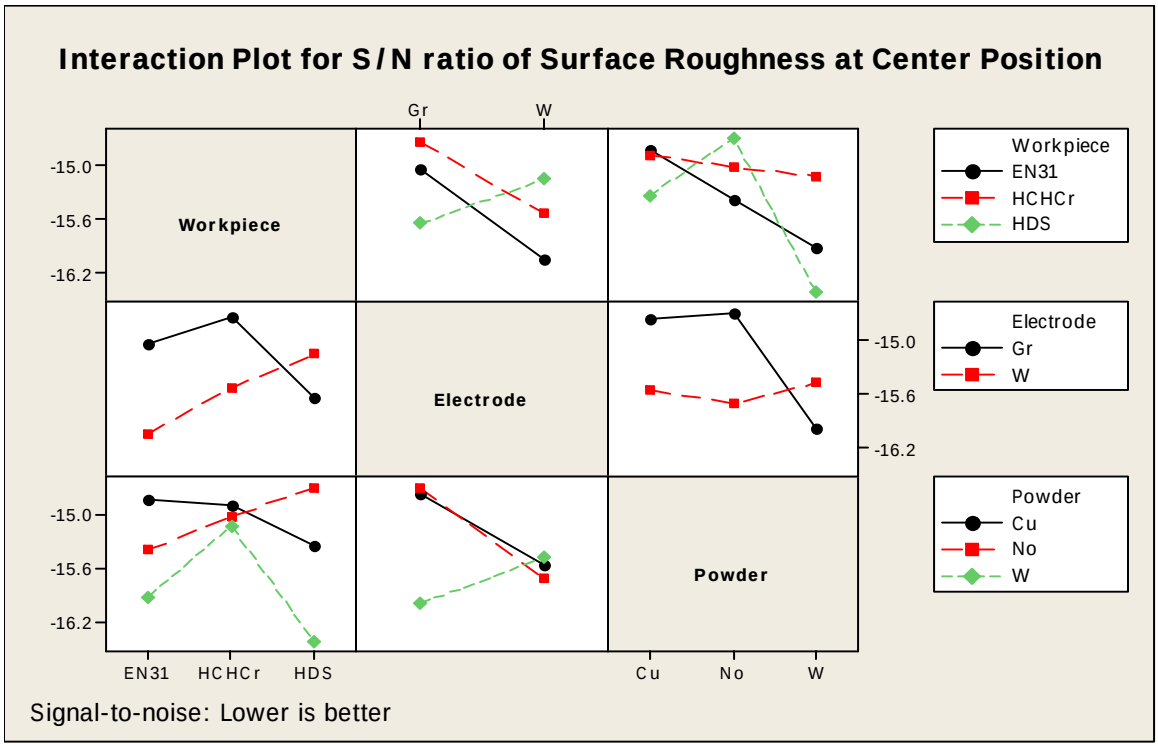

Figure 7.4: Interaction plot for of S/N ratio of surface roughness center position

7.5 OPTIMAL DESIGN

In this experimental analysis, the main effect plot in Figure 7.1 used to estimate the mean value surface roughness with. From the, Table 7.6 it is concluded that least surface roughness was observed when pulse on time 10µs, current 2Amp were chosen in the treatment conditions. In this case, the same levels of the significant factors provide the higher average and reduced variability so nothing has to be compromised.

Table 7.6: Significant factors and interactions for surface roughness at center position

Factors	Affecting mean		Affecting variation (S/N ratio)	
	Contribution	Best level	Contribution	Best level
Workpiece (A)	Insignificant	-	Insignificant	-
Dielectric (B)	Insignificant	-	Insignificant	-
Electrode (C)	Insignificant	-	Insignificant	-
Pulse off time (D)	Insignificant	-	Insignificant	-
Pulse on time (E)	Significant	Level 1-10 µs	Significant	Level 1- 10 µs
Current (F)	Significant	Level 1- 2 Amp	Significant	Level 1- 2 Amp
Powder (G)	Insignificant	-	Insignificant	-
(A × C)	Insignificant	-	Insignificant	-
(A × G)	Insignificant	-	Insignificant	-
(C × G)	Insignificant	-	Insignificant	-

Estimating the mean

In experimental analysis, the surface roughness is a lower average response is better (LB) characteristic. Depending on the characteristic, different treatment combinations has chosen to obtain satisfactory results. After conducting the experiments the optimum treatment condition within the experiments determined on the basis of prescribed combination of factor levels is determined to one of those in the experiment.

Estimating the mean

Mean value of surface roughness at center position:

$\mu_{E_1F_1} = \overline{E_1} + \overline{F_1} - \overline{T}$

$\mu_{E_1F_1}$ = 4.65+4.65-5.96 =3.34 microns

Confidence Interval around the Estimated Mean

The confidence interval is a maximum and minimum value between which the true average should fall at some stated percentage of confidence. The estimate of the mean μ is only a point estimate based on the averages of results obtained from the experiment. Statistically this provides a 50% chance of the true averages being greater than μ and a 50% chance of the true average being less than μ.

Confidence Interval around the estimated mean of surface roughness at center position

$CI_1 = \sqrt{\frac{F_{\alpha,\nu_1,\nu_2} V_e}{n_{eff}}}$ Where $F_{\alpha\nu_1\nu_2} = F\ ratio$

$\alpha = risk\ (0.01)$ $confidence = 1-\alpha$

$\nu_1 = dof\ for\ mean\ which\ is\ always = 1$

$\nu_2 = dof\ for\ error = \nu_e$

n_{eff} = Number of tests under that condition using the participating factors

$$n_{eff} = \frac{N}{1 + dof_{E,F}} = \frac{27}{1+2+2} = 5.4$$

$$CI_1 = \sqrt{\frac{F_{\alpha,\nu_1,\nu_2} V_e}{n_{eff}}} = \sqrt{\frac{0.22 \times 0.47}{5.4}} = 0.13$$

So the confidence interval around the surface roughness at center position is given by 3.34±0.13 microns.

7.6 ANALYSIS OF VARIANCE- SURFACE ROUGHNESS AT LEFT POSITION

The results for surface roughness at left position for each of the 27 treatment conditions with repetition are given in Table 7.1. The Analysis of Variance (ANOVA) for the mean surface roughness at 99% confidence interval is given in Table 7.7. The two factors, namely, current and pulse on time were found to be significant in surface roughness at center position. All other factors, namely, workpiece, dielectric, electrode, pulse off time, powder and interactions studied during trials were found to be insignificant for surface roughness. Table 7.8 shows the ranks to various factors according to significance in surface roughness; current has higher rank which has highest contribution in surface roughness. Main effect plot and interaction plot for surface roughness at left position are shown in the Figure 7.5 and Figure 7.6 respectively. As the current, pulse on time and pulse off time increases, surface roughness increased. With tungsten powder, surface roughness of machined surface increases.

Table 7.7: ANOVA for surface roughness at left position

Sources	SS	v	V	F	F (critical)	SS'	% contribution
Workpiece (A)	0.20	2	0.10	0.31			
Dielectric (B)	0.18	1	0.18	0.56			
Electrode (C)	0.16	1	0.16	0.48			
Pulse off time (D)	0.71	2	0.36	1.10			
Pulse on time (E)	14.92	2	7.46	23.07	10.9	14.12	25.951
Current (F)	30.74	2	15.37	47.53	10.9	29.94	55.023
Powder (G)	2.27	2	1.14	3.52			
(A × C)	1.74	2	0.87	2.69			
(A × G)	0.19	4	0.05	0.15			
(C × G)	1.36	2	0.68	2.11			
Error	1.94	6	0.32				
TOTAL	54.41	26	2.09			54.41	100
e pooled	8.76	22	0.40			10.35	19.02

Table 7.8: Response table for means of surface roughness at left position

Level	Workpiece (A)	Dielectric (B)	Electrode (C)	Pulse off time (D)	Pulse on time (E)	Current (F)	Powder (G)
1	5.904	6.141	5.972	5.834	5.078	4.645	5.892
2	6.079	5.968	6.134	6.012	6.107	6.189	5.757
3	6.094			6.232	6.893	7.243	6.429
Delta	0.190	0.173	0.161	0.397	1.815	2.598	0.672
Rank	5	6	7	4	2	1	3

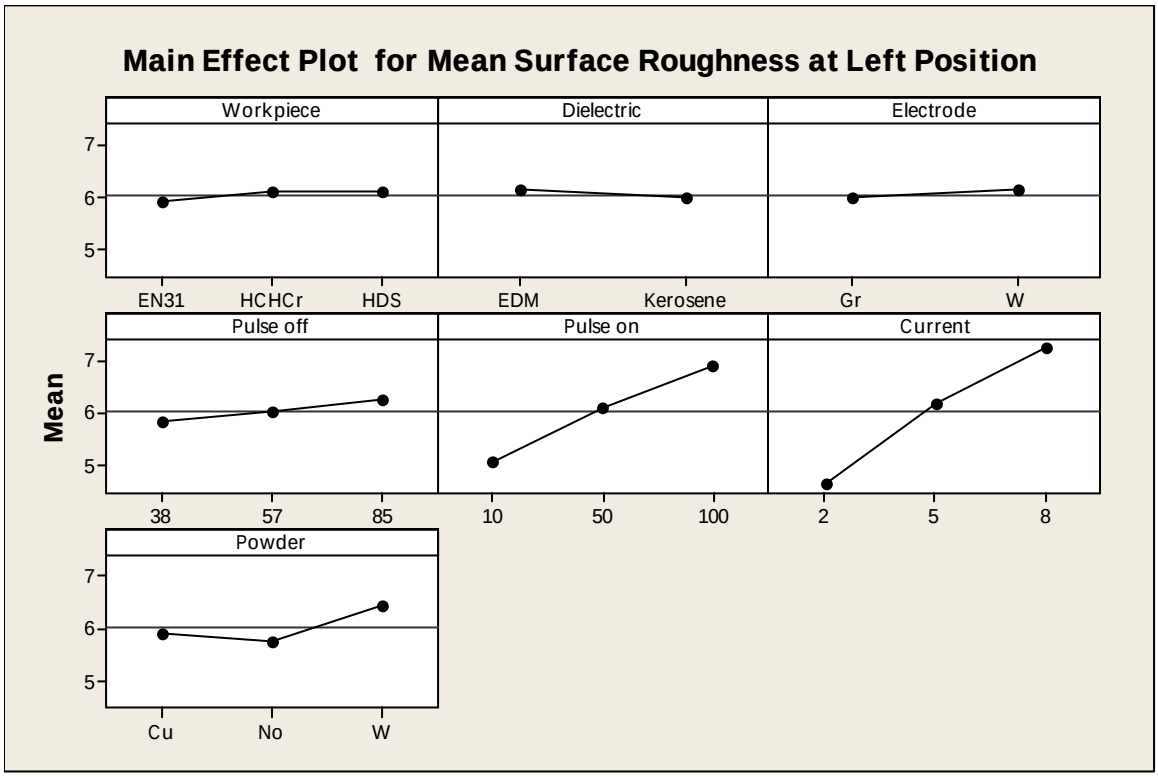

Figure 7.5: Main effect plot for of surface roughness at left position

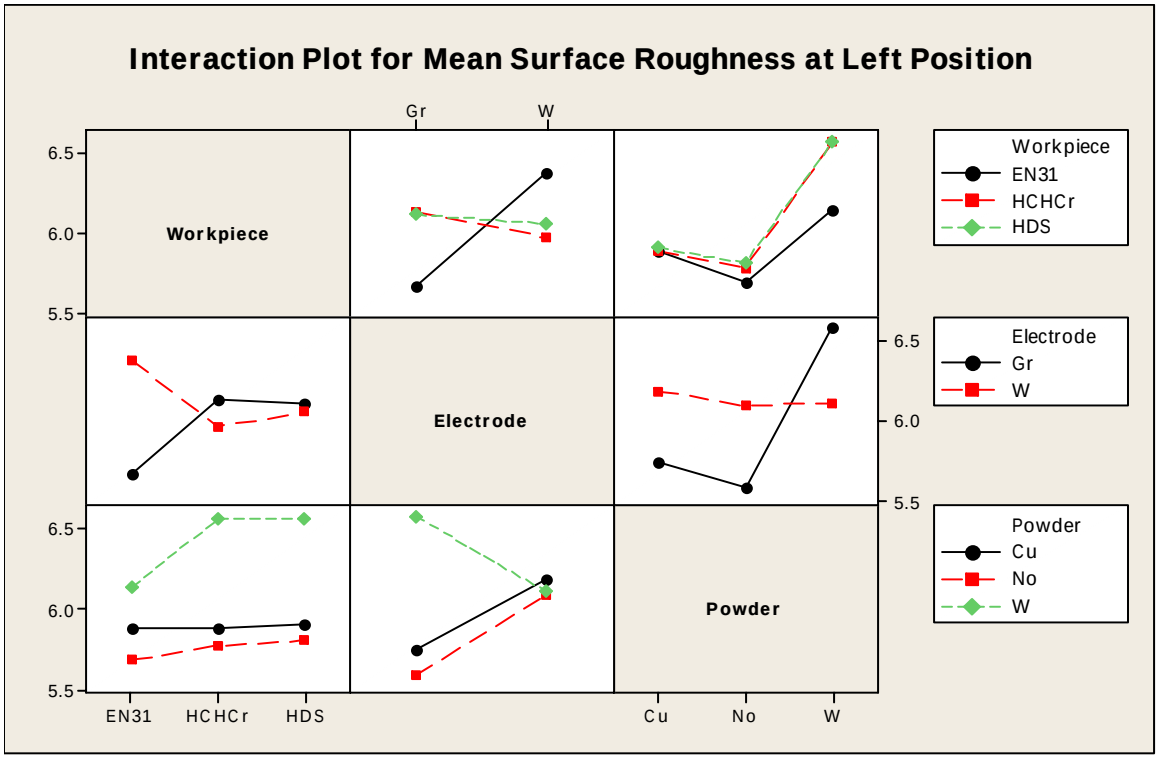

Figure 7.6: Interaction plot for surface roughness at left position

7.7 RESULTS FOR S/N RATIO -SURFACE ROUGHNESS AT LEFT POSITION

The S/N ratios have been calculated to identify the major contributing factors and interactions that cause variation in surface roughness. Surface roughness is a "Lower is better", type response and is given by a logarithmic function based on the mean square deviation (MSD) given by:

$$S/N_{LB} = -10\log(MSD) = -10\log[(\frac{1}{r}\sum_{i=1}^{r} y^2{}_i)$$

Table 7.9 shows the ANOVA for S/N ratio for roughness at 99% confidence interval. The two factors, namely, current and pulse on time was found to be significant in surface roughness. Remaining factors and all interactions studied during the trials were found to be insignificant. Table 7.10 shows the ranks to various factors in terms of their relative significance. Current has the highest rank, signifying the highest contribution to surface roughness and dielectric has the lowest rank and was observed to be insignificant in affecting surface roughness. Main effect plot and interaction plot for S/N ratio are shown in Figure 7.7 and Figure 7.8 respectively.

Table 7.9: ANOVA for S/N ratio of surface roughness at left position

Sources	SS	v	V	F	F (critical)	SS'	% contribution
Workpiece (A)	0.68	2	0.34	0.74			
Dielectric (B)	0.66	1	0.66	1.43			
Electrode (C)	0.59	1	0.59	1.29			
Pulse off time (D)	1.37	2	0.69	1.49			
Pulse on time (E)	32.36	2	16.18	35.21	10.9	31.06	26.870
Current (F)	68.96	2	34.48	75.03	10.9	67.66	58.532
Powder (G)	4.29	2	2.14	4.66			
(A × C)	2.25	2	1.12	2.44			
(A × G)	0.20	4	0.05	0.11			
(C × G)	1.49	2	0.74	1.62			
Error	2.76	6	0.46				
TOTAL	115.59	26	4.45			115.59	100
e pooled	14.28	22	0.65			16.88	14.599

Table 7.10: Response table for S/N ratio of surface roughness at left position

Level	Workpiece (A)	Dielectric (B)	Electrode (C)	Pulse off time (D)	Pulse on time (E)	Current (F)	Powder (G)
1	-15.30	-15.59	-15.26	-15.09	-13.94	-13.24	-15.22
2	-15.22	-15.26	-15.58	-15.37	-15.57	-15.78	-14.97
3	-15.59			-15.65	-16.60	-17.09	-15.92
Delta	0.37	0.33	0.31	0.55	2.66	3.85	0.94
Rank	5	6	7	4	2	1	3

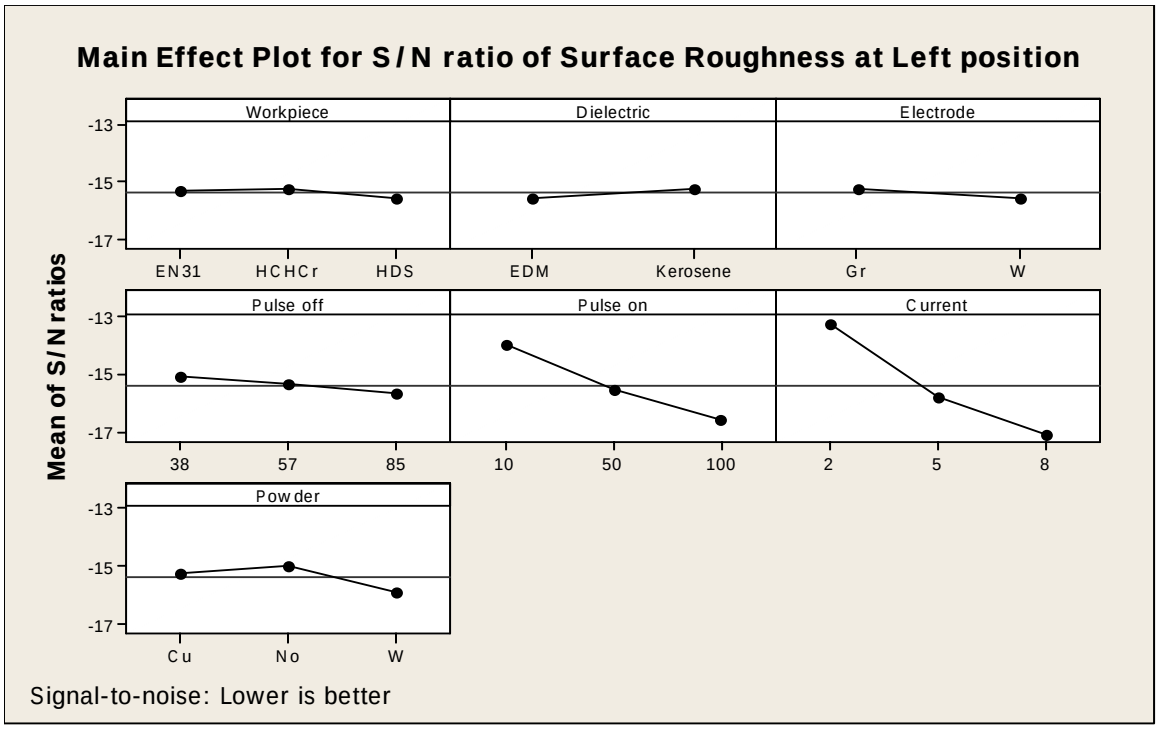

Figure 7.7: Main effect plot for S/N ratio of surface roughness at left position

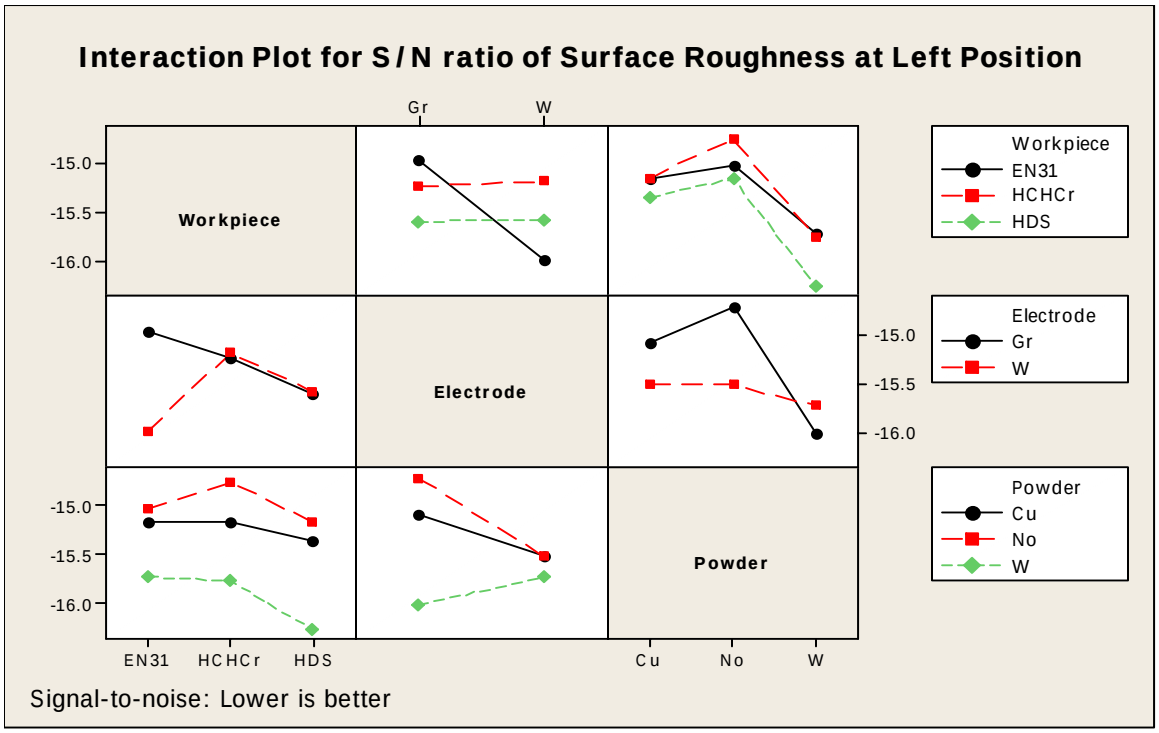

Figure 7.8: Interaction plot for S/N ratio of surface roughness at left position

7.8 OPTIMAL DESIGN

In this experimental analysis, the main effect plot in Figure 7.5 used to estimate the mean surface roughness. From the, Table 7.11 it is concluded that least surface roughness was observed when pulse on time 10µs and current 2Amp was chosen in the treatment conditions. In this case, the same levels of the significant factors provide the higher average and reduced variability so nothing has to be compromised.

Table 7.11: Significant factors and interactions for surface roughness at left position

Factors	Affecting mean		Affecting variation (S/N ratio)	
	Contribution	Best level	Contribution	Best level
Workpiece (A)	Insignificant	-	Insignificant	-
Dielectric (B)	Insignificant	-	Insignificant	-
Electrode (C)	Insignificant	-	Insignificant	-
Pulse off (D)	Insignificant	-	Insignificant	-
Pulse on (E)	Significant	Level 1-10 µs	Significant	Level 1- 10 µs
Current (F)	Significant	Level 1- 2 Amp	Significant	Level 1- 2 Amp
Powder (G)	Insignificant	-	Insignificant	-
(A × C)	Insignificant	-	Insignificant	-
(A × G)	Insignificant	-	Insignificant	-
(C × G)	Insignificant	-	Insignificant	-

Estimating the mean

Mean value of surface roughness at left position:

$$\mu_{E_1F_1} = \overline{E_1} + \overline{F_1} - \overline{T}$$

$$\mu_{E_1F_1} = 4.64+5.07-6.02 = 3.69 \text{ microns}$$

Confidence Interval around the Estimated Mean

Confidence Interval around the estimated surface roughness at left position:

$$CI_1 = \sqrt{\frac{F_{\alpha,\nu_1,\nu_2} V_e}{n_{eff}}} \quad \text{Where} \quad F_{\alpha\nu_1\nu_2} = F\ ratio$$

$\alpha = risk\ (0.01)$ $\qquad$ $confidence\ = 1-\alpha$

$\nu_1 = dof\ \ for\ mean\ which\ is\ always = 1$

$\nu_2 = dof\ \ for\ error = \nu_e$

n_{eff} = Number of tests under that condition using the participating factors

$$n_{eff} = \frac{N}{1 + dof_{E,F}} = \frac{27}{1+2+2} = 5.4$$

$$CI_1 = \sqrt{\frac{F_{\alpha,\nu_1,\nu_2} V_e}{n_{eff}}} = \sqrt{\frac{0.22 \times 0.40}{5.4}} = 0.12$$

So the confidence interval around the surface roughness at left position is given by 3.69±0.12 microns.

7.9 ANALYSIS OF VARIANCE- SURFACE ROUGHNESS AT RIGHT POSITION

The results for surface roughness at right position for each of the 27 treatment conditions with repetition are given in Table 7.1. The results were analyzed using ANOVA for identifying the significant factors affecting the performance measures. The Analysis of Variance (ANOVA) for the mean surface roughness at 99% confidence interval is given in Table 7.12. The factors, namely, current, pulse on time, powder and electrode were found to be significant for surface roughness at right position. The factors, namely, workpiece, pulse off time and interaction between workpiece × powder were found to be insignificant in surface roughness. Table 7.13 shows the ranks to various factors relative to their significance in surface roughness. The current has the highest rank which has highest contribution in surface roughness and dielectric has lowest rank and was observed insignificant to surface roughness at right position. Main effect plot and interaction plot for surface roughness at left position are shown in the Figure 7.9 and

Figure 7.10 respectively. As the current, pulse on time and pulse off time increases, surface roughness increased.

Table 7.12: ANOVA for surface roughness at right position

Sources	SS	v	V	F	F (critical)	SS'	% contribution
Workpiece (A)	0.18	2	0.09	2.86			
Dielectric (B)	0.00	1	0.00	0.00			
Electrode (C)	0.64	1	0.64	20.56	13.7	0.55	1.154
Pulse off time (D)	0.04	2	0.02	0.70			
Pulse on time (E)	13.60	2	6.80	217.27	10.9	13.42	28.025
Current (F)	28.57	2	14.29	456.40	10.9	28.39	59.288
Powder (G)	2.15	2	1.08	34.37	10.9	1.97	4.113
(A × C)	0.69	2	0.35	11.08	10.9	0.51	1.069
(A × G)	0.95	4	0.24	7.63			
(C × G)	0.86	2	0.43	13.68	10.9	0.67	1.408
Error	0.19	6	0.03				
TOTAL	47.88	26	1.84			47.88	100
e pooled	1.37	15	0.09			2.37	4.943

Table 7.13: Response table for means of surface roughness at right position

Level	Workpiece (A)	Dielectric (B)	Electrode (C)	Pulse off time (D)	Pulse on time (E)	Current (F)	Powder (G)
1	5.876	5.921	5.813	5.882	5.014	4.591	5.811
2	5.854	5.923	6.141	5.908	6.006	6.081	5.646
3	6.037			5.977	6.747	7.096	6.310
Delta	0.183	0.002	0.327	0.095	1.733	2.505	0.664
Rank	5	7	4	6	2	1	3

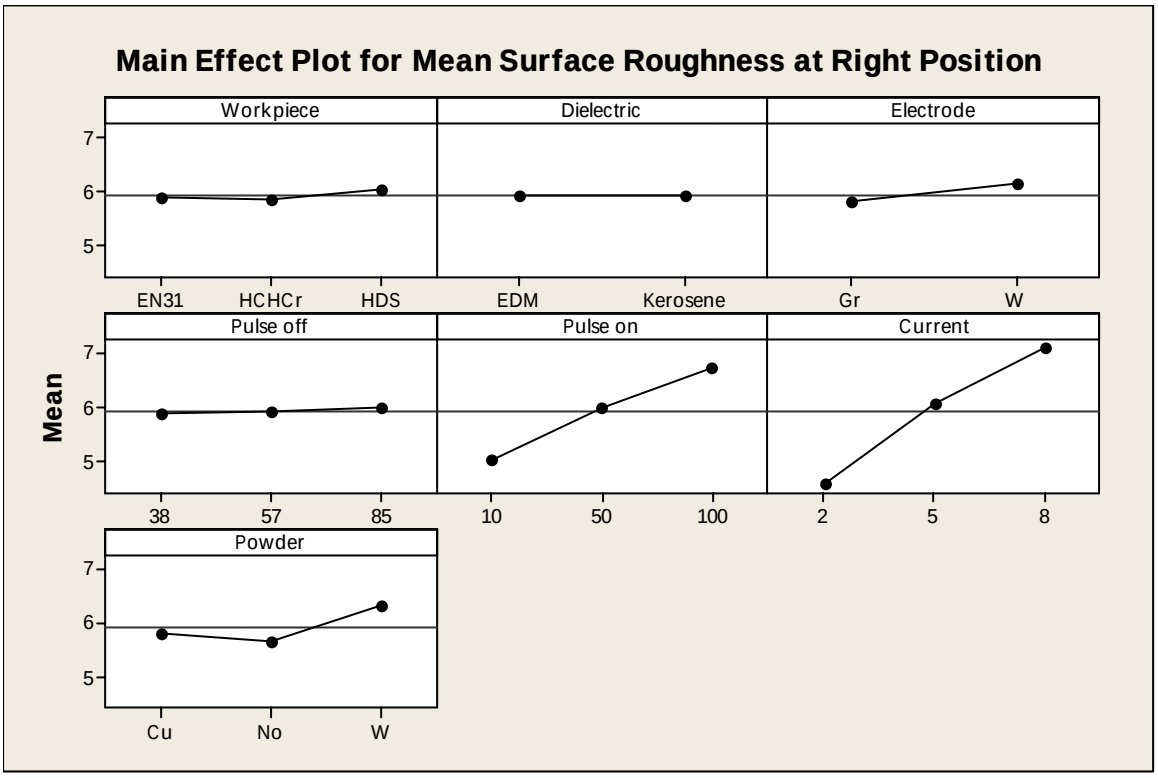

Figure 7.9: Main effect plot for of surface roughness at right position

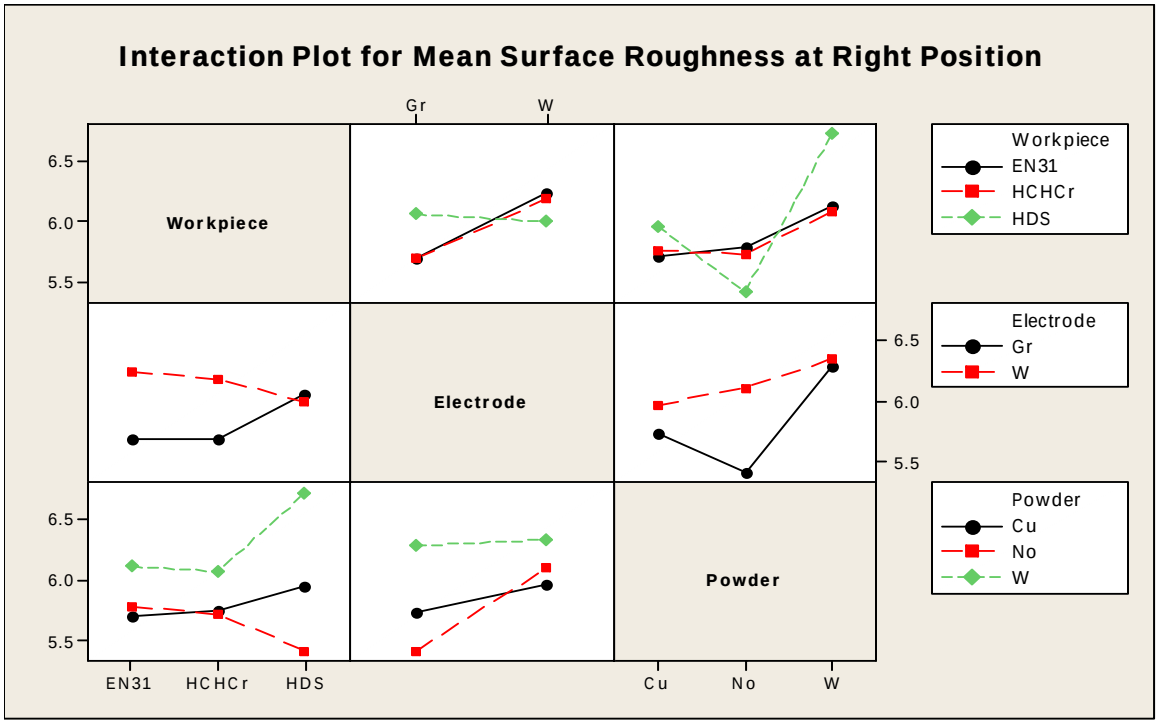

Figure 7.10: Interaction plot for surface roughness right at position

7.10 RESULTS FOR S/N RATIO FOR SURFACE ROUGHNESS AT RIGHT POSITION

The S/N ratios have been calculated to identify the major contributing factors and interactions that cause variation in surface roughness. Surface roughness is a "Lower is better", type response and is given by a logarithmic function based on the mean square deviation (MSD) given by:

$$S/N_{LB} = -10\log(MSD) = -10\log[(\frac{1}{r}\sum_{i=1}^{r} y^2{}_i)$$

Table 7.14 shows the ANOVA for S/N ratio for roughness at 99% confidence interval. The factors, namely, current pulse on time, electrode, powder and interaction between workpiece × electrode was found to be significant in surface roughness. Remaining factors and all interactions studied during the trials were found to be insignificant. Table 7.15 shows the ranks to various factors in terms of their relative significance. Current has the highest rank, signifying the highest contribution to surface roughness and dielectric has the lowest rank and was observed to be insignificant in affecting surface roughness. Main effect plot and interaction plot for S/N ratio are shown in Figure 7.11 and Figure 7.12 respectively.

Table 7.14: ANOVA for S/N ratio of surface roughness at right position

Sources	SS	V	V	F	F (critical)	SS'	% contribution
Workpiece (A)	1.32	2	0.66	8.66			
Dielectric (B)	0.03	1	0.03	0.38			
Electrode (C)	1.71	1	1.71	22.42	13.7	1.38	1.203
Pulse off (D)	0.36	2	0.18	2.34			
Pulse on (E)	32.23	2	16.11	211.41	10.9	31.58	27.464
Current (F)	68.69	2	34.35	450.59	10.9	68.04	59.179
Powder (G)	4.99	2	2.49	32.71	10.9	4.33	3.770
(A × C)	1.81	2	0.91	11.90	10.9	1.16	1.010
(A × G)	1.98	4	0.49	6.49			
(C × G)	1.40	2	0.70	9.20			

Error	0.46	6	0.08				
TOTAL	114.98	26	4.42			114.98	100
e pooled	5.54	17	0.33			8.48	7.374

Table 7.15: Response table for S/N ratio of surface roughness at right position

Level	Workpiece (A)	Dielectric (B)	Electrode (C)	Pulse off (D)	Pulse on (E)	Current (F)	Powder (G)
1	-15.24	-15.27	-15.04	-15.11	-13.80	-13.10	-15.09
2	-1494	-15.20	-15.58	-15.18	-15.39	-15.62	-14.77
3	-15.48			-15.38	-16.46	-16.94	-15.80
Delta	0.54	0.07	0.53	0.27	2.66	3.85	1.03
Rank	4	7	5	6	2	1	3

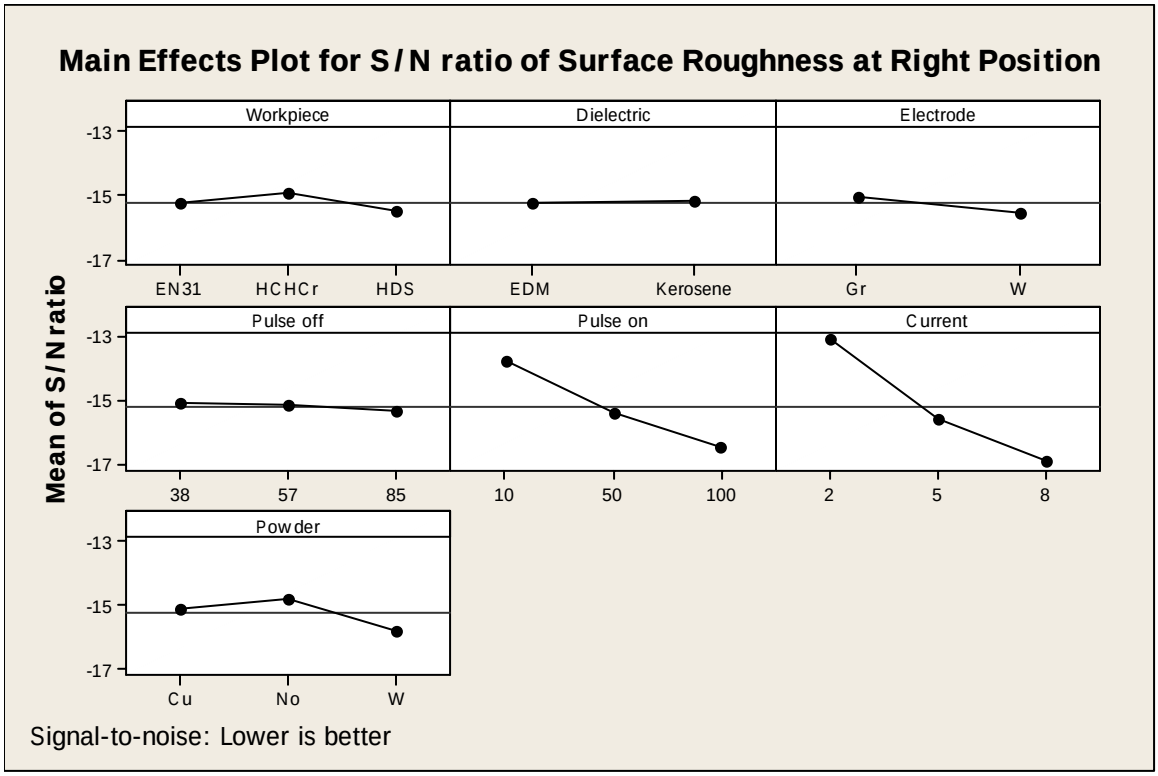

Figure 7.11: Main effect plot for S/N ratio of surface roughness at right position

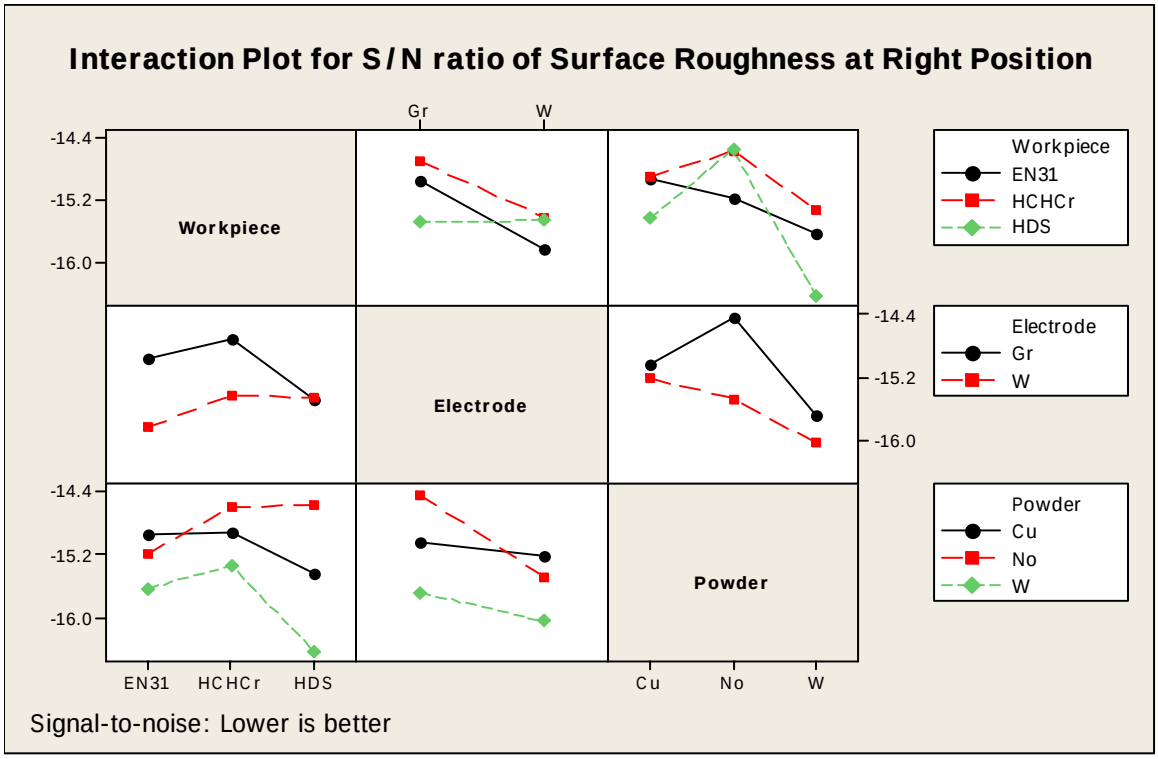

Figure 7.12: Interaction plot for S/N ratio of surface roughness at right position

7.11 OPTIMAL DESIGN

In this experimental analysis, the main effect plot and interaction plot in Figure 7.9 and Figure 7.10 used to estimate the mean surface roughness. From the, Table 7.16 it is concluded that least surface roughness was observed when pulse on time 10µs, current 2Amp, graphite as electrode was chosen in the treatment conditions. In this case, the same levels of the significant factors and interactions provide the higher average and reduced variability so nothing has to be compromised. In some situations, the levels of factors which improve the average and improve the uniformity may conflict, so a compromise may have to be reached. Also, a compromise may have to occur when multiple responses are considered and the same factor level may cause one response to improve and another to deteriorate.

Table 7.16: Significant factors and interactions for surface roughness at right position

Factors	Affecting mean		Affecting variation (S/N ratio)	
	Contribution	Best level	Contribution	Best level
Workpiece (A)	Insignificant	-	Insgnificant	-
Dielectric (B)	Insignificant	-	Insignificant	-
Electrode (C)	Significant	Level 1-Gr	Significant	Level 1-Gr
Pulse off (D)	Insignificant	-	Insignificant	-
Pulse on (E)	Significant	Level 1-10 µs	Significant	Level 1- 10 µs
Current (F)	Significant	Level 1- 2 Amp	Significant	Level 1- 2 Amp
Powder (G)	Significant	Level 1- No	Significant	Level 1-No
(A × C)	Significant	A_1C_1	Significant	A_1C_1
(A × G)	Insignificant	-	Insignificant	-
(C × G)	Significant	C_1G_1	Insignificant	-

Estimating the mean

Mean value of surface roughness at right position

$$\mu_{C_1E_1F_1G_1A_1\times C_1C_1\times G_1} = \overline{C_1} + \overline{E_1} + \overline{F_1} + \overline{G_1} + \overline{A_1 \times C_1} + \overline{C_1 \times G_1} - 5\overline{T}$$

$$\mu_{C_1E_1F_1G_1A_1\times C_1C_1\times G_1} = 5.81+4.59+5.01+5.64+5.21+5.18-5\times5.92 = 3.35 \text{ microns}$$

Confidence Interval around the Estimated Mean

Confidence Interval around the estimated surface roughness at right position

$$CI_1 = \sqrt{\frac{F_{\alpha,\nu_1,\nu_2} V_e}{n_{eff}}} \quad \text{Where} \quad F_{\alpha\nu_1\nu_2} = F \text{ ratio}$$

$\alpha = risk\ (0.01)$ $\qquad$ $confidence = 1-\alpha$

$\nu_1 = dof\ for\ mean\ which\ is\ always = 1$

$\nu_2 = dof\ for\ error = \nu_e$

n_{eff} = Number of tests under that condition using the participating factors

$$n_{eff} = \frac{N}{1 + dof_{C,E,F,G,AC,CG}} = \frac{27}{1 + 2 + 2 + 2 + 2 + 2} = 2.45$$

$$CI_1 = \sqrt{\frac{F_{\alpha,v_1,v_2} V_e}{n_{eff}}} = \sqrt{\frac{0.15 \times 0.09}{2.45}} = 0.074$$

So the confidence interval around the surface roughness at right position is given by 3.35±0.074 microns.

Chapter 8

FURTHER ANALYSIS

8.1 INTRODUCTION

In the present work, the effect of various input parameters i.e. current, pulse on time, pulse off time, electrode material, powder on the surface properties of the workpiece material was evaluated. During machining, temperature between tool and workpiece very high and this high temperature causes fusion or partial vaporization of the molten metal and the dielectric fluid at the point of discharge. Due to very high temperature the workpiece material is subjected to, re-crystallization of the metal grains take place and subsequent cooling of the heated metal causes change in the micro structure. The heating and cooling rate decides the shape of grains and properties of surface of machined area. Also, material is transferred from the powder suspended in the dielectric, as well as from the electrode, on to the machined surface. The chemical composition of the machined surface was determined with the help of X-Ray Diffraction (XRD) analysis. Micro structural analysis was carried using Scanning Electron Microscope (SEM) and Lieca Metallurgical Microscope. During this analysis chemical composition of machined surface and micro structure of machined surface determined

8.2 XRD ANALYSIS

During machining of the workpiece, material is transferred from suspended powder in the dielectric and from the electrode material, resulting in improvement of surface properties. The material transferred to the workpiece, forms various compound on the surface of workpiece. To analyze this, the workpiece was tested for XRD on selected samples. The range of 2θ from 5^0 to 100^0 was used at a scan speed of 5^0/minute at wavelength 1.54 angstrom for each test. After the XRD analysis, each sample was tested on Optical Emission Spectrometry to quantitatively confirm the results of XRD.

8.2.1. XRD Analysis of High Carbon High Chromium (HCHCr)

The XRD pattern of HCHCr machined with tungsten-copper electrode in EDM oil with no powder mixed in dielectric medium is shown in the Figure 8.1. The pattern shows the presence of cohenite synthetic (Fe_3C). The cohenite is rich iron meteorites, having carbon content not more than 0.4-0.6% less than α-γ eutectoid composition. The presence cohenite increase the hardness. As shown in the Figure 8.1 Fe_3C compound formed increases the hardness of the surface. Pattern list are given shown in the Table 8.1 which shows the percentage of the compound according to the score. After the spectrometer analysis, it was observed that carbon percentage increased from 1.60% to 1.63% and tungsten increased from 0.02% to 0.024%.

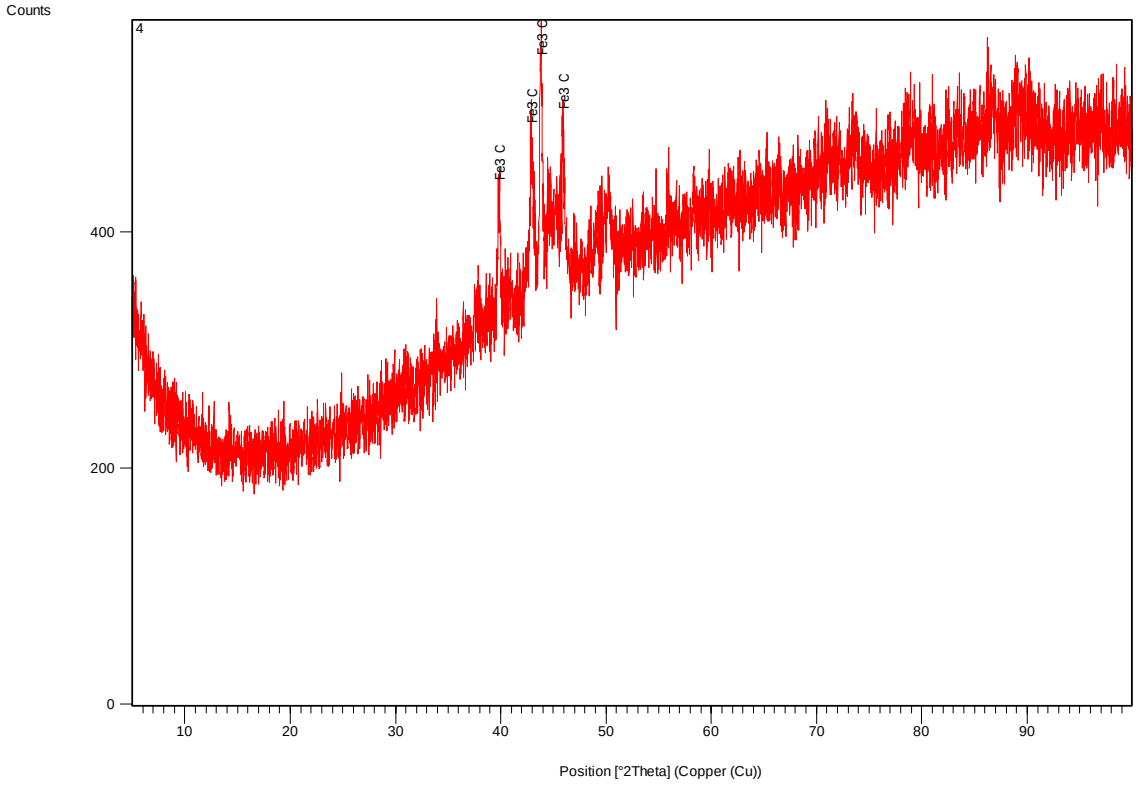

Figure 8.1: XRD pattern of HCHCr machined with W-Cu electrode in edm oil without powder mixing. (I 8Amp, Pulse on time 100µs, Pulse off time 57µs)

Table 8.1: Pattern list for HCHCr machined with W-Cu in EDM oil without powder mixing

Visible	Score	Compound	Scale	Chemical	SemiQuant [%]

			Factor	Formula	
1	10	Cohenite – synthetic	1.274	Fe_3 C	100

The XRD pattern of HCHCr machined with W-Cu electrode with tungsten powder mixed in kerosene dielectric medium is shown in the Figure 8.2. The XRD pattern shows the traces of tungsten carbide (W_2C), chromium molybdenum and copper germanium iron on the surface of sample. Tungsten carbide is an inorganic chemical compound containing tungsten and carbon atoms. The tungsten carbide has very high strength thus imparts hardness rigidity to the material. Compressive strength is also higher. In addition, mechanical and physical properties such as toughness, wear resistance were also improved with tungsten carbide. In chromium molybdenum compound a hexagonal and a Face Centered Cubic (FCC) phase was formed. The hardness of hexagonal phase increased and FCC compounds decreased. Copper germanium iron improved the hardness and wear resistance. The changes in chemical composition after machining are given in Table 8.2. Pattern list of XRD pattern are given in Table 8.3.

Table 8.2: Chemical composition of HCHCr machined with W-Cu electrode in kerosene with tungsten powder mixing. (I=5 Amp, Pulse on= 50µs, Pulse off=38µs)

Composition	Before machining (%)	After machining (%)
Carbon	1.6	1.74
Tungsten	0.02	1.37
Chromium	13.3	12.9
Molybdenum	0.05	0.09
Copper	0.05	0.94

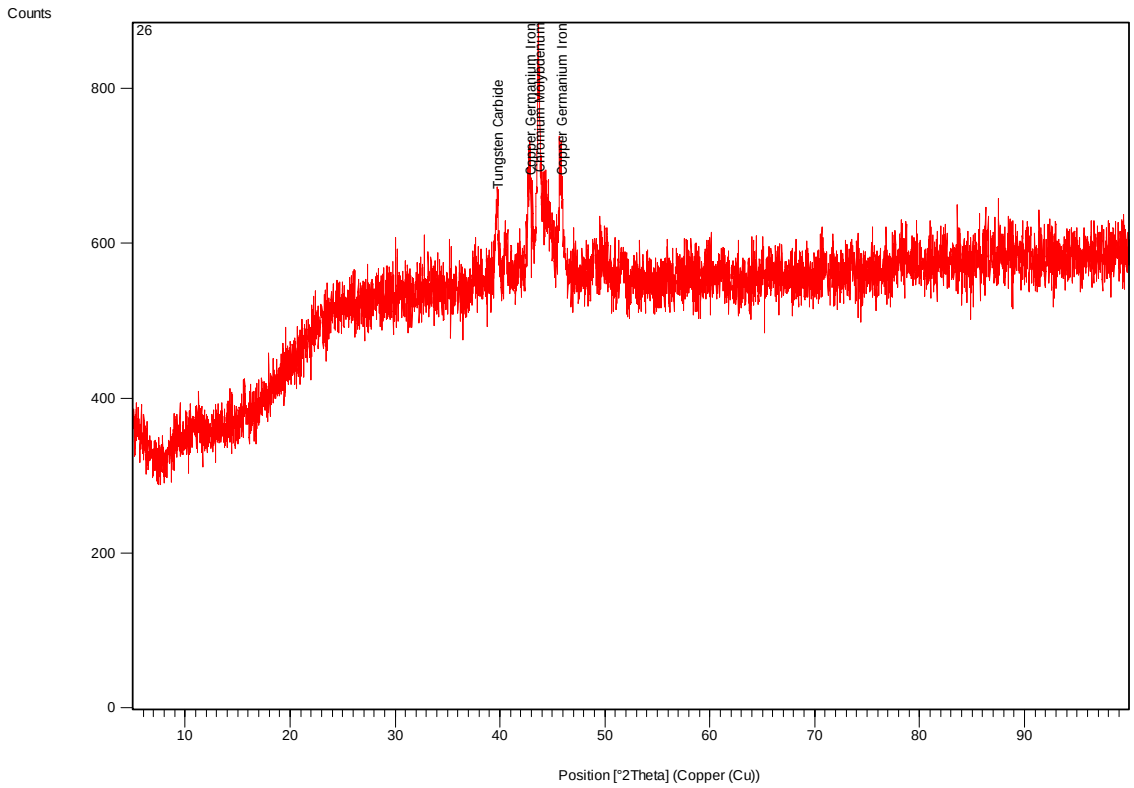

Figure 8.2: XRD pattern of HCHCr machined with W-Cu electrode in kerosene with tungsten powder mixing. (I=5 Amp, Pulse on= 50µs, Pulse off=38µs)

Table 8.3: Pattern list HCHCr machined with W-Cu electrode in kerosene with tungsten powder mixed dielectric

Visible	Score	Compound	Scale Factor	Chemical Formula	SemiQuant [%]
1	2	Tungsten Carbide	0.249	$W_2 C$	19
2	26	Chromium Molybdenum	0.478	$(Cr_{0.7} Mo_{0.3})$	33
3	31	Copper Germanium Iron	0.531	$Cu_{1.6} Fe_{0.1} Ge_{0.3}$	48

The XRD pattern HCHCr machined with graphite electrode with copper powder mixed in kerosene dielectric is shown in Figure 8.3. The XRD pattern shows the traces of copper, chromium and carbon and has not formed any compound. The chromium has transferred in α-

chromium which reduces the stresses and improves the corrosion resistance. After the spectrometer analysis, it was observed that percentage of copper increased from 0.03% to 1.12% and carbon increased from 1.6% to 1.94%. Pattern list of XRD are given in Table 8.4.

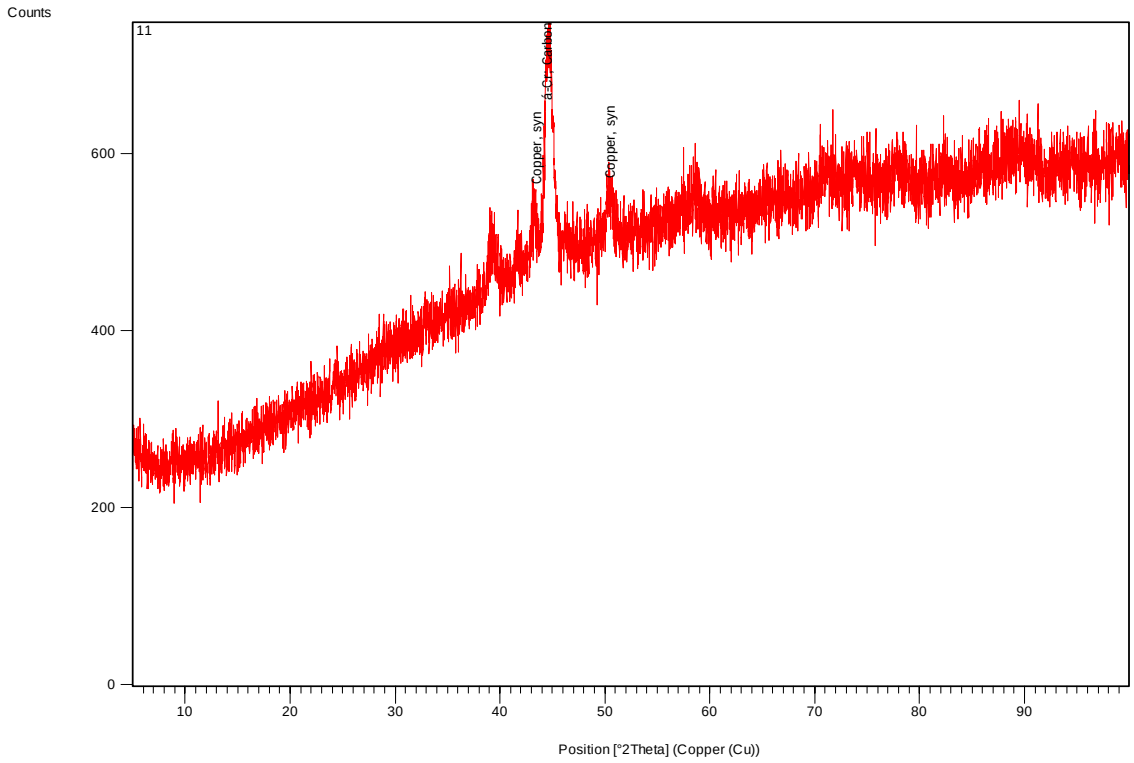

Figure 8.3: XRD pattern of HCHCr machined with graphite electrode in kerosene with Cu powder mixing. (I=5 Amp, Pulse on= 50µs, Pulse off=57µs)

Table 8.4: Peak list of HCHCr machined with graphite electrode in kerosene with Cu powder mixed dielectric

Visible	Score	Compound	Scale Factor	Chemical Formula	SemiQuant [%]
1	16	Copper, syn	0.262	Cu	5
2	28	á-Cr	0.792	Cr	14
3	27	Carbon	0.486	C	81

8.2.2. XRD Analysis of EN31

The XRD pattern of EN31 machined with graphite electrode with tungsten powder mixing in kerosene dielectric medium is shown in the Figure 8.4. The pattern shows the some traces of chromium iron carbide and iron carbide. The chromium forms solid solution with iron and has high solubility in α-ferrite as well as γ-iron. The iron atoms of cementite phase can be substituted in chromium atoms and forms carbides in steel. The chromium carbides and chromium iron carbides are formed by carburization of chromium at high temperature. When chromium is more than 5%, the high temperature properties and corrosion resistance of steels is improves and also the, hardenability. The thermal expansion coefficient of chromium carbide is almost equal to that of steel, reducing the mechanical stress buildup at the layer boundary. The changes in the chemical composition after machining of EN31with graphite electrode in tungsten mixed powder are given in Table 8.5. Table 8.6 shows the pattern list and compound which was formed.

Table 8.5: Chemical composition of EN31 after machining with graphite electrode in tungsten powder in kerosene dielectric (I 5 Amp, Pulse on time 100μs, Pulse off time 85μs)

Composition	Before machining %	After machining %
Carbon	0.35	0.47
Tungsten	0.01	0.22
Nickel	0.09	0.13

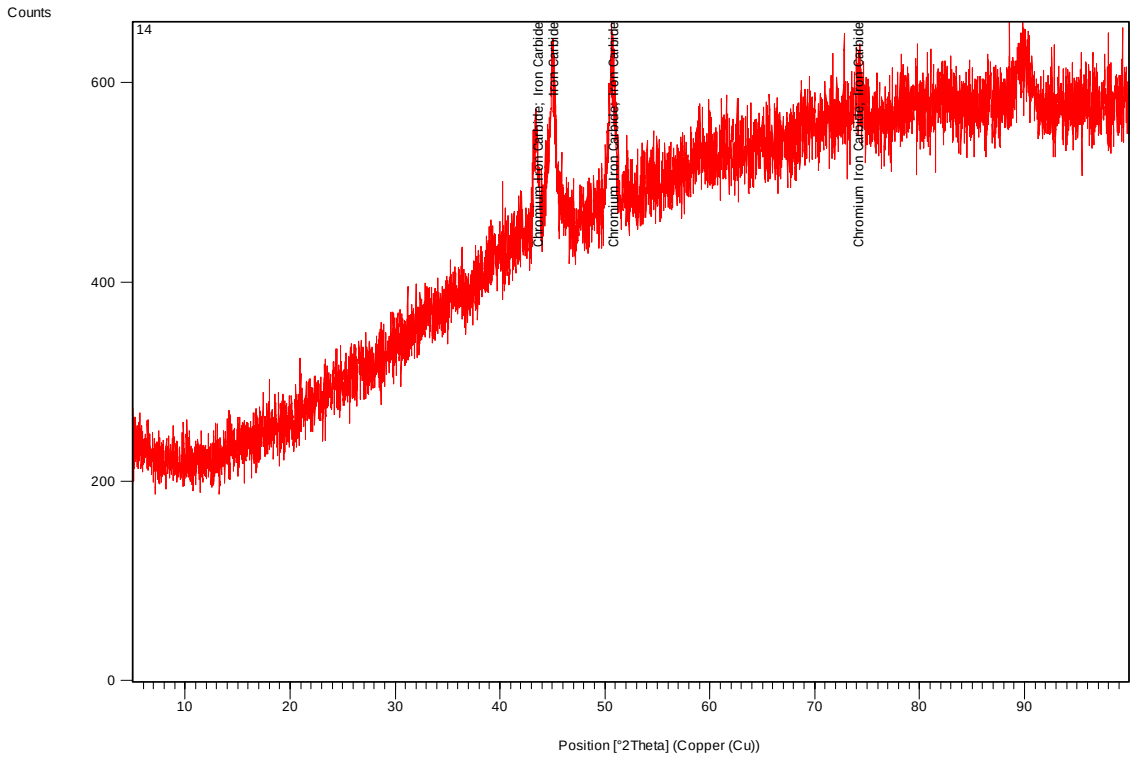

Figure 8.4: XRD pattern of EN 31 machined with graphite electrode in kerosene with tungsten powder mixing. (I 5Amp, Pulse on time 100µs, Pulse off time 85µs)

Table 8.6: Pattern list EN 31 machined with graphite electrode in kerosene with tungsten powder mixing

Visible	Score	Compound	Scale Factor	Chemical Formula	SemiQuant [%]
1	45	Chromium Iron Carbide	0.673	$Cr_2 Fe_{14} C$	43
2	39	Iron Carbide	0.803	$Fe_4 C_{.63}$	57

The XRD pattern of EN31 machined with graphite electrode in copper powder mixed kerosene dielectric is shown in the Figure 8.5. The XRD pattern shows the traces of copper iron ($Fe Cu_4$) and carbon. The carbon imparts the strength, wear resistance and hardness but reduces the toughness and ductility. The carbon has contributed by electrode wear as well as the pyrolysis of the dielectric. Iron copper ($Fe Cu_4$) has good corrosion resistance and have some effect on

hardness. After the spectrometer analysis, it was observed that carbon percentage increased from 0.35% to 0.79% and copper increased from 0.03% to 1.12%.

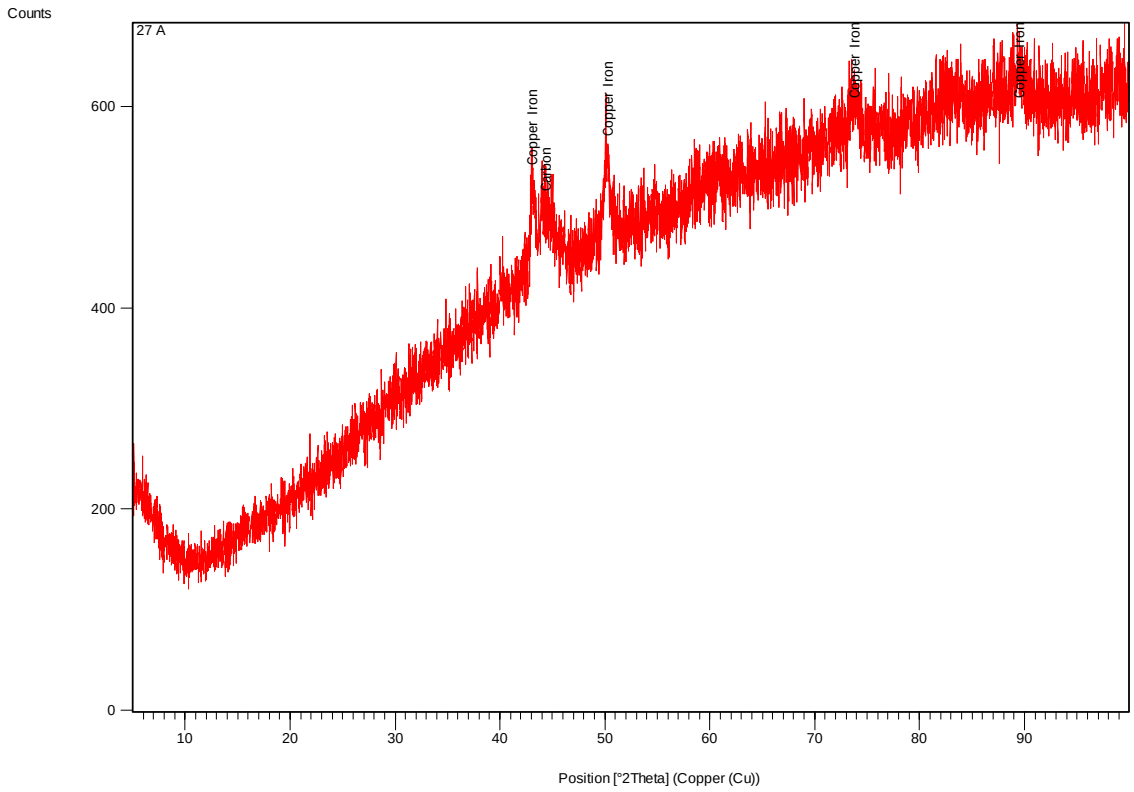

Figure 8.5: XRD pattern of EN 31 machined with graphite electrode in kerosene with Cu powder mixing. (I 2Amp, Pulse on time 50µs, Pulse off time 57µs)

Table 8.7: Pattern list of EN 31 machined with graphite electrode in kerosene with Cu powder mixing

Visible	Score	Compound	Scale Factor	Chemical Formula	SemiQuant [%]
1	13	Copper Iron	0.709	$Fe\ Cu_4$	15
2	16	Carbon	0.495	C	85

The XRD patterns of EN 31 machined with W-Cu electrode in copper powder mixed in EDM oil is shown in the Figure 8.6. The XRD pattern shows the traces of copper and cementite compound. Copper has transferred from powder which was suspended in the dielectric and as well as from the electrode material. The cementite is iron carbide with an orthorhombic crystal

structure. The cementite increases the hardness of material. The copper has not formed any compound. After the spectrometer analysis, it was observed that percentage of copper increased from 0.03% to 1.12%.

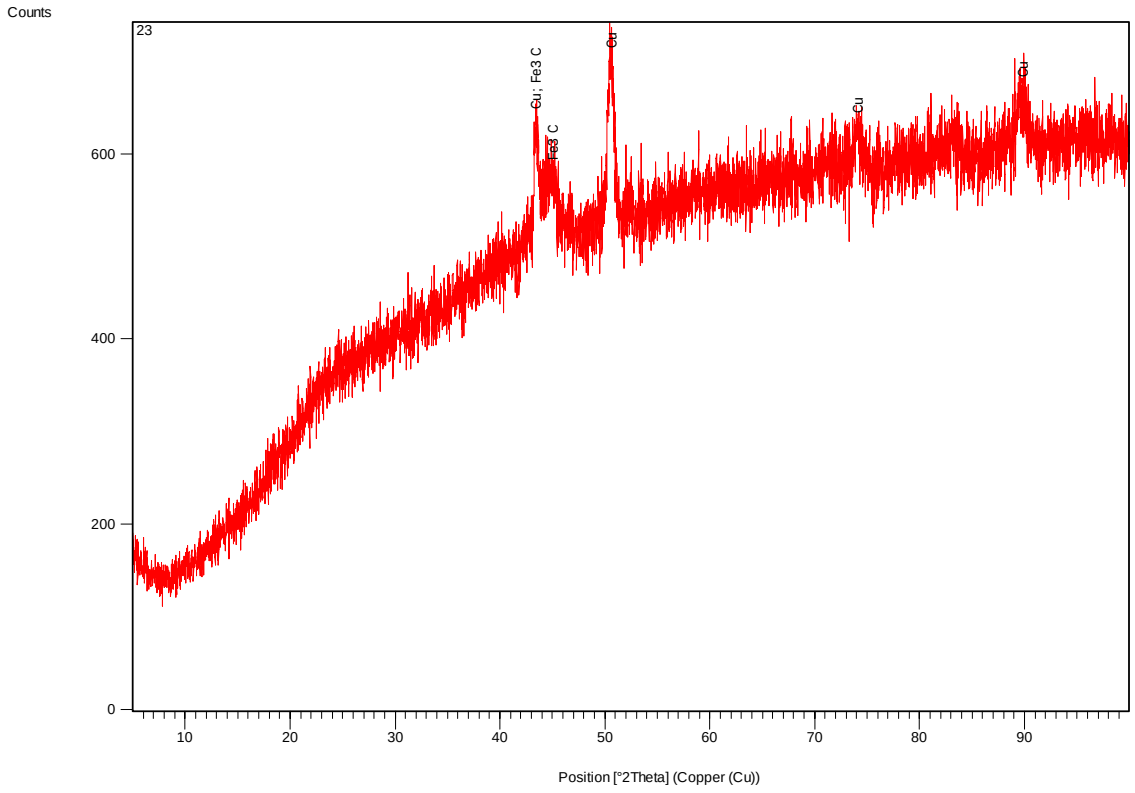

Fig 8.6: XRD pattern of EN 31 machined with W-Cu electrode in EDM oil with Cu powder mixing. (I=5 Amp, Pulse on= 100µs, Pulse off=38µs)

Table 8.8 Peak list of EN 31 machined with W-Cu electrode in EDM oil with Cu powder mixing

Visible	Score	Compound	Scale Factor	Chemical Formula	SemiQuant [%]
1	85	Copper, syn	0.655	Cu	67
2	8	Cementite	0.352	$Fe_3 C$	33

8.2.3 XRD Analysis of Hot Die Steel

The XRD pattern of hot die steel machined with graphite electrode in copper mixed in kersoene dielctric is shown in the Figure 8.7. The pattern shows the formation of iron carbide and copper on the machined surface. The iron carbide (Fe_7C_3) with an orthorhombic crystal structure increased the hardness of material. After the spectrometer analysis, it was observed that carbon percentage increased from 0.4% to 0.68% and copper increased from 0.01% to 1.22%.

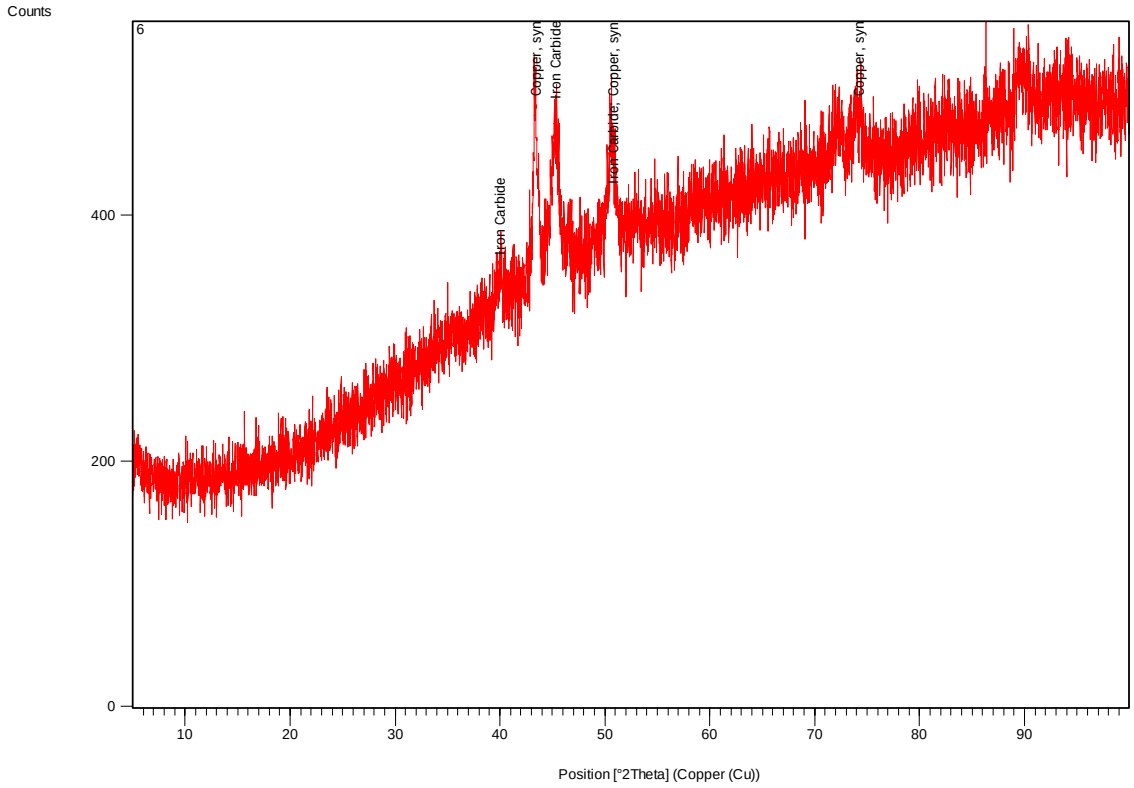

Figure 8.7: XRD pattern of hot die steel machined with graphite electrode in kerosene with copper powder mixing. (I 2Amp, Pulse on time 100µs, Pulse off time 38µs)

Table 8.9: Pattern list of hot die steel machined with graphite electrode in kerosene with copper powder mixing

Visible	Score	Compound	Scale Factor	Chemical Formula	SemiQuant [%]
1	11	Iron Carbide	0.466	$Fe_7 C_3$	41
2	43	Copper, syn	0.824	Cu	59

The XRD pattern of hot die steel machined with graphite electrode in tungsten powder mixed dielectric is shown in the Figure 8.8. The XRD pattern shows chromium carbide compound. Corrosion resistance of steels improved and hardenability improved with chromium carbide. After the spectrometer analysis, it was observed that tungsten increased from 0.1% to 1.15% and chromium decreased from 5.32% to 5.23% because some replacement of chromium with tungsten on surface.

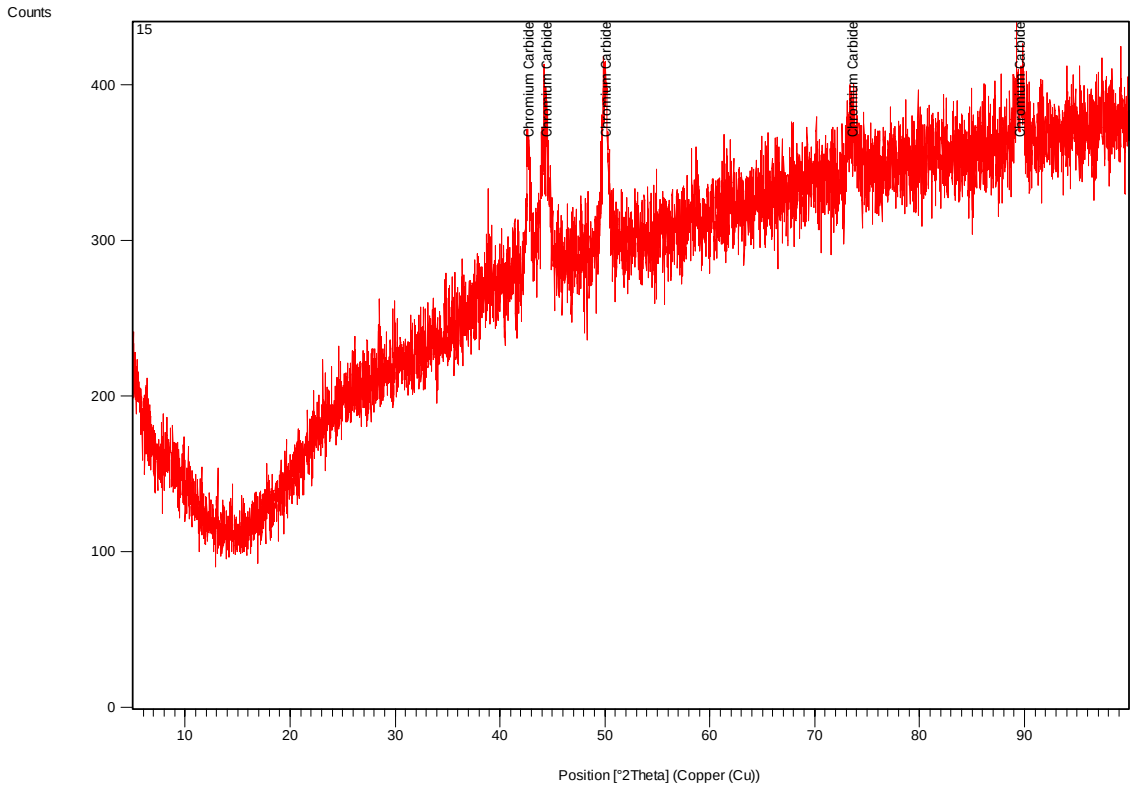

Figure 8.8: XRD pattern of hot die steel machined with graphite electrode in kerosene with tungsten powder mixing. (I=8 Amp, Pulse on= 50µs, Pulse off=38µs)

Table 8.10: Pattern list of hot die steel machined with graphite electrode in kerosene with tungsten powder mixing

Visible	Score	Compound	Scale Factor	Chemical Formula	SemiQuant [%]
1	19	Chromium Carbide	1.172	$Cr_7 C_3$	100

The XRD pattern of hot die steel machined with W-Cu electrode in copper mixed in kerosene dielectric is shown in Figure 8.9. The XRD pattern shows the cohenite compound which contributes to increase the hardness but copper has not formed any compound. The copper has not formed any carbide in tool steel after machining and has generally found as a solid solution with iron. The effect of copper in improving the mechanical properties of ferrite phase is only marginal but in any case, the presence of copper is not detrimental to properties.

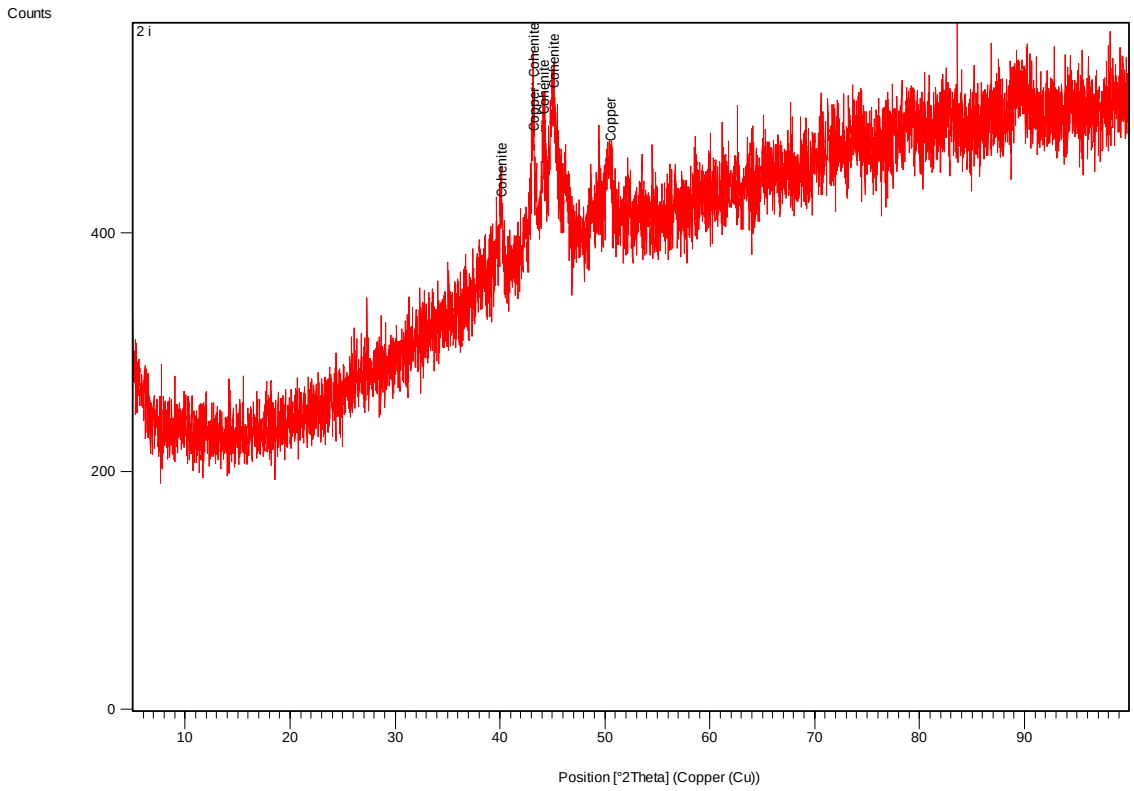

Figure 8.9: XRD pattern of hot die steel machined with W-Cu electrode in kerosene with copper powder mixing. (I 8Amp, Pulse on time 50µs, Pulse off time 57µs)

Table 8.11: Pattern list of HDS machined with W-Cu electrode in kerosene with Cu powder

Visible	Score	Compound	Scale Factor	Chemical Formula	SemiQuant [%]
1	30	Copper	0.645	Cu	43
2	21	Cohenite	0.700	Fe_3C	57

8.3 SUMMARY OF XRD ANALYSIS

The summary of the XRD analysis is tabulated in Table 8.12.

Table 8.12: Summary of XRD analysis

Workpiece	Electrode	Powder	Dielectric	Results
HCHCr	W-Cu	No	EDM oil	• Shows the Cohenite synthetic (Fe3C). • Increase the corrosion resistance and hardenability. • Reduce the mechanical stress at layer boundary.
HCHCr	W-Cu	tungsten	Kerosene	• Shows the traces of W_2C, Cr 0.7Mo 0.3, Cu 1.6Fe 0.1 Ge 0.3. • Increase the hardness and rigidity. • Toughness, wear resistance were improved
HCHCr	graphite	copper	Kerosene	• Shows the traces of Cu, C, α-Cr. • Chromium reduces the stresses and improves the corrosion.
EN31	graphite	tungsten	Kerosene	• Shows the traces of chromium carbide and iron carbide. • Temperature properties and corrosion resistance improved. • Reduced the mechanical stresses.
EN31	graphite	copper	kerosene	• Shows the traces of copper iron and carbon.

				• Iron carbon has improved the corrosion resistance and hardness.
EN31	W-Cu	copper	EDM oil	• Shows the traces of copper and cementite. • Cementite increased the hardness of machined surface. • Copper has not formed any compound.
HDS	graphite	copper	Kerosene	• Shows the formation of iron carbide and copper. • Iron carbide contributed to increase the hardness of material.
HDS	graphite	tungsten	Kerosene	• Chromium carbide compound has formed. • Corrosion resistance of materials improves. • Hardenability improved with chromium carbide.
HDS	W-Cu	copper		• Cohenite compound has formed but copper has not formed any compound. • Cohenite contributes to increase the hardness.

8.4 MICROSTRUCTURE ANALYSIS

Microstructure analysis was carried out on some selected samples using Scanning Electron Microscope to study the change in the microstructure after machining. The samples were

prepared as per standard before SEM analysis on three different magnifications, namely, 200×, 500× and 1000×.

8.4.1 Method of Sample Preparation

The steps for the sample preparation for SEM are given below:

1) Cut out the samples in 13×16mm on wire cut EDM.
2) Clean the surface with wire brush.
3) Clean the samples with acetone.
4) Clean the samples with ultrasonic gel to remove any dust particles.

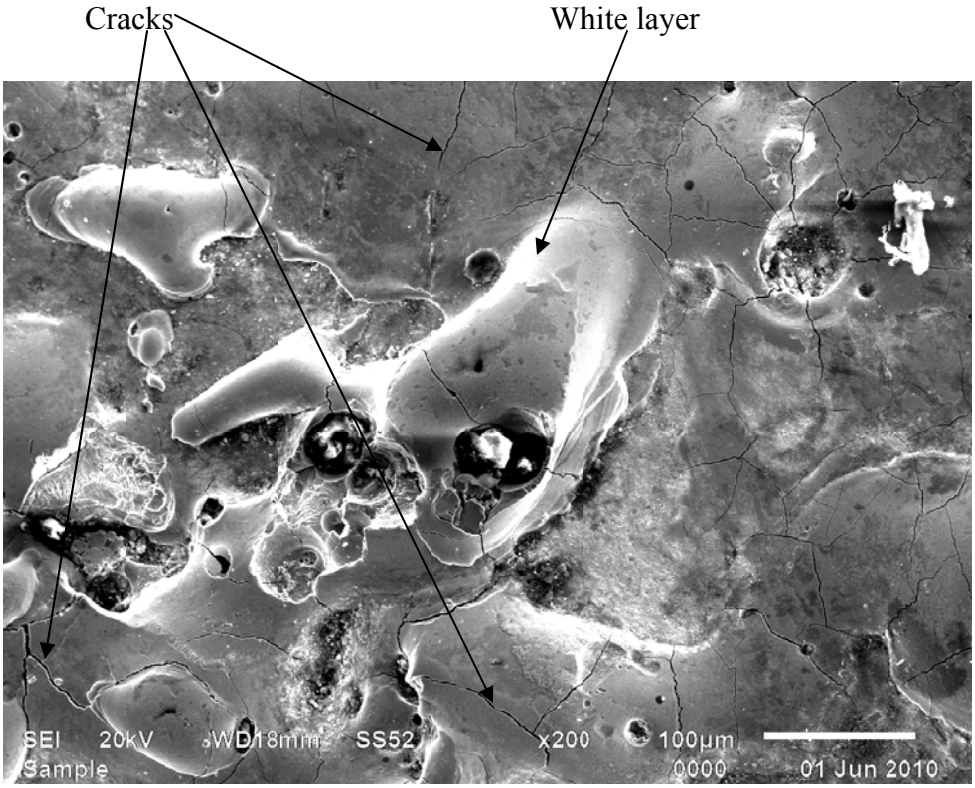

Figure 8.10: SEM micrograph at 200× of HCHCr machined with W-Cu electrode in without powder mixed in EDM oil (I 8Amp, pulse on time 100µs, pulse off time 57µs)

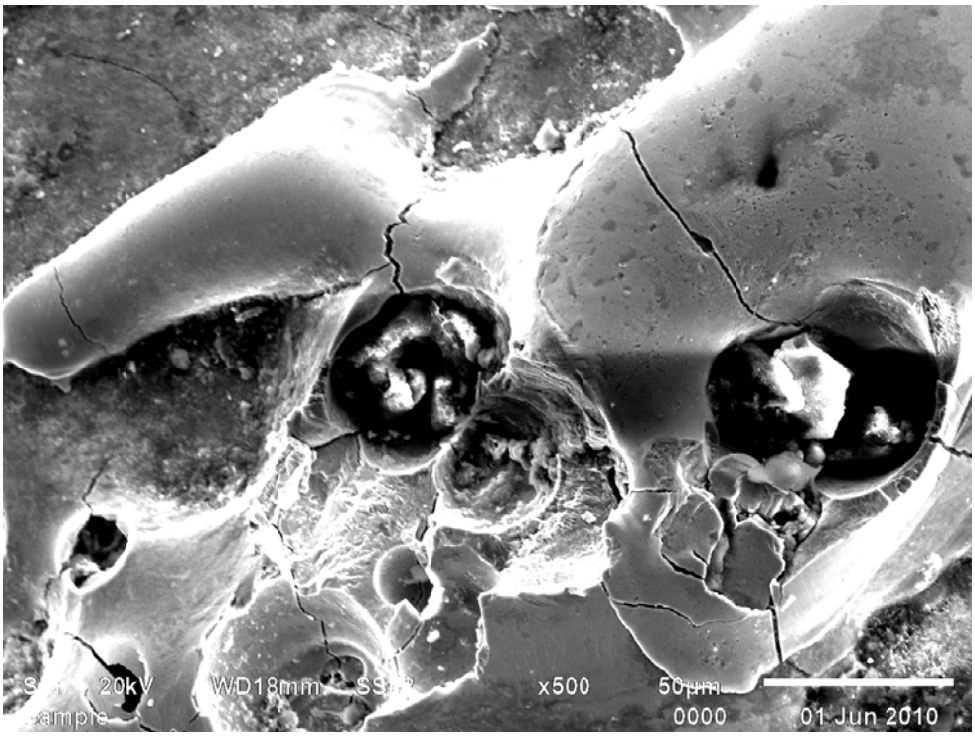

Figure 8.11: SEM micrograph at 500× of HCHCr machined with W-Cu electrode in without powder mixed in EDM oil (I 8Amp, pulse on time 100µs, pulse off time 57µs)

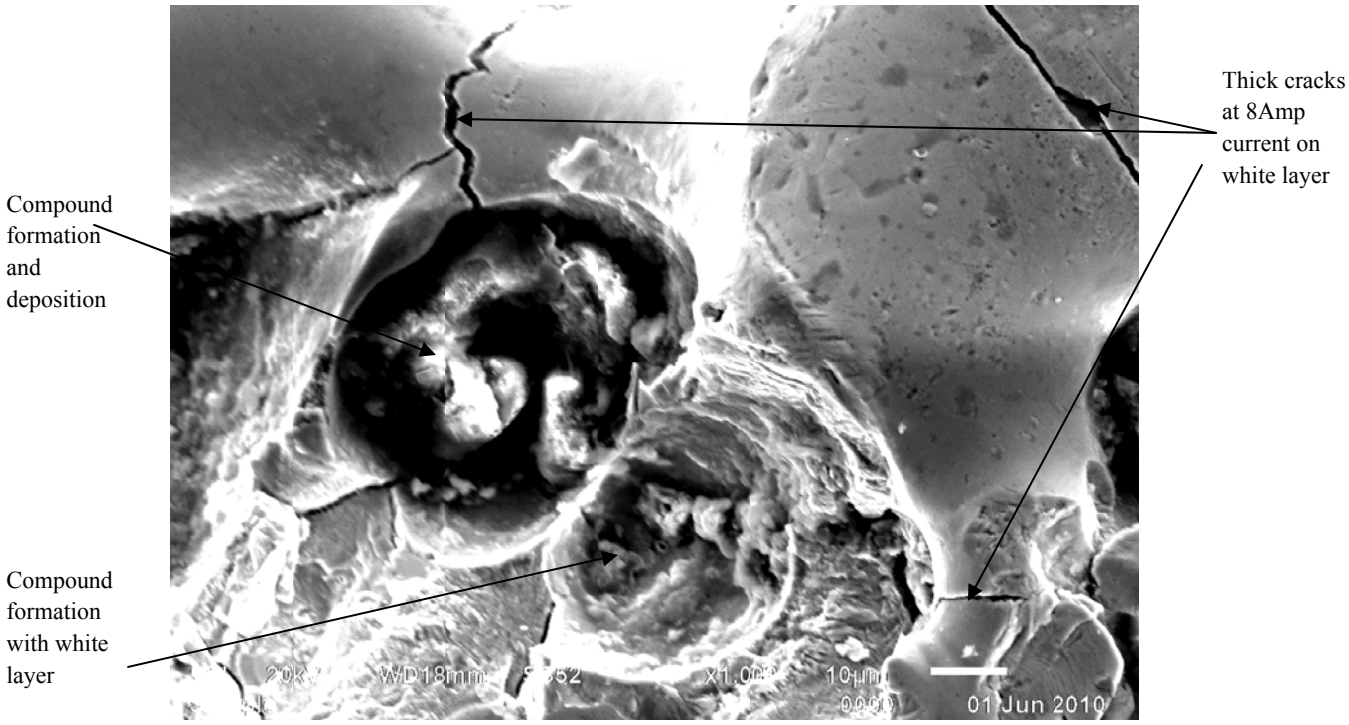

Figure 8.12: SEM micrograph at 1000× of HCHCr machined with W-Cu electrode in without powder mixed in EDM oil (I 8Amp, pulse on time 100µs, pulse off time 57µs)

Figure 8.13: SEM micrograph at 200× of HCHCr machined with graphite electrode in copper powder mixed in EDM oil (I 5Amp, pulse on time 50µs, pulse off time 57µs)

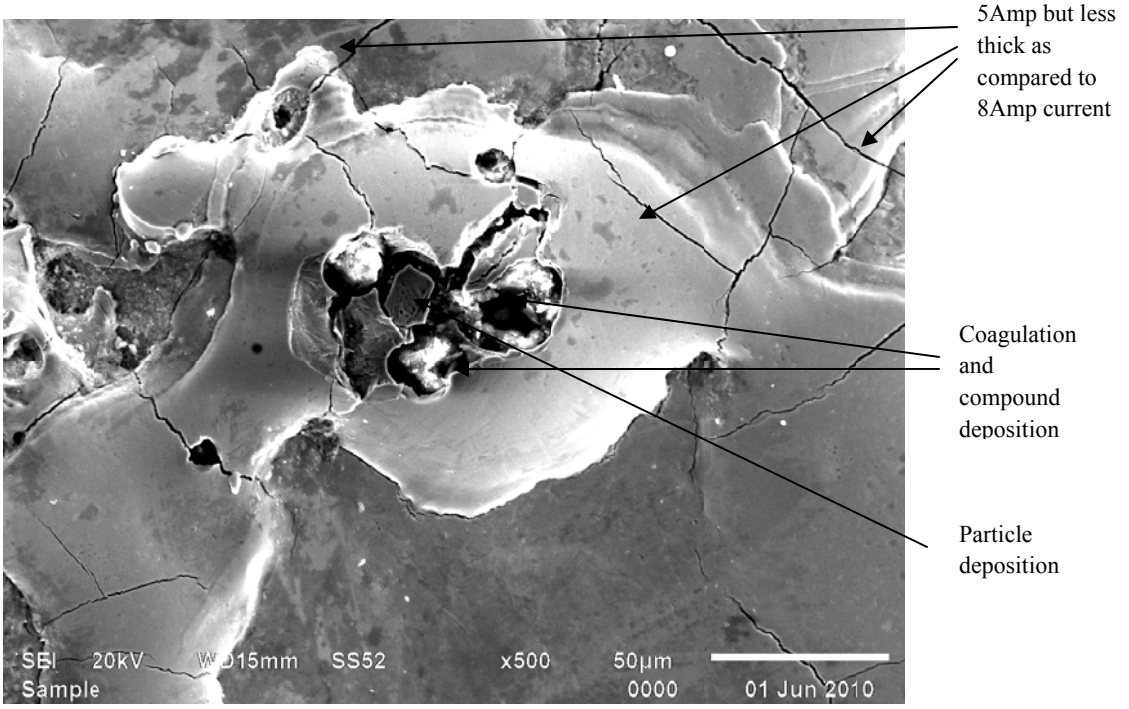

Figure 8.14: SEM micrograph at 500× of HCHCr machined with graphite electrode in copper powder mixed in EDM oil (I 5Amp, pulse on time 50µs, pulse off time 57µs)

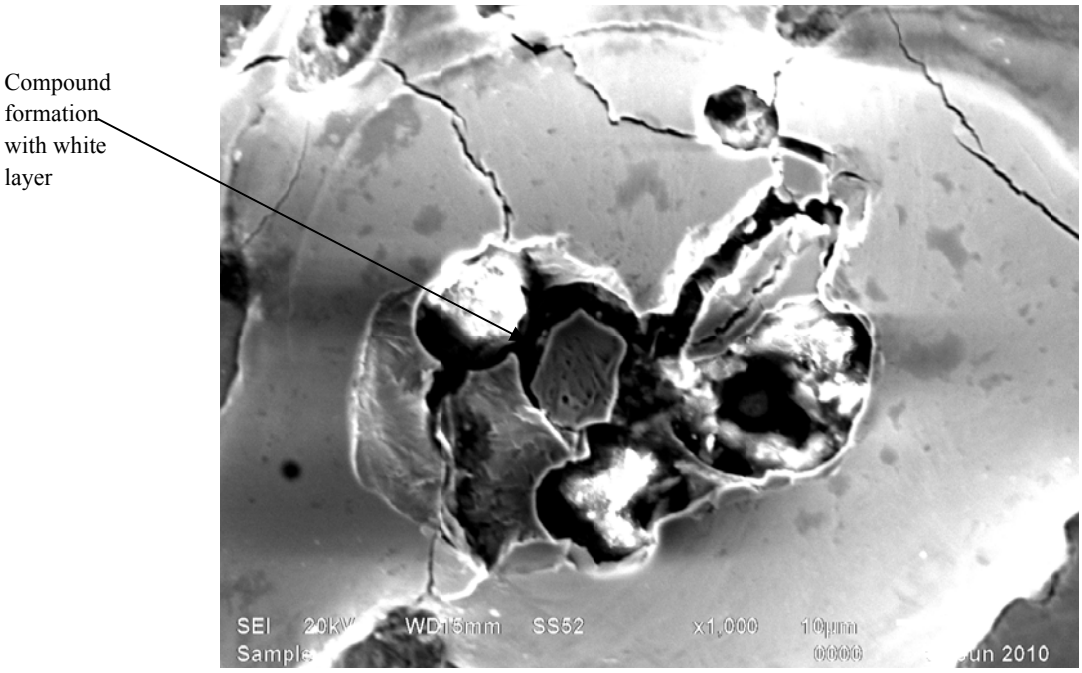

Figure 8.15: SEM micrograph at 1000× of HCHCr machined with graphite electrode in copper powder mixed in EDM oil (I 5Amp, pulse on time 50µs, pulse off time 57µs)

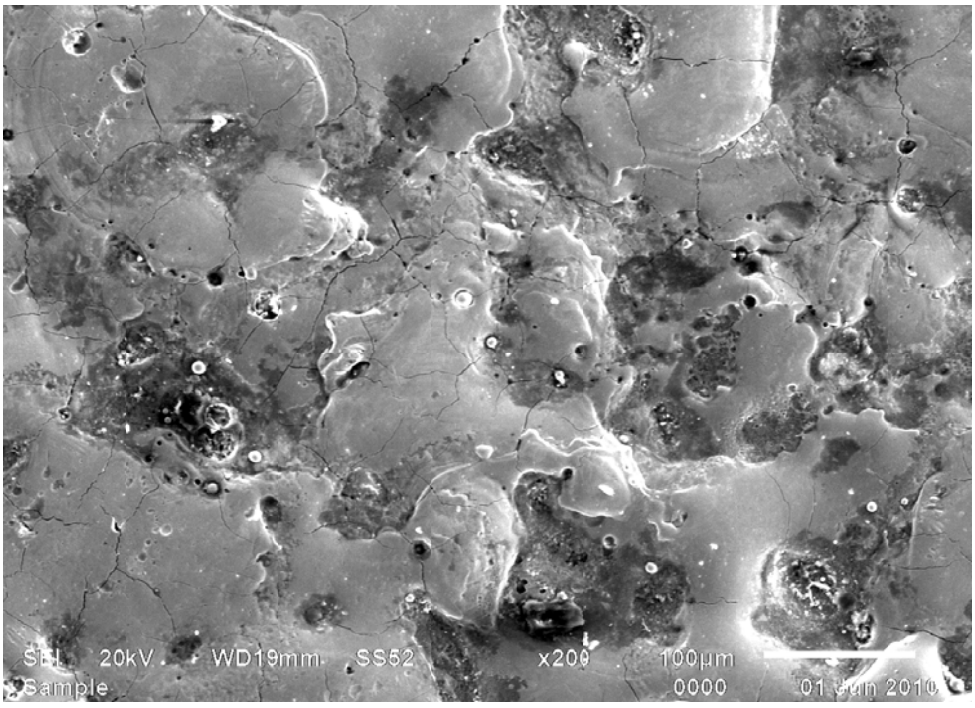

Figure 8.16: SEM micrograph at 200× of EN 31 machined with graphite electrode in copper mixed in kerosene (I 2Amp, pulse on time 50µs, pulse off time 57µs)

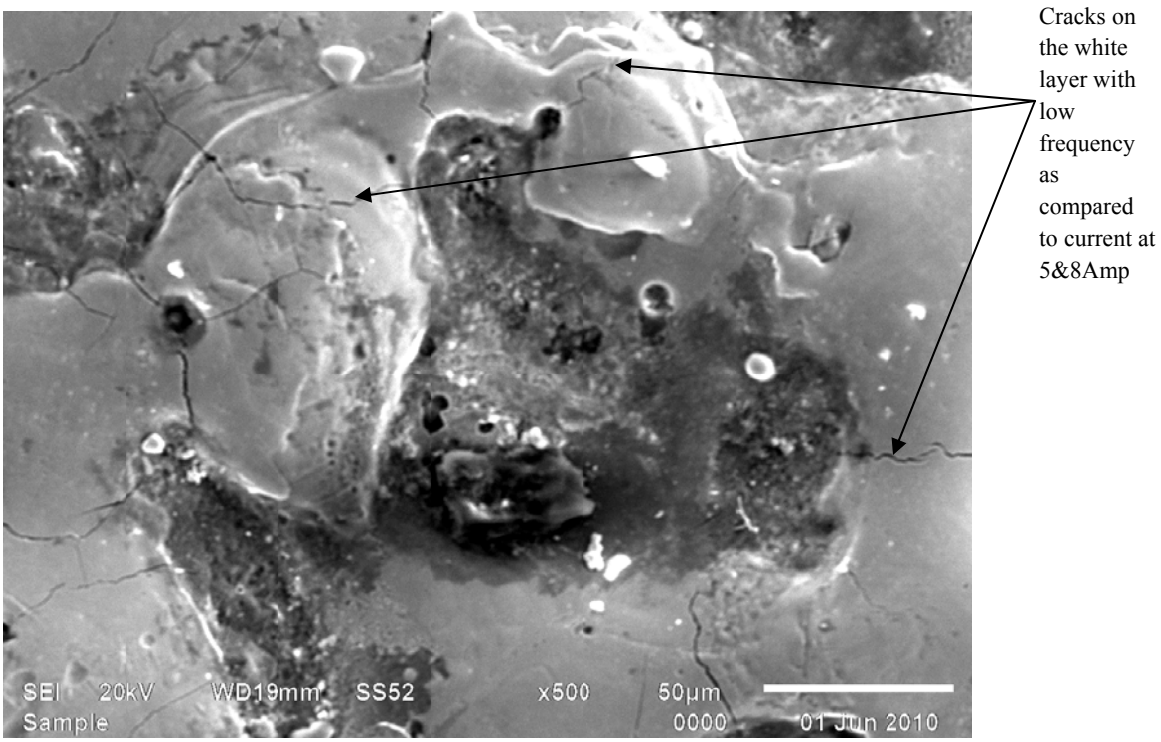

Figure 8.17: SEM micrograph at 500× of EN 31 machined with graphite electrode in copper mixed in kerosene (I 2Amp, pulse on time 50µs, pulse off time 57µs)

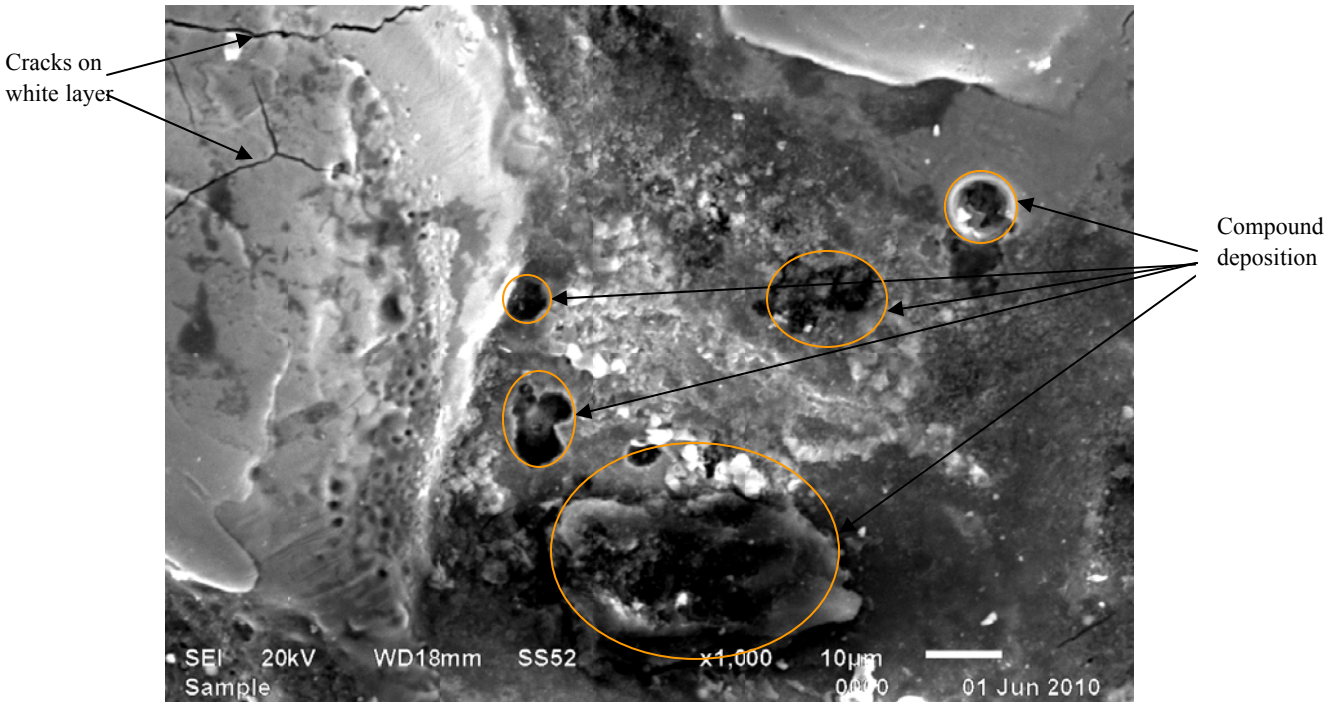

Figure 8.18: SEM micrograph at 1000× of EN 31 machined with graphite electrode in copper mixed in kerosene (I 2Amp, pulse on time 50µs, pulse off time 57µs)

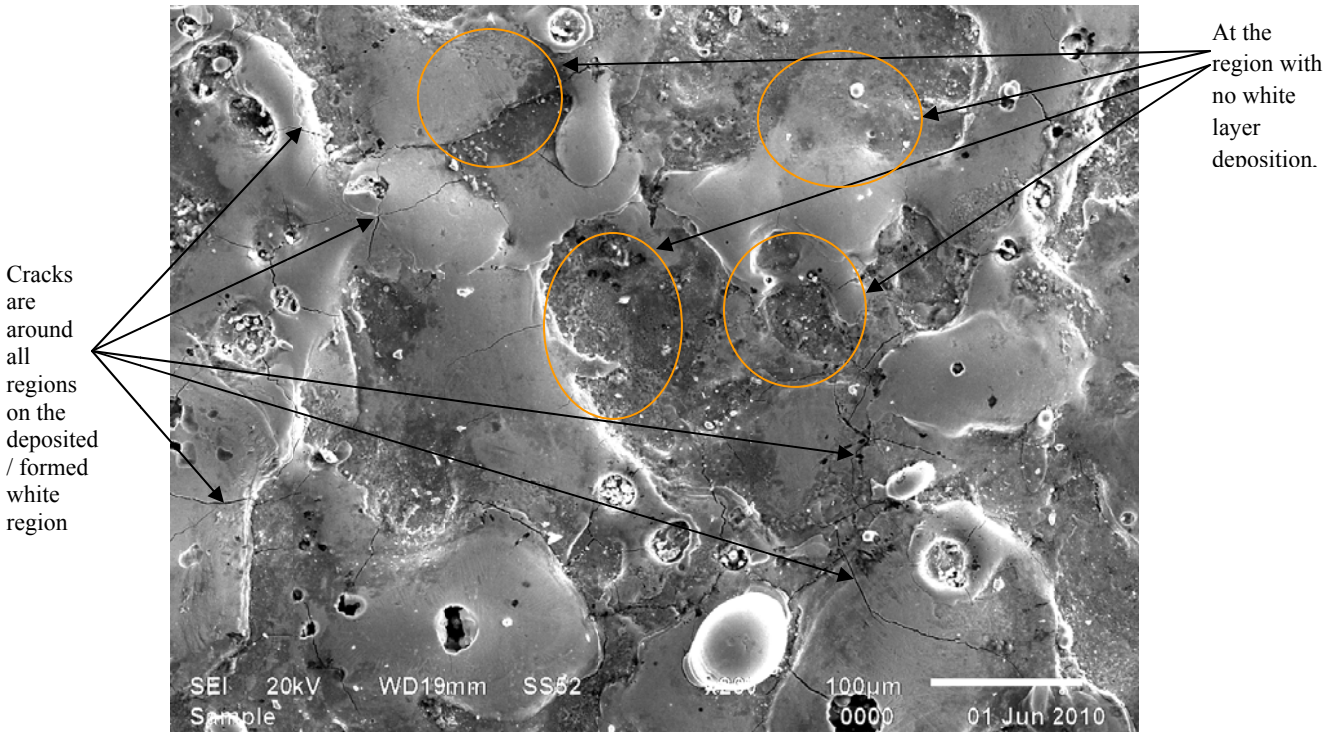

Figure 8.19: SEM micrograph at 200× of EN 31 machined with graphite electrode in tungsten mixed in kerosene (I 5Amp, pulse on time 100µs, pulse off time 85µs)

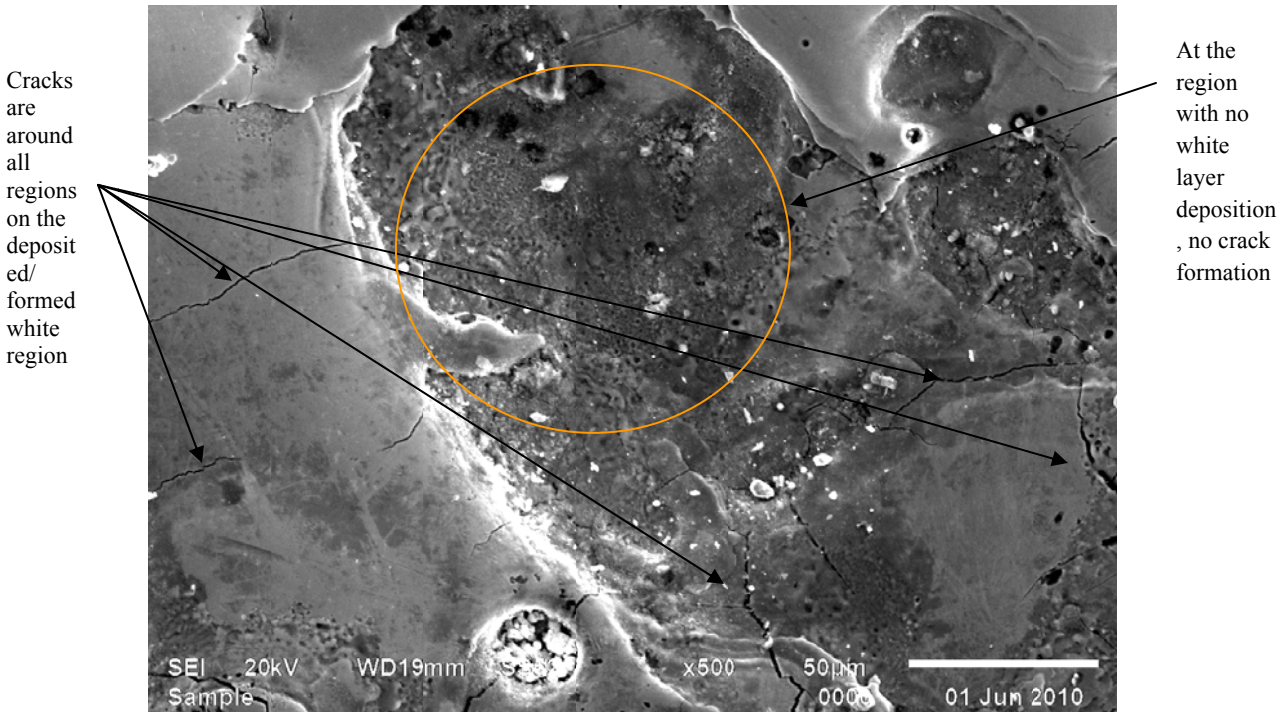

Figure 8.20: SEM micrograph at 500× of EN 31 machined with graphite electrode in tungsten mixed in kerosene (I 5 Amp, pulse on time 100µs, pulse off time 85µs)

5.21: SEM micrograph at 1000× of EN 31 machined with graphite electrode in tungsten mixed in kerosene (I 5Amp, pulse on time 100µs, pulse off time 85µs)

SEM micrograph at 200×, 500× and 1000× of high carbon high chromium machined with tungsten-copper electrode in without powder mixed in EDM oil (I=8 Amp, pulse on 100µs, pulse off 57µs) are shown in the Figure 5.10-5.12 which shows formation of cracks on the white layer. The crater size is more when machined at 8Amp without powder in dielectric. Crater size increased with increase in current. A recast layer has observed on the machined surface. The surface was observed to be rough because of debris which were not flashed away completely from the machining zone. Different layers which were formed in the machined are shown in the Figure 5.22. The discharge between the workpiece and tool melts the metal and metal vaporizes which created thermally altered layers of the cavity. The white layer readily formed and was observed to remains stable on the surface. The white layer is typically fine grained and hard and is alloyed with carbon from the material transferred from electrode. In the white layer material was taken to molten state but neither ejected nor removed by flushing action of the dielectric. The depth of this top melted zone depends upon the pulse energy and duration. The carbon content in the layer can also be affected by carburization from the flushing fluid or electrode material, but decarburization also occurs. The action of EDM altered the metallurgical structure

and characteristics in the recast layer. The recast layer is formed by the un-expelled molten metal solidifying in the craters. The white layer is densely infiltrated with carbon to the point that its structure is different than that of the base material.

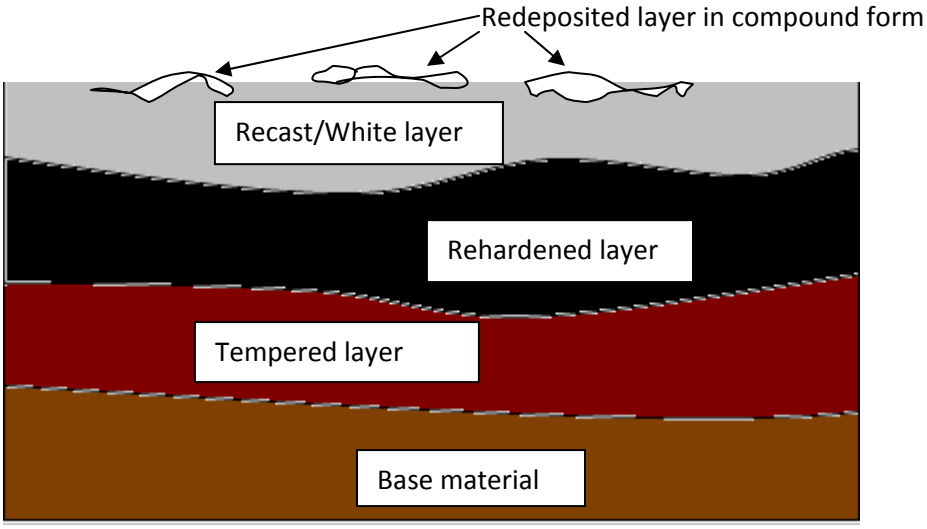

Figure 5.22: Different layers formed on the EDM machined surface

The white layer consists mainly of martensite, residual austenite, and some undissolved carbide. In addition, the high-temperature conditions induced during the EDM procedure prompt some carbon atoms from the kerosene dielectric fluid to migrate into the surface of the machined component. As the thickness of the white layer increases, it becomes more brittle and therefore fractures more readily. As a result, the fatigue life reduces as the thickness of the white layer increases. The next layer is rehardened layer, in this layer temperature has risen above the hardening temperature and martensite formed and which become more hard and brittle. The last layer which is formed that is tempered layer in which material has not heated up to reach hardening temperature and tempering back occurred. This layer retains the metallurgical structure same as the base material because temperature absorbed is not to the level to change the structure. Below the tempered layer is the base material and this is unaffected by EDM process. When workpiece material was machined without powder in the dielectric then crater size is more and more in the depth. Increasing the current or reducing the pulse-on duration suppresses the formation of surface cracks in the machined surface.[12, 44] The fundamental cause of cracking lies in the existence of the internal stresses which are created at the time of the machining operation. The surface density and the depth of these cracks are directly related to the machining

conditions, more increase the current (2Amp-8Amp), more the appearance frequency of these cracks increases. The cracks are formed with the result of high thermal stresses prevailing at the workpiece surface as the latter was cooled at fast rate after the discharge. Figure 5.16-5.17 shows the uniform dispersion of the particles and less micro cracks on the surface of machined when machined with copper powder mixed dielectric. The fine dispersion of hard particles is shown in the Figure 5.19-5.21 which shows the region with no white layer deposition, no crack formation and also shows the cracks all around the region of deposited and white layer. The size of the craters is smaller. With addition of cooper powder in the dielectric craters size is less as compared to tungsten powder.

CHAPTER 9

RESULTS, CONCLUSIONS AND RECOMMENDATIONS

9.1 RESULTS

The effect of parameters i.e. workpiece, dielectric, electrode, pulse on time, pulse off time, current, powder and some of their interactions were evaluated using ANOVA and factorial design analysis. The purpose of the ANOVA was to identify the important parameters in prediction of MRR, TWR, micro hardness, surface roughness. Some results consolidated from ANOVA and plots are given below:

9.1.1 PILOT EXPERIMENT

- It was observed that at low current, MRR is low but increases sharply with increased current.
- MRR was observed to increase when copper powder was suspended in dielectric and reduce with graphite powder.
- The electrode material was found to be most significant factor effecting TWR.
- Increase in current caused high tool wear

9.1.2 MRR

- Current was found the most significant factor with F value 41.03 and its contribution to MRR was 22.54% and followed by electrode (F value 60.22), pulse on time (F value 26.75), powder (F value16.05), pulse off time (F value11.73) were the factors that significantly affected the MRR which had contribution to MRR was 17.17%, 13.77%, 7.93%, 4.5% respectively.
- Others two factors, namely, dielectric and workpiece material and interactions were found to be insignificant.
- In S/N ratio workpiece material and interactions were found to be significant affecting MRR for reducing the variation.

- The estimated mean value of MRR when six factors, namely, workpiece material (HCHCr), pulse off time (57μs), current (5Amp), pulse on time (100μs), powder (tungsten) and interactions were considered with 99% confidence interval was found to be 38.33±1.38 mm^3/min.

9.1.2 TWR

- Current (F value 36.19), electrode (F value 30.08) and powder (F value 17.03) were the factors that significantly affected the TWR.
- Factors, namely, workpiece material, dielectric, pulse on time, pulse off time and interactions were found to be insignificant for TWR.
- In S/N ratio pulse off time, interaction between electrode and powder was the significant for TWR to reducing the variation.
- The estimated mean value of TWR when four factors, namely, electrode (W-Cu) pulse off time (57μs), current (5Amp), powder (tungsten) and interaction between electrode and powder were considered with 99% confidence interval was found to be 1.35±0.134mm^3/min.

9.1.3 MICRO HARDNESS

- Current (F value 17.27) and powder (F value 13.22) were the factors that has significantly affected the micro hardness at non-deposited region.
- Factors, namely workpiece material, dielectric, electrode material, pulse on time, pulse off time and interactions studied in trials were found to be insignificant for micro hardness at non-deposited region.
- The estimated mean value of micro hardness at non-deposited region when current 8Amp and tungsten powder were considered with 99% confidence interval was found to be 835±7.18 hvn.
- Powder (F value 133.15), electrode material (F value 13.93) and current (F value 13.09) were found to be significant for micro hardness at deposited region and all other factors studied in trials were found to be insignificant.

- The estimated mean value of micro hardness at non-deposited region when current 8Amp, tungsten-copper electrode and tungsten powder were considered with 99% confidence interval was found to be 1218.94±13.20 hvn.

9.1.4 SURFACE ROUGHNESS

- Current (F value 52.63) and pulse on time (F value 21.27) were found to be significant in surface roughness at center and left position. All other factors, namely, workpiece, dielectric, electrode, pulse off time, powder and interactions studied during trials were found to be insignificant for surface roughness.
- The estimated mean value of surface roughness at center and left position when current 2Amp and pulse on time 10μs were considered with 99% confidence interval was found to be 3.34±0.13 microns and 3.69±0.12 microns.
- Current, pulse on time, powder and electrode were found to be significant for surface roughness at right position. The factors, namely, workpiece, pulse off time and interaction between workpiece and powder were found to be insignificant.
- The estimated mean value of surface roughness at center and left position when current 2Amp, graphite electrode pulse on time 10μs and interaction between workpiece (HCHCr) and electrode (graphite) were considered with 99% confidence interval was found to be 3.35±0.074 microns.

9.1.5 XRD ANALYSIS

HCHCr

When HCHCr workpiece material was machined with W-Cu electrode in EDM oil with no powder mixing, Cohenite synthetic (Fe_3C) was formed which increases the corrosion resistance and hardenability and reduce the stresses. Also, same material was machined with W-Cu electrode in kerosene oil with tungsten powder mixed, forming tungsten carbide (W_2C) compound which increases hardness and rigidity. Traces of Cu, C, α-Cr have been formed on the surface of HCHCr as machined with graphite electrode with copper powder mixing in kerosene oil.

EN31

Chromium carbide and iron carbide were formed on the surface of EN31 when machined with graphite electrode with tungsten powder mixed in kerosene oil which improved the thermal characteristics and corrosion resistance and reduced the mechanical stresses. Corrosion resistance and hardness were improved when machined with graphite electrode in copper mixed kerosene oil.

Hot Die Steel

Iron carbide was formed on the surface of HDS as machined with graphite electrode in copper mixed kerosene oil. Iron carbide contributed to increase the hardness of material. Chromium carbide was formed when machined with graphite electrode in tungsten powder mixed kerosene. Cohenite compound was formed but copper did not formed any compound.

9.1.6. MICROSTRUCTURE ANALYSIS

SEM micrograph carried out on selected samples at three different magnifications, namely at 200×, 500× and 1000×. It was observed that crater size was more when machined at 8Amp without powder in dielectric as compared to when machined with powder mixed in dielectric. The white layer formed readily and remained stable on the surface. The white layer was observed to be typically fine grained and hard and was alloyed with carbon from the material transferred from electrode. With increase in current micro cracks on the white layer also increased. The fundamental cause of cracking lies in the existence of the internal stresses which were created at the time of the machining operation. The uniform dispersion of the particles and less micro cracks on the surface of machined were observed when machined with copper powder mixed dielectric. With addition of cooper powder in the dielectric craters size was less as compared to tungsten powder.

9.2 CONCLUSIONS

The present study was carried out to study the effect of input parameters on the MRR, TWR, surface roughness, micro hardness and on the surface properties. The following conclusions were drawn from the study:

- The MRR and TWR are mainly affected by the current and electrode material.
- All three workpiece materials showed improvement in micro hardness when machining has been carried out with tungsten powder and the highest value of micro hardness 1193hvn has been achieved in EN31. The tungsten was found in the form of intermetallic compounds as carbide (W_2C).
- Micro hardness also affected with current.
- Surface roughness was mainly affected by the current and pulse on time. At higher value of current causes the more surface roughness.
- Tungsten and copper was found on the surface of workpiece material when machining was carried out with tungsten-copper electrode and with tungsten or copper suspended in the dielectric medium. In HCHCr material, tungsten has been increased from 0.02% to 1.37% and copper from 0.05% to 0.94% when machining has been carried out with tungsten-copper electrode in tungsten powder mixed in dielectric medium.
- With addition of powder in dielectric medium, crater size reduced and with copper crater size was less as compared with tungsten powder.
- Thickness of cracks increased with increase in current.
- Higher surface finish can be achieved at low current value.
- To increase the hardness of material tungsten powder can be used.
- Dielectric medium has less effect on the output responses.

9.3 RECOMMENDATIONS FOR FUTURE WORK

Only three workpiece materials, namely, HCHCr, hot die steel and EN31 has been used. Other materials such as titanium, OHNS die steel and tungsten hot work die steel can be used. Machining was carried out only with two powders, copper and tungsten. Other powders, namely, silicon, nickel, vanadium can be used. Particle size and powder concentration can also be varied.

TECHNICAL SPECIFICATION OF EDM MACHINE

The experiment has been conducted on Electrical Discharge Machine model T-3822M, Victory Electromech, Kolhapur, India. Technical data of machine is as under:

1.Electrical Data

Supply voltage	415V, 3Ø, 50 Hz
Connected load	3 KVA
Open gap voltage output	135±5% V
Max. Machine current	12Amp
Current range	3 ranges of 4Amp each
Current adjustment	0-4Amp in each current range

2. *Machine Tool*

Height	1300mm
Width	730mm
Depth	840mm
Net weight	325 kg
Quill travel	150mm

3. Work Tank

Length	600mm
Width	350mm

APPENDIX-B

SPECIFICATIONS OF MEASURING INSTRUMENTS

1. OPTICAL EMISSION SPECTROMETER

Make and model	Baird, DV-6, USA
Base	Iron, Aluminum, Copper
Medium	Argon gas
Accuracy	0.0001%

2. PERTHOMETER

Make andmodel	Mahr. M4Pi, Germany
Measurement method	Stylus
Profile resolution	100nm
Cut-off wavelength	0.8mm
Tracing length	4.8mm

3. MICRO HARDNESS TESTER

Make and model	Metatech, MVH-2, Pune, India,
Software used	Quantimet
Load	1 kg

Dwell time	20 sec

4. SCANNING ELETRON MICROSCOPE

Make and model	JSM-840A Joel, Japan
Magnification range	10× to 3,00,000×

5. X-RAY DIFFRACTION TESTER

Make and model	ME 210 LA 2, Rigaku corporation
Scan speed	5^0/minute
Range of 2θ	5^0 to 100^0

SPECIFICATIONS OF DIELECTRIC MEDIUM

1. Kerosene oil

Appearance	Clear, transparent, light
Density (kg/m^3)	817.15
Flash Point (^0C)	40
Boiling Point (^0C)	600
Viscosity (centistokes)	2.71

2. EDM oil

Appearance	Clear, light
Density (kg/m^3)	835
Flash Point (^0C)	130
Viscosity (centistokes)	3.12
Specific gravity	0.78±0.02
Dielectric strength	45 kv

[1] Fuller J.E. (1996), "Electrical Discharge Machining", ASM Machining handbook, Vol. 16, pp 557-564.

[2] Pandey P.C. and Shan H.S. (1995), "Modern Machining Processes", Tata McGrawHill, New Delhi, India, ISBN 0-07-096553-9.

[3] Jain V.K. (2004), "Advanced Machining processes", Allied Publishers, New Delhi, India, ISBN 81-7764-294-4.

[4] McGeough J.A. (1998), "Advanced Methods of Machining", Chapman and Hall, USA, ISBN 0-41231970-5.

[5] Mishra P.K. (2005), "Nonconventional Machining", Narosa Publishing House, New Delhi, India, ISBN 81-7319-192-19.

[6] Kumar S., Singh R., Singh T.P., Sethi B.L. (2009), "Surface modifaction by electrical discharge machining: A review", *Journal of Material Processing Technology* Vol. 209, pp 3675-3687.

[7] Sommer C. (2000), "Non-Traditional Machining Handbook", Advance Publishing Inc. Houston, USA, ISBN 1-57537-325-4.

[8] Schumacher B.M. (2004), "After 60 years of EDM the discharge process remains still disputed", *Journal of Material Processing Technology,* Vol. 149, pp 376-381.

[9] Kansal H.K., Singh S., Kumar P., (2007), "Effect of silicon powder mixed EDM on machining rate of AISI D2 die steel", *Journal of Manufacturing proces*ses, Vol. 9, pp 13-21.

[10] Uno Y., Okada A., Cetin S., (2001), "Surface modification of EDMed surface with powder mixed fluid", *2nd International Conference on Design and Production of dies and molds*.

[11] Pecas P., Henriques E., (2008), "Effect of powder concentration and dielectric flow in the surface morphology in electrical discharge machining with powder mixed dielectric (PMD-EDM)", *International Journal of Advanced Manufacturing Technology,* Vol. 37, pp. 1120-1132.

[12] Simao J., Lee H.G, Aspinwall D.K, Dewes R.C, Aspinwall E.N., (2003), "Workpiece surface modification using electrical discharge machining", *International Journal of Machine Tools & Manufacture,* Vol. 43, pp. 121-128.

[13] Furutani K., Sanetoa A., Takezawaa, Mohria N., Miyakeb H., (2001), "Accretion of titanium carbide by electrical discharge machining with powder suspended in working fluid", *Journal of International Societies for Precision Engineering and Nanotechnology,* Vol. 25, pp. 138-144.

[14] Wong Y. S, Lim L.C, Rahuman I., Tee W. M, (1998), "Near-mirror-finish phenomena in EDM using powder-mixed dielectric", *Journal of Material Processing Technology,* Vol. 79, pp. 30-40.

[15] Wu K.L., Yan B.H., Huang F.Y., Chen S.C., (2005), "Improvement of surface finish on SKD steel using electro-discharge machining with aluminum and surfactant added dielectric", *International Journal of Machine Tools & Manufacture,* Vol. 45, pp. 1195-1201.

[16] Pecas P., Henriques E., (2003), "Influence of silicon powder-mixed dielectric on conventional electrical discharge machining", *International Journal of Machine Tools & Manufacture,* Vol. 43, pp. 1465-1471.

[17] Jeswani M.L., (1981), "Effect of the addition of graphite powder to kerosene used as a dielectric fluid in electrical discharge machining", *International Journal of Material Processing Technology,* Vol. 70, pp. 133-139.

[18] Furutani K., Shimizu Y., (2003), "Deposition of lubricant layer by electrical discharge machining during finishing process (2^{nd} report)-Estimation of deposit process through condition monitoring", *Journal of Japan Society for Precision Engineering,* Vol. 70, pp. 683-688.

[19] Prihandana G.S., Mahardika M., Hamdi M., Wong Y.S., Mitsui K. (2009), "Effect of micro powder suspension and ultrasonic vibration of dielectric fluid in micro-EDM process- Taguchi approach", *International Journal of Machine Tools & Manufacture,* Vol. 49, pp. 1035-1041.

[20] Zhao W.S., Meng Q.G., Wang Z.L., (2002), "The application of research on powder mixed EDM in rough machining", *Journal of Material Processing Technology,* Vol. 129, pp. 30-33.

[21] Ming Q.Y., He L.Y., (1995), "Powder suspension dielectric fluid for EDM", *Journal of Materials Processing Technology,* Vol. 52, pp. 44-54.

[22] Kozak J., Rozenek M., Dabrowski L., (2003), "Study of electrical discharge machining using powder suspended working fluid", *Journal of Engineering Manufacture,* Vol. 217, pp. 1597-1602.

[23] Kansal H.K., Singh S., Kumar P.,(2005), "Parametric optimization of powder mixed electrical discharge machining by response surface methodology", *Journal of Materials Processing Technology,* Vol. 169, pp. 427-436.

[24] Tzeng Y., Chen F., (2005), "Investigation into some surface characteristics of electrical discharged machined SKD-11 using powder suspension dielectric oil", *International Journal of Material Processing Technology,* Vol. 170, pp. 385-391.

[25] Chow H.M., Yan B.H., Huang F.Y., Hung J.C., (2000), "Study of added powder in kerosene for the micro slit machining of titanium alloy using electrical discharge machining", *Journal of Materials Processing* Technology, Vol. 101, pp. 95-103.

[26] Chen Y.F., Lin Y.C. (2009), "Surface modification of Al-Zn-Mg alloy using combined EDM with ultrasonic machining and addition of TiC particles into dielectric", *Journal of Materials Processing* Technology, Vol. 209, pp. 4343-4350.

[27] Tsai H.C., Yan B.H., Huang F.Y. (2003), "EDM performance of Cr/Cu-based electrodes", *International Journal of Machine Tools and Manufacture,* Vol. 43, pp. 245-252.

[28] Mohri N., Saito N., Tsunekawa Y., Kinoshtia N. (1993), "Metal surface modification by electrical discharge machining with composite electrode" *CIRP Annals-Manufacturing Technology,* Vol. 42, pp. 219-222.

[29] Koshy P., Jain V.K., Lal G.K. (1993), "Experimental investigation into electrical discharge machining with a rotating disk electrode", *Precision Engineering,* Vol. 15, pp. 6-15.

[30] Singh S., Maheshwari S., Pandey P.C. (2004), "Some investigation into electrical discharge machining of hardened tool steel using different electrode materials", *Journal of Materials Processing Technology,* Vol. 149, pp. 272- 277.

[31] Khanra A.K., Sarkar B.R., Bhattacharya B., Pathak C., Godkhindi M.M. (2004),"Performance of ZrB2-Cu composite as an EDM electrode", *Journal of Materials processing Technology,* Vol. 183, pp. 122-126.

[32] Erden A., Bilgin S. (1980), "Role of impurities in EDM", Proc. 21st IMTDR Conference, pp. 345-350.

[33] Curodeau A., Marceau L.F., Richard M., Lessard J. (2005), "New EDM polishing and texturing with conductive polymer electrodes", *Journal of Materials Processing Technology,* Vol. 159, pp. 17-26.

[34] Marfona J., Wykes C. (2000), "A new method of optimizing material removal rate using EDM with tungsten electrode", *International Journal of Machine Tools & Manufacture,* Vol. 40, pp. 153-164.

[35] Muttamara A., Fukuzawa Y., Mohri N., Tani T. (2009), "Effect of electrode material on electrical discharge machining of alumina", *Journal of Materials Processing Technology,* Vol. 209, pp. 2545-2552.

[36] Haron C.H.C., Ghani J.A., Burhanuddin Y., Seong Y.K., Swee C.Y. (2008),"Copper and graphite electrodes performance in electrical discharge machining of XW42 tool steel", *Journal of Materials Processing Technology,* Vol. 201, pp. 570-573.

[37] Mohan B., Rajadurai A., Satyanarayana K.G. (2002), "Effect of SiC and rotation of electrode on discharge machining of Al-SiC composite", *Journal of Materials Processing Technology,* Vol. 124, pp. 297-304.

[38] Mohri N., TakeZawa H., Furutani K., Ito Y., Sata T., (2000), "A new process of additive and removal machining by EDM with a thin electrode", *CIRP-Annals-Manufacturing Technology,* Vol. 40, pp. 123-126.

[39] Li L., Wong Y.S., Fuh J.Y.H., Lu L. (2001), "Effect of TiC in copper tungsten electrodes on EDM performance", *Journal of Materials Processing Technology,* Vol. 113, pp. 563-567.

[40] Roethel F., Garbajs V. (1976), "Contribution of the micro-analysis of spark eroded surfaces", *CIRP-Annals- Manufacturing Technology,* Vol. 25, pp. 135-140.

[41] Jeswni M.L., Basu S., (1976), "Electron microprobe study of deposition and diffusion of tool material in electrical discharge machining", *International Journal of Production Research,* Vol. 17, pp. 1-14.

[42] Roy R.K., (1990), "A primer on the Taguchi method", *Van Nostrand Reinhold,* New York.

[43] Ross Phillip J., (1990), "Taguchi Techniques for Quality Engineering", McGraw-Hill, ISBN 0-07-053866-2

[44] Krawczyk J., Pacyna J., (2006), "Effect of the tool microstructure on the white layer formation", *Journal of Achievements in Materials and Manufacturing Engineering,* Vol. 17, pp. 93-96.